Experiments on Surface Elevation Probability Distribution and Statistics in Surf and Swash Zones

by

Michael N. Herrman, Nobuhisa Kobayashi,
Bradley D. Johnson and Mark D. Orzech

RESEARCH REPORT NO. CACR-97-01
January, 1997

CENTER FOR APPLIED COASTAL RESEARCH

Ocean Engineering Laboratory
University of Delaware
Newark, Delaware 19716

MASTER COPY KEEP FOR REPRODUCTION PURPOSES

REPORT DOCUMENTATION PAGE

Form Approved
OMB NO. 0704-0188

1. AGENCY USE ONLY *(Leave blank)*	2. REPORT DATE	3. REPORT TYPE AND DATES COVERED
	Jan 97	Technical

4. TITLE AND SUBTITLE

Experiments on Surface Elevation Probability Distribution and Statistics in Surf and Swash Zones

5. FUNDING NUMBERS

DAAL03-92-G-0116

6. AUTHOR(S)

Michael N. Herrman, Nobuhisa Kobayaski, Bradley D. Johnson, Mark D. Orzech

7. PERFORMING ORGANIZATION NAMES(S) AND ADDRESS(ES)

Univ of Delaware
Center for Applied Coastal Research
Ocean Engineering Laboratory
Newark, DE 19716

8. PERFORMING ORGANIZATION REPORT NUMBER

9. SPONSORING / MONITORING AGENCY NAME(S) AND ADDRESS(ES)

U.S. Army Research Office
P.O. Box 12211
Research Triangle Park,, NC 27709-2211

10. SPONSORING / MONITORING AGENCY REPORT NUMBER

ARO 30379.50-GS-URI

11. SUPPLEMENTARY NOTES

The views, opinions and/or findings contained in this report are those of the author(s) and should not be construed as an official Department of the Army position, policy or decision, unless so designated by other documentation.

12a. DISTRIBUTION / AVAILABILITY STATEMENT

Approved for public release; distribution unlimited.

12 b. DISTRIBUTION CODE

13. ABSTRACT ***(Maximum 200 words)***

Three irregular wave tests, with distinct breaker characteristics. were conducted on a 1:16 smooth slope to investigate the detailed cross-shore variations of the probability distributions and statistics of the free surface elevations and mid-depth horizontal velocities in the shoaling, surf and swash zones. The exponential gamma distribution. with measured mean. standard deviation. and skewness, is

(abstract continued on reverse side)

14. SUBJECT TERMS			15. NUMBER IF PAGES
			16. PRICE CODE
17. SECURITY CLASSIFICATION OR REPORT	18. SECURITY CLASSIFICATION OF THIS PAGE	19. SECURITY CLASSIFICATION OF ABSTRACT	20. LIMITATION OF ABSTRACT
UNCLASSIFIED	UNCLASSIFIED	UNCLASSIFIED	UL

shown to be capable of describing the measured probability distributions in a unified manner. The probability distribution of the free surface elevation, limited by the beach face in the swash zone, becomes exponential with the skewness $s = 2$ and the root-mean-square wave height $H_{\rm rms} = \sqrt{8}\,\overline{h}$, with $\overline{h}$ = mean water depth. These upper limits of s and $H_{\rm rms}/\overline{h}$ in the swash zone are in agreement with the data, and indicate that the swash zone is very different from the surf zone. The cross-shore variations of the mean (undertow) and standard deviation of the mid-depth horizontal velocity measured in the shoaling and surf zones can be predicted using the simple relationships derived using linear long-wave theory together with the measured values of $\overline{h}$ and $H_{\rm rms}$.

ABSTRACT

Three irregular wave tests, with distinct breaker characteristics, were conducted on a 1:16 smooth slope to investigate the detailed cross-shore variations of the probability distributions and statistics of the free surface elevations and mid-depth horizontal velocities in the shoaling, surf and swash zones. The exponential gamma distribution, with measured mean, standard deviation, and skewness, is shown to be capable of describing the measured probability distributions in a unified manner. The probability distribution of the free surface elevation, limited by the beach face in the swash zone, becomes exponential with the skewness $s = 2$ and the root-mean-square wave height $H_{\rm rms} = \sqrt{8}\,\overline{h}$, with $\overline{h}$ = mean water depth. These upper limits of s and $H_{\rm rms}/\overline{h}$ in the swash zone are in agreement with the data, and indicate that the swash zone is very different from the surf zone. The cross-shore variations of the mean (undertow) and standard deviation of the mid-depth horizontal velocity measured in the shoaling and surf zones can be predicted using the simple relationships derived using linear long-wave theory together with the measured values of $\overline{h}$ and $H_{\rm rms}$.

ACKNOWLEDGMENTS

This work was supported by the U.S. Army Research Office, University Research Initiative under Contract No. DAAL03-92-G-0116, and by the NOAA Office of Sea Grant, Department of Commerce, under Grant No. NA85AA-D-SG033 (Project SG97 R/OE-22). A special thanks goes to Joseph Hammack for designing, fabricating and installing the wave paddle used in these experiments.

TABLE OF CONTENTS

LIST OF FIGURES

LIST OF TABLES

Chapter 1

INTRODUCTION

The swash zone on a beach forms the boundary zone between the surf and backshore. A predictive model for swash dynamics is required for modeling the erosion and recovery of natural and artificial beaches. Swash data on natural beaches provided the qualitative understanding of swash dynamics [e.g., Guza and Thornton (1982); Holman and Sallenger (1985); Douglas (1992)] but it may not be possible to develop simple empirical relationships in view of the various possible combinations of different beach profiles and incident wave characteristics. On the other hand, the time-dependent numerical model based on the finite-amplitude shallow-water equations including bottom friction (Kobayashi and Wurjanto 1992) has been shown to be capable of predicting the swash characteristics on a natural beach within errors of about 20% (Raubenheimer *et al.* 1995). However, this shallow-water model can not be extended to intermediate water depth. Furthermore, the time-dependent numerical model requires significant computation time to resolve the breaking wave profiles varying rapidly in time and space. This leads to the study of possible statistical methods for predicting swash dynamics.

1.1 Previous Statistical Work

The time-averaged models for random waves represented by the root-mean-square wave height (Battjes and Janssen 1978; Thornton and Guza 1983) or expressed as the superposition of regular waves (Dally and Dean 1986; Mase and Kobayashi 1991) are more efficient computationally at the expense of the loss of

detailed temporal information, such as the skewness of the wave profile, which is regarded to be an important characteristic in cross-shore sediment transport [e.g., Guza and Thornton (1985)]. Moreover, the existing time-averaged models may considerably underpredict the wave setup and root-mean-square wave height in the swash zone (Cox et al. 1994).

Guza and Thornton (1985) computed the various moments of the fluid velocity field measured on a gently sloping beach in estimating nearshore sediment transport rates. The time averaging and probabilistic averaging of a random variable were assumed to be equivalent. The comparisons of the computed moments with monochromatic and linear (Gaussian) random wave models indicated major shortcomings in the monochromatic representation of random waves. The Gaussian model, with given mean and standard deviation, was shown to predict the even moments fairly accurately but to be incapable of predicting the odd moments associated with nonlinearities. In relatively deep water, attempts were made to predict the skewed distribution of the free surface elevation using higher-order expansions [e.g., Longuet-Higgins (1963); Huang and Long (1980); Tayfun (1980)]. In shallow water, Bitner (1980) compared a Gram-Chalier expansion with field data. This higher-order distribution, with measured skewness and kurtosis, predicted the measured free surface probability density functions only slightly better than the Gaussian distribution.

1.2 Objective

The probabilistic approach has recently been neglected, probably for lack of a reasonably simple skewed distribution, in favor of time-dependent numerical modeling. In this study, the exponential gamma distribution [e.g., Gran (1992)] with given mean, standard deviation, and skewness is adopted to describe the probability density function of the free surface elevation from outside the surf zone through the swash zone. The range of the skewness, s, allowed in this distribution is $s = 0 - 2$.

The skewness determines the shape of this distribution and the distribution becomes Gaussian for $s = 0$ and exponential for $s = 2$. The Gaussian distribution may be appropriate in relatively deep water, far seaward of the breaker zone, where local nonlinearity may be negligible. The exponential distribution may be a good approximation in the swash zone where the lower limit of the free surface elevation is limited by the bottom elevation. Since there is no theoretical justification for the adopted exponential gamma distribution, an experiment was conducted to evaluate the applicability of the exponential gamma distribution, as well as to examine the cross-shore variations of the mean, standard deviation, and skewness of the free surface elevation from outside the surf zone to the swash zone.

In the following, the exponential gamma distribution is explained first because the present experiment was designed to assess the cross-shore variation of this distribution. The laboratory experiment is then described concisely. The measured free surface elevation and velocities are analyzed to obtain the probability distributions of these variables. A summary of this study has been submitted for publication (Kobayashi et al. 1996).

Chapter 2

EXPONENTIAL GAMMA DISTRIBUTION

The free surface elevation, η, above the still water level (SWL) is assumed to be a stochastic process satisfying the conditions of stationality and ergodicity [e.g., Goda (1985)]. The time and probabilistic averaging of the stochastic variable, denoted by an overbar in the following, can then be regarded to be equivalent. The probability density function of η is assumed to be expressed by the exponential gamma distribution [e.g., Gran (1992)]. The mean, standard deviation, and skewness coefficient of η are denoted by $\bar{\eta}$, σ and s, respectively. It is assumed that $0 \leq s \leq 2$ on the basis of available field and laboratory data (Bitner 1980; Thompson 1980; Huang and Long 1980; Goda 1985; Mase and Kobayashi 1991; Raubenheimer *et al.* 1995).

2.1 Exponential Gamma Distribution

The normalized free surface elevation, η_*, is defined as $\eta_* = (\eta - \bar{\eta})/\sigma$, whose mean and standard deviation are zero and unity respectively. The skewness, s, of η_* is the same as s of η. The exponential gamma distribution for η_* can be shown to be expressed as

$$f(\eta_*) = [\Gamma(a)]^{-1} \sqrt{\psi'(a)}\, e^{-ay} \exp\left(-e^{-y}\right) \tag{2.1}$$

with

$$y = \sqrt{\psi'(a)}\, \eta_* - \psi(a) \tag{2.2}$$

in which a = shape parameter; Γ = gamma function; ψ = digamma function; and ψ' = trigamma function. The relationship between s and a is given by

$$s = -\psi''(a)\,[\psi'(a)]^{-1.5} \tag{2.3}$$

in which ψ'' = tetragamma function. The kurtosis K of η_* and η is given by

$$K = \psi'''(a)\,[\psi'(a)]^{-2} + 3 \tag{2.4}$$

in which ψ''' = pentagamma function.

The gamma and related functions are explained in Abramowitz and Stegun (1972) and tabulated by Gran (1992). Moreover, the values of $\Gamma(a)$, $\psi(a)$, $\psi'(a)$, $\psi''(a)$, and $\psi'''(a)$ for given a can be found using *Mathematica* (Wolfram 1991). The value of a for given s can be obtained by solving (2.3) using an iteration method (Gran 1992). Figure 2.1 shows the variations of a and $(K-3)$ with respect to s where use can be made of $a = (0.5 + s^{-2})$ for $s < 0.4$ (Gran 1992). The shape parameter, a, decreases from infinity at $s = 0$ to zero at $s = 2$. The kurtosis K increases from $K = 3$ at $s = 0$ to $K = 9$ at $s = 2$.

2.2 Limits of the Exponential Gamma Distribution

For $s = 0$, equation (2.1) reduces to the Gaussian distribution

$$f(\eta_*) = \frac{1}{\sqrt{2\pi}} \exp\left(-\frac{\eta_*^2}{2}\right) \qquad \text{for } s = 0 \tag{2.5}$$

On the other hand, for $s = 2$ equation (2.1) becomes the exponential distribution

$$f(\eta_*) = e^{-(\eta_* + 1)} \qquad \text{for } s = 2 \tag{2.6}$$

which is limited for the range $\eta_* = [(\eta - \overline{\eta})/\sigma] \geq -1$. This lower limit may be interpreted in terms of the instantaneous water depth $h = (\eta - z_b)$ where z_b = fixed bottom elevation which is taken to be positive above SWL. It is required that $h \geq 0$ and hence $\eta \geq z_b$. The lower limit of η for $s = 2$ may be assumed to be imposed by

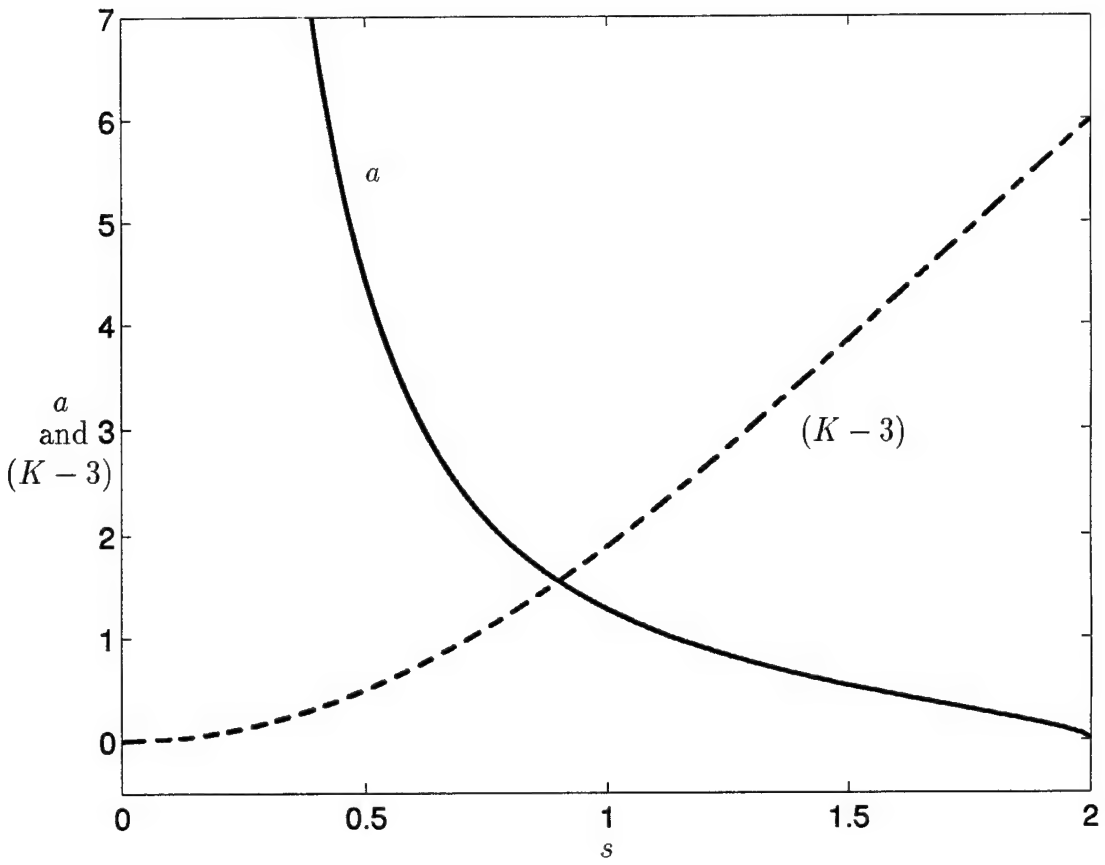

Figure 2.1: Shape Parameter, a, and Kurtosis, K, as a Function of Skewness, s

z_b, resulting in $(\bar{\eta} - \sigma) = z_b$. Since the mean water depth $\bar{h}$ is given by $\bar{h} = (\bar{\eta} - z_b)$, this intuitive assumption requires

$$\bar{h} = \sigma \qquad \text{for } s = 2 \tag{2.7}$$

2.3 Limitations of Available Data

One of the objectives in this study is to investigate whether equations (2.6) and (2.7) hold in the swash zone. The available surf zone laboratory data [e.g., Mase and Kobayashi (1991)] indicates a landward decrease in skewness s toward the still water shoreline. It is hence uncertain whether s increases landward of the still water shoreline, and approaches two in the swash zone as implied by (2.6).

Moreover, Raubenheimer *et al.* (1995) measured the free surface oscillations using runup wires placed parallel to a natural beach face and obtained small and negative values of s for the sea swell frequency range. However, the free surface elevation η used herein corresponds to that measured by a vertical gage with its lower limit on the beach face.

The root-mean-square wave height, $H_{\rm rms}$, is defined in this paper using the standard deviation, σ, (Thornton and Guza 1983; Battjes and Stive 1985)

$$H_{\rm rms} = \sqrt{8}\sigma \tag{2.8}$$

If equation (2.7) holds in the swash zone, $H_{\rm rms}/\overline{h} = \sqrt{8}$ which is much larger than $H_{\rm rms}/\overline{h} \simeq 0.42$ in the inner surf zone measured on a natural beach by Thornton and Guza (1982). On the other hand, the free surface elevation time series measured by vertical capacitance wave gages buried partially in the sand beach in the SUPERTANK Project (Kriebel 1994) indicated that $H_{mo}/\overline{\eta} = 3 - 4$ at the still water shoreline, where H_{mo} = zero-moment wave height given by $H_{mo} = 4\sigma$. Since $z_b = 0$ and $\overline{h} = \overline{\eta}$ at the still water shoreline, this observed range corresponds to $H_{\rm rms}/\overline{h} = 2.1 - 2.8$. This suggests that equation (2.7) may be reasonable in the swash zone, and that the value of $H_{\rm rms}/\overline{h}$ may increase appreciably from the inner surf zone to the swash zone.

Chapter 3

EXPERIMENTAL PROCEDURES

Experiments were conducted to obtain a dense array of measurements for free surface elevation and mid-depth horizontal fluid velocity in the shoaling, surf, and swash zones.

3.1 Experimental Setup

The experiments were conducted in a wave tank that was 30 m long, 2.44 m wide, and 1.5 m high with a constant water depth of 76.2 cm (30 in). Irregular waves, based on the TMA spectrum (Bouws *et al.* 1985) using linear wave theory and random phases, were generated with a piston-type wave paddle. A rock beach with a 1:8 slope was located opposite the wave paddle to absorb waves propagating landward. A divider wall was constructed along the center line in the tank to reduce the effects of re-reflection from the wave paddle. The experimental setup is shown in Figure 3.1. A plywood beach with a 1:16 slope was installed in the 1.22-m-wide flume. Eight capacitance wave gages were used to measure the temporal variations of free surface elevations. One acoustic-Doppler velocimeter (Kraus *et al.* 1994) was employed to measure the temporal variations of fluid velocities. The sampling rate for the free surface and fluid velocity measurements was 20 Hz.

Three sets of tests were conducted on the 1:16 slope. The wave paddle motion, controlled by a computer, was identical for each test. Wave gages 1, 2, and 3 were fixed for each test and used to separate the incident and reflected waves using the procedure described by Kobayashi and Raichle (1994). Wave gage 1 was located at

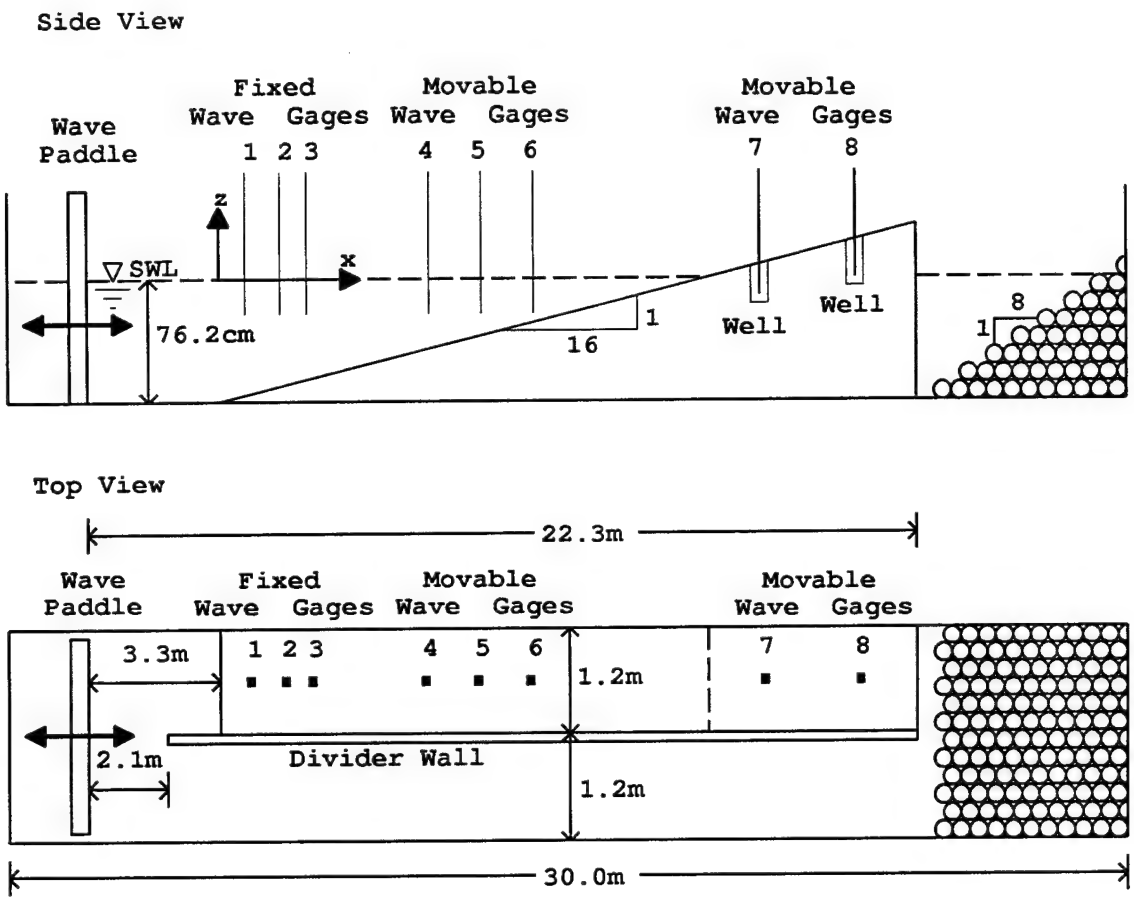

Figure 3.1: Wave Tank Experimental Setup

the water depth below SWL, $d = 75$ cm, for tests 1 and 2 with the incident wave spectral peak period $T_p = 1.5$ and 2.8s, respectively. The horizontal coordinate x in this paper is taken to be positive landward with $x = 0$ at $d = 75$ cm. To better resolve the incident and reflected waves for test 3, with $T_p = 4.7$ s, wave gage 1 was moved to $x = -1$ m where $d = 76.2$ cm above the horizontal bottom. For all three tests, wave gages 2 and 3 were located at $x = 0.38$ m with $d = 72.6$ cm and at $x = 0.50$ m with $d = 71.9$ cm respectively.

3.2 Free Surface Tests

Each test set consisted of 17 runs performed for the free surface measurements along the center line on the 1:16 slope. The duration of each run was 400 s, of which the initial transient duration of 75 s was removed. The remaining 325 s of each time series was used for the subsequent data analyses. The runs from each test set were numbered 1 through 17 for the free surface tests. For wave gages 4–6, the horizontal spacing of the two adjacent gages was 0.16 m, corresponding to a 1-cm increment of the water depth, d. These three gages were moved in the region of $x = 1.44$–9.44 m, where $d = 16$–66 cm, to measure the free surface oscillations at a horizontal interval of 0.16 m. Simultaneously, wave gages 7 and 8 were partially immersed in gage

Table 3.1: Depth of Water at each Gage Position for Free Surface Test 1

	Water Depth d (cm)			*Bottom Elevation Z_b(cm)*	
Run	*Gage 4*	*Gage 5*	*Gage 6*	*Gage 7*	*Gage 8*
1-1	66	65	64	-12.5	-10.0
1-2	63	62	61	-12.5	-10.0
1-3	60	59	58	-10.0	-7.5
1-4	57	56	55	-10.0	-7.5
1-5	54	53	52	-7.5	-5.0
1-6	51	50	49	-7.5	-5.0
1-7	48	47	46	-5.0	-2.5
1-8	45	44	43	-5.0	-2.5
1-9	42	41	40	-2.5	0.0
1-10	39	38	37	-2.5	0.0
1-11	36	35	34	0.0	2.5
1-12	33	32	31	0.0	2.5
1-13	30	29	28	2.5	5.0
1-14	27	26	25	2.5	5.0
1-15	24	23	22	5.0	7.5
1-16	21	20	19	5.0	7.5
1-17	18	17	16	5.0	7.5

wells as illustrated in Figure 3.1. The horizontal spacing of the 16 gage wells was

Table 3.2: Depth of Water at each Gage Position for Free Surface Test 2

	Water Depth d (cm)			*Bottom Elevation Z_b(cm)*	
Run	*Gage 4*	*Gage 5*	*Gage 6*	*Gage 7*	*Gage 8*
2-1	66	65	64	-12.5	-10.0
2-2	63	62	61	-10.0	-7.5
2-3	60	59	58	-7.5	-5.0
2-4	57	56	55	-5.0	-2.5
2-5	54	53	52	-2.5	0.0
2-6	51	50	49	0.0	2.5
2-7	48	47	46	2.5	5.0
2-8	45	44	43	5.0	7.5
2-9	42	41	40	7.5	10.0
2-10	39	38	37	10.0	12.5
2-11	36	35	34	10.0	12.5
2-12	33	32	31	12.5	15.0
2-13	30	29	28	12.5	15.0
2-14	27	26	25	15.0	17.5
2-15	24	23	22	15.0	17.5
2-16	21	20	19	17.5	20.0
2-17	18	17	16	17.5	20.0

0.4 m in the region 10 m $\leq x \leq$ 16 m, corresponding to the 2.5-cm increment of the water depth d. Tables 3.1 – 3.3 show the water depth at each gage position for tests 1–3, respectively. Note that the water depth is given by d for gages 4–6 and by z_b, where $z_b = -d$, for gages 7 and 8 to avoid a negative water depth connotation in the swash zone, where $d < 0$. Rubber lids were placed on the 14 gage wells that were not in use for the free surface measurements in individual runs. Rubber lids were also attached to wave gages 7 and 8 to seal the gage wells used for the free surface measurements. The rubber lids were used to provide a continuous, smooth slope over the wells to eliminate disturbances in the sensitive shallow water and swash regions. Wave gages 7 and 8 with the attached rubber lids, which were calibrated before and after each test, were deployed in the region of $x \geq 10$ m and $d \leq 12.5$ cm

Table 3.3: Depth of Water at each Gage Position for Free Surface Test 3

	Water Depth d (cm)			*Bottom Elevation Z_b(cm)*	
Run	*Gage 4*	*Gage 5*	*Gage 6*	*Gage 7*	*Gage 8*
3-1	66	65	64	-12.5	-10.0
3-2	63	62	61	-10.0	-7.5
3-3	60	59	58	-7.5	-5.0
3-4	57	56	55	-5.0	-2.5
3-5	54	53	52	-2.5	0.0
3-6	51	50	49	0.0	2.5
3-7	48	47	46	2.5	5.0
3-8	45	44	43	5.0	7.5
3-9	42	41	40	7.5	10.0
3-10	39	38	37	10.0	12.5
3-11	36	35	34	12.5	15.0
3-12	33	32	31	15.0	17.5
3-13	30	29	28	17.5	20.0
3-14	27	26	25	20.0	22.5
3-15	24	23	22	20.0	22.5
3-16	21	20	19	22.5	25.0
3-17	18	17	16	22.5	25.0

up to the upper limit of wave runup for each test. The free surface measurements at the gage wells were made more than once because the 17 runs for each test allowed 34 free surface measurements using wave gages 7 and 8.

3.3 Velocity Tests

The velocity measurements for each of the three tests were made at mid-depth, $z = (-d/2)$, at the horizontal locations of $d = 10$, 12.5 and $(15 + 3j)$ cm with $j = 1, 2, \ldots, 17$ where z = vertical coordinate taken to be positive upward with $z = 0$ at SWL. The velocity test runs are numbered 18 through 34 for each test set. The fixed wave gages 1–3 were also deployed to ensure the repeatability of the wave conditions during the velocity measurements for each test. The free surface elevations at the locations of the velocity measurements were measured separately

in the 17 runs described above. A 3D side-looking probe attached to an acoustic doppler velocimeter was used to measure the three velocity components in the region d = 18–66 cm, whereas a 2D side-looking probe was employed to measure the two horizontal velocity components in the region d = 10–12.5 cm. The velocity measurements for test 1 were performed twice for the range of d = 18–66 cm, with the 2D probe used from d = 18–27 cm in the second test set, to check the repeatability of the velocity measurements and the sensitivity of the 3D probe in shallow water. The cross-shore horizontal and vertical velocity components were analyzed in the same way as the free surface elevations. The measured cross-tank horizontal velocity components were negligible. The measured vertical velocity components were small relative to the corresponding horizontal velocity components and affected more by the turbulence generated by wave breaking. Consequently, only the horizontal velocity components are presented herein.

3.4 Repeatability of Tests

After completing the 17 runs for the free surface and velocity measurements for the three test sets, the repeatability of the incident and reflected waves was checked for each set. The separated incident and reflected wave spectra at the location of wave gage 1 were plotted together for the 17 runs of each free surface and velocity test. The plotted 17 spectra for each individual test set were almost identical, as shown in Figure 3.2 – 3.7.

Comparisons were also made of the spectral parameters such as the incident wave spectral peak period, T_p, the spectral estimate of the incident significant wave height, $H_{mo} = 4\sqrt{m_0}$, with m_0 = zero-moment of the incident wave spectrum, and the average reflection coefficient, $R = \sqrt{(m_0)_r/m_0}$, with $(m_0)_r$ = zero-moment of the reflected wave spectrum. In addition, the separated incident wave time series were analyzed using a zero-upcrossing method to obtain the time series parameters such as the significant wave period T_s and the significant wave height H_s. Tables 3.4

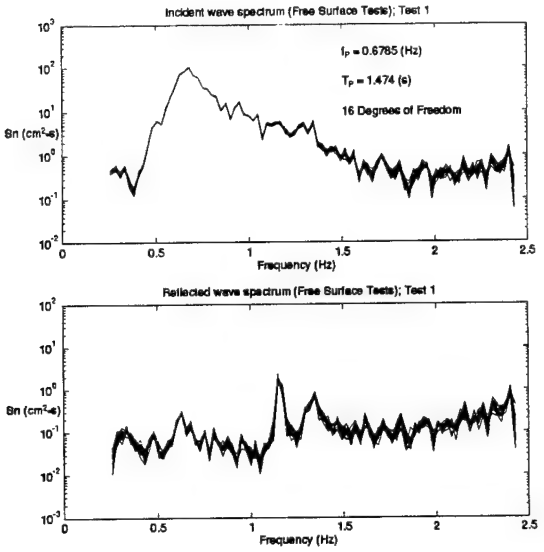

Figure 3.2: Smoothed Power Density Spectrum; Incident and Reflected Waves for Free Surface Test 1

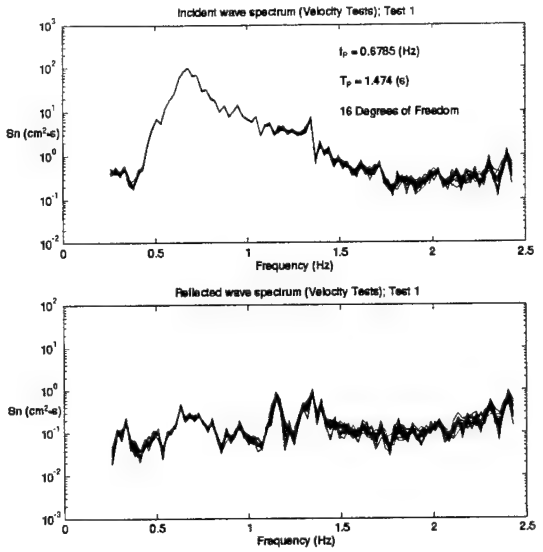

Figure 3.3: Smoothed Power Density Spectrum; Incident and Reflected Waves for Velocity Test 1

and 3.5 list the average values of T_s, H_s, T_p, H_{mo} and R for the 17 runs for each of the three free surface tests. The deviations from the average values of T_s, H_s, T_p and H_{mo} among the 17 runs were generally less than 1% and did not exceed 4%. The reflection coefficient R varied more and, for example, R was in the range $R =$ 0.14–0.15 for test 1, $R = 0.13$–0.19 for test 2, and $R = 0.16$–0.17 for test 3 as shown in Table 3.4. Finally, the surf similarity parameter ξ (Battjes 1974) based on T_p and H_{mo} for the 1:16 slope is listed in Tables 3.4 and 3.5 to indicate the transition from mostly spilling breakers for test 1 to predominantly plunging breakers for test 3. Tables 3.6 – 3.11 show the values of T_s, H_s, H_{mo}, H_{rms} and R for each run in test set 1 through test set 3 for the free surface and velocity tests.

Additionally, the values for wave setup $\overline{\eta}$, root-mean-square wave height H_{rms}, skewness, and kurtosis were compared for gages 1–3 for each run in each test set. The values, shown in Tables 3.12 – 3.17, are consistent through each test set and were generally within small percentage points of error.

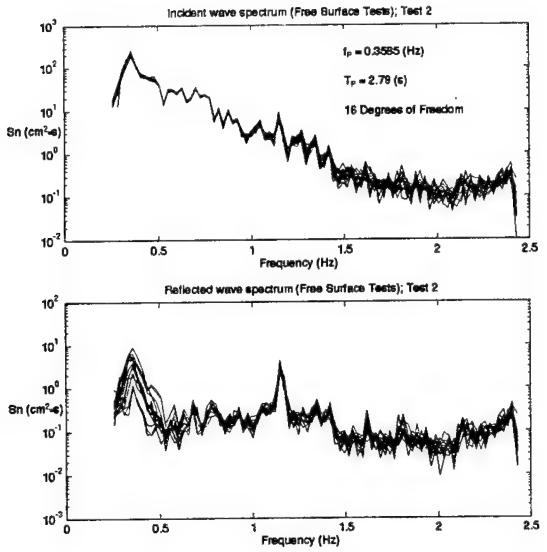

Figure 3.4: Smoothed Power Density Spectrum; Incident and Reflected Waves for Free Surface Test 2

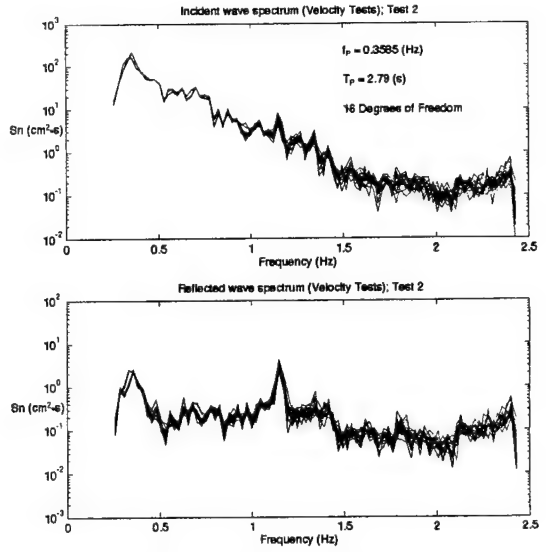

Figure 3.5: Smoothed Power Density Spectrum; Incident and Reflected Waves for Velocity Test 2

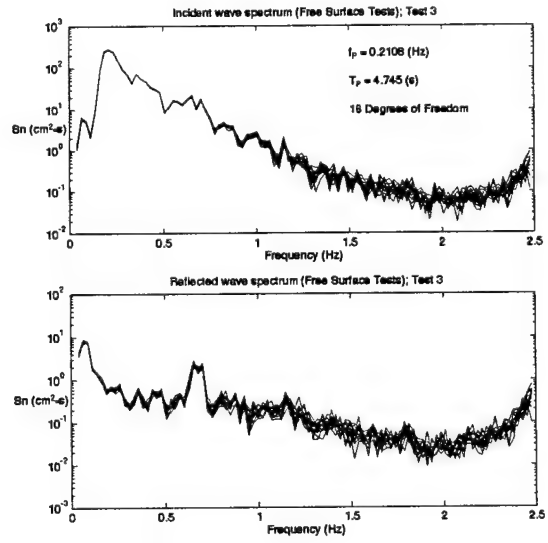

Figure 3.6: Smoothed Power Density Spectrum; Incident and Reflected Waves for Free Surface Test 3

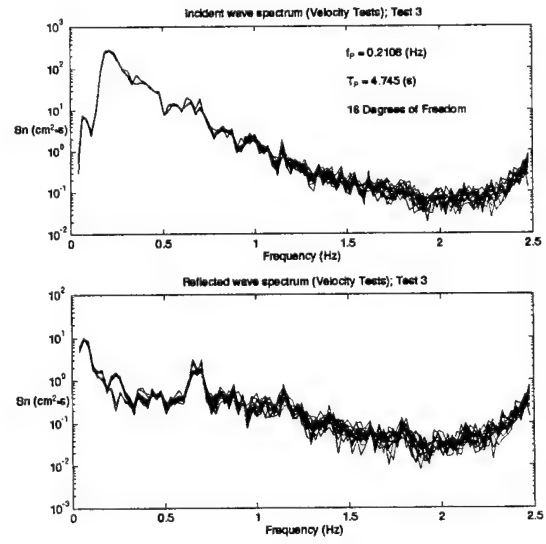

Figure 3.7: Smoothed Power Density Spectrum; Incident and Reflected Waves for Velocity Test 3

Table 3.4: Incident Wave Characteristics for Three Free Surface Tests

Test	T_s (s)	H_s (cm)	T_p (s)	H_{mo} (cm)	R	ξ
1	1.4	17.3	1.5	17.3	0.14	0.28
2	2.5	22.8	2.8	22.3	0.15	0.46
3	4.1	26.1	4.7	26.1	0.17	0.72

Table 3.5: Incident Wave Characteristics for Three Velocity Tests

Test	T_s (s)	H_s (cm)	T_p (s)	H_{mo} (cm)	R	ξ
1	1.4	16.5	1.5	16.8	0.15	0.29
2	2.5	22.6	2.8	22.1	0.14	0.47
3	4.2	25.8	4.7	25.9	0.18	0.72

Table 3.6: Time Series and Spectral Parameters for Free Surface Test 1

	Time Series		*Spectral*		
Run	$T_s(s)$	$H_s(cm)$	$H_{mo}(cm)$	$H_{rms}(cm)$	R
1-1	1.4	17.3	17.3	12.2	0.14
1-2	1.4	17.3	17.3	12.2	0.14
1-3	1.4	17.4	17.3	12.2	0.14
1-4	1.4	17.1	17.2	12.2	0.14
1-5	1.4	17.3	17.3	12.2	0.14
1-6	1.4	17.4	17.4	12.3	0.14
1-7	1.4	17.5	17.4	12.3	0.14
1-8	1.4	17.4	17.4	12.3	0.14
1-9	1.4	17.4	17.4	12.3	0.14
1-10	1.4	17.5	17.4	12.3	0.15
1-11	1.4	17.2	17.1	12.1	0.14
1-12	1.4	17.1	17.2	12.1	0.14
1-13	1.4	17.3	17.2	12.2	0.14
1-14	1.4	17.3	17.3	12.2	0.14
1-15	1.4	17.2	17.2	12.2	0.14
1-16	1.4	17.3	17.3	12.2	0.14
1-17	1.4	17.4	17.3	12.2	0.14
Mean	1.4	17.3	17.3	12.2	0.14
Max	1.4	17.5	17.4	12.3	0.15
Min	1.4	17.1	17.1	12.1	0.14

Table 3.7: Time Series and Spectral Parameters for Velocity Test 1

	Time Series		*Spectral*		
Run	$T_s(s)$	$H_s(cm)$	$H_{mo}(cm)$	$H_{rms}(cm)$	R
1-18	1.4	16.4	16.7	11.8	0.15
1-19	1.4	16.5	16.7	11.8	0.15
1-20	1.4	16.5	16.7	11.8	0.15
1-21	1.4	16.6	16.8	11.9	0.15
1-22	1.4	16.5	16.8	11.8	0.15
1-23	1.4	16.7	16.8	11.9	0.15
1-24	1.4	16.5	16.8	11.9	0.15
1-25	1.4	16.6	16.9	11.9	0.15
1-26	1.4	16.6	16.8	11.9	0.15
1-27	1.4	16.6	16.8	11.9	0.15
1-28	1.4	16.6	16.8	11.9	0.15
1-29	1.4	16.5	16.8	11.8	0.14
1-30	1.4	16.6	16.8	11.9	0.15
1-31	1.4	16.5	16.6	11.8	0.14
1-32	1.4	16.6	16.8	11.9	0.15
1-33	1.4	16.7	16.8	11.9	0.14
1-34	1.4	16.7	16.8	11.9	0.15
1-35	1.4	16.3	16.6	11.7	0.15
1-36	1.4	16.5	16.8	11.8	0.14
Mean	1.4	16.5	16.8	11.9	0.15
Max	1.4	16.7	16.9	11.9	0.15
Min	1.4	16.3	16.6	11.7	0.14

Table 3.8: Time Series and Spectral Parameters for Free Surface Test 2

	Time Series		*Spectral*		
Run	$T_s(s)$	$H_s(cm)$	$H_{mo}(cm)$	$H_{rms}(cm)$	R
2-1	2.5	22.4	21.8	15.4	0.13
2-2	2.5	22.3	21.7	15.3	0.13
2-3	2.4	22.1	21.7	15.3	0.13
2-4	2.5	22.6	22.0	15.5	0.13
2-5	2.5	22.7	22.2	15.7	0.14
2-6	2.5	23.0	22.3	15.8	0.14
2-7	2.5	23.1	22.4	15.8	0.15
2-8	2.5	22.9	22.5	15.9	0.16
2-9	2.5	23.0	22.4	15.8	0.17
2-10	2.5	23.1	22.6	15.9	0.17
2-11	2.5	22.9	22.5	15.9	0.16
2-12	2.5	23.0	22.5	15.9	0.16
2-13	2.5	22.8	22.4	15.8	0.14
2-14	2.5	22.8	22.3	15.8	0.16
2-15	2.5	23.5	23.0	16.2	0.16
2-16	2.5	23.2	23.0	16.2	0.17
2-17	2.5	22.8	22.1	15.6	0.19
Mean	2.5	22.8	22.3	15.8	0.15
Max	2.5	23.5	23.0	16.2	0.19
Min	2.4	22.1	21.7	15.3	0.13

Table 3.9: Time Series and Spectral Parameters for Velocity Test 2

	Time Series		*Spectral*		
Run	$T_s(s)$	$H_s(cm)$	$H_{mo}(cm)$	$H_{rms}(cm)$	R
2-18	2.4	22.2	22.0	15.6	0.14
2-19	2.5	22.4	22.0	15.6	0.14
2-20	2.5	22.3	22.0	15.6	0.14
2-21	2.5	22.8	22.2	15.7	0.14
2-22	2.5	22.8	22.1	15.6	0.15
2-23	2.5	22.5	22.1	15.6	0.14
2-24	2.5	22.5	22.2	15.7	0.14
2-25	2.5	22.8	22.2	15.7	0.14
2-26	2.5	22.5	22.2	15.6	0.15
2-27	2.5	22.7	22.2	15.7	0.15
2-28	2.5	22.6	22.1	15.6	0.14
2-29	2.5	22.7	22.1	15.6	0.14
2-30	2.5	22.6	22.2	15.7	0.15
2-31	2.5	22.7	22.2	15.7	0.15
2-32	2.5	22.8	22.2	15.7	0.14
2-33	2.5	22.6	22.2	15.7	0.14
2-34	2.5	22.8	22.3	15.7	0.14
2-35	2.5	22.2	21.7	15.3	0.15
2-36	2.5	22.5	21.8	15.4	0.16
Mean	2.5	22.6	22.1	15.6	0.14
Max	2.5	22.8	22.3	15.7	0.16
Min	2.4	22.2	21.7	15.3	0.14

Table 3.10: Time Series and Spectral Parameters for Free Surface Test 3

	Time Series		*Spectral*		
Run	$T_S(s)$	$H_S(cm)$	$H_{mo}(cm)$	$H_{rms}(cm)$	R
3-1	4.2	26.0	26.0	18.4	0.17
3-2	4.2	26.1	26.0	18.4	0.17
3-3	4.2	26.5	26.0	18.4	0.16
3-4	4.2	26.1	26.1	18.4	0.17
3-5	4.2	26.0	26.1	18.4	0.16
3-6	4.2	26.3	26.1	18.4	0.17
3-7	4.1	26.1	26.1	18.4	0.17
3-8	4.1	26.1	26.1	18.4	0.17
3-9	4.2	25.8	26.0	18.4	0.17
3-10	4.1	25.8	26.0	18.4	0.17
3-11	4.2	26.1	26.0	18.4	0.16
3-12	4.2	26.2	26.1	18.4	0.16
3-13	4.1	26.3	26.1	18.4	0.16
3-14	4.1	26.2	26.1	18.4	0.17
3-15	4.1	26.0	26.1	18.4	0.17
3-16	4.1	25.8	26.0	18.4	0.17
3-17	4.0	25.8	26.1	18.4	0.16
Mean	4.2	26.1	26.1	18.4	0.17
Max	4.2	26.5	26.1	18.4	0.17
Min	4.0	25.8	26.0	18.4	0.16

Table 3.11: Time Series and Spectral Parameters for Velocity Test 3

	Time Series		*Spectral*		
Run	$T_S(s)$	$H_S(cm)$	$H_{mo}(cm)$	$H_{rms}(cm)$	R
3-18	4.2	25.8	25.9	18.3	0.18
3-19	4.2	25.9	25.9	18.3	0.18
3-20	4.2	25.9	25.9	18.3	0.18
3-21	4.3	25.9	25.9	18.3	0.18
3-22	4.3	25.8	25.9	18.3	0.18
3-23	4.2	25.9	25.9	18.3	0.18
3-24	4.3	26.1	25.9	18.3	0.18
3-25	4.2	25.6	25.9	18.3	0.18
3-26	4.2	26.0	25.9	18.3	0.18
3-27	4.2	25.8	25.9	18.3	0.18
3-28	4.3	25.7	25.9	18.3	0.18
3-29	4.1	25.5	25.9	18.3	0.18
3-30	4.1	25.8	26.0	18.3	0.18
3-31	4.3	25.6	26.0	18.3	0.18
3-32	4.3	25.9	26.0	18.3	0.18
3-33	4.2	25.5	26.0	18.4	0.18
3-34	4.3	26.3	26.0	18.3	0.18
3-35	4.2	26.2	25.5	18.0	0.18
3-36	4.2	25.7	25.5	18.0	0.18
Mean	4.2	25.8	25.9	18.3	0.18
Max	4.3	26.3	26.0	18.4	0.18
Min	4.1	25.5	25.5	18.0	0.18

Table 3.12: $\overline{\eta}$, H_{rms}, Skewness, and Kurtosis for Free Surface Test 1

	Setup, $\overline{\eta}$*(cm)*			H_{rms}*(cm)*			*Skewness s*			*Kurtosis K*		
Run	*Gage 1*	*Gage 2*	*Gage 3*	*Gage 1*	*Gage 2*	*Gage 3*	*Gage 1*	*Gage 2*	*Gage 3*	*Gage 1*	*Gage 2*	*Gage 3*
1-1	0.11	-0.18	-0.23	12.45	12.53	12.40	0.36	0.37	0.35	3.24	3.20	3.16
1-2	0.11	-0.18	-0.22	12.41	12.51	12.39	0.35	0.38	0.36	3.21	3.20	3.19
1-3	0.11	-0.18	-0.22	12.47	12.55	12.44	0.35	0.38	0.36	3.20	3.21	3.18
1-4	0.12	-0.14	-0.19	12.41	12.44	12.33	0.35	0.35	0.34	3.24	3.15	3.13
1-5	0.11	-0.15	-0.20	12.44	12.51	12.40	0.36	0.39	0.37	3.22	3.22	3.19
1-6	0.11	-0.15	-0.20	12.52	12.57	12.47	0.36	0.37	0.36	3.23	3.19	3.17
1-7	0.11	-0.15	-0.21	12.51	12.58	12.46	0.37	0.39	0.36	3.26	3.25	3.19
1-8	0.10	-0.15	-0.21	12.48	12.59	12.49	0.37	0.39	0.37	3.25	3.20	3.19
1-9	0.10	-0.15	-0.21	12.48	12.61	12.49	0.37	0.39	0.37	3.25	3.24	3.21
1-10	0.10	-0.15	-0.21	12.48	12.59	12.49	0.37	0.40	0.38	3.25	3.27	3.22
1-11	-0.06	-0.09	-0.14	12.34	12.38	12.27	0.36	0.37	0.35	3.17	3.17	3.12
1-12	-0.07	-0.09	-0.16	12.37	12.38	12.25	0.35	0.36	0.33	3.20	3.15	3.15
1-13	-0.08	-0.10	-0.16	12.43	12.42	12.30	0.36	0.36	0.35	3.23	3.16	3.13
1-14	-0.08	-0.11	-0.17	12.45	12.43	12.33	0.37	0.36	0.34	3.24	3.18	3.17
1-15	-0.08	-0.11	-0.16	12.42	12.42	12.30	0.37	0.38	0.36	3.25	3.21	3.17
1-16	-0.09	-0.11	-0.17	12.46	12.45	12.33	0.37	0.39	0.36	3.25	3.22	3.18
1-17	-0.09	-0.11	-0.17	12.44	12.44	12.34	0.38	0.39	0.37	3.27	3.23	3.21
Mean	0.03	-0.13	-0.19	12.44	12.49	12.38	0.36	0.38	0.36	3.23	3.20	3.17
Max	0.12	-0.08	-0.14	12.52	12.61	12.49	0.38	0.40	0.38	3.27	3.27	3.22
Min	-0.09	-0.18	-0.23	12.34	12.38	12.25	0.35	0.35	0.33	3.17	3.15	3.13

Table 3.13: $\overline{\eta}$, H_{rms}, Skewness, and Kurtosis for Velocity Test 1

	Setup, $\overline{\eta}$*(cm)*			H_{rms}*(cm)*			*Skewness s*			*Kurtosis K*		
Run	*Gage 1*	*Gage 2*	*Gage 3*	*Gage 1*	*Gage 2*	*Gage 3*	*Gage 1*	*Gage 2*	*Gage 3*	*Gage 1*	*Gage 2*	*Gage 3*
1-18	-0.19	-0.22	-0.27	12.29	12.21	12.15	0.33	0.27	0.22	3.20	3.04	3.00
1-19	-0.20	-0.24	-0.28	12.31	12.24	12.15	0.34	0.27	0.21	3.20	3.05	3.01
1-20	-0.21	-0.23	-0.28	12.32	12.27	12.19	0.33	0.28	0.22	3.23	3.05	3.02
1-21	-0.21	-0.24	-0.29	12.36	12.33	12.21	0.33	0.27	0.23	3.19	3.06	3.05
1-22	-0.21	-0.24	-0.29	12.36	12.29	12.19	0.34	0.28	0.22	3.20	3.05	3.02
1-23	-0.21	-0.25	-0.29	12.41	12.35	12.24	0.33	0.27	0.22	3.20	3.04	3.03
1-24	-0.21	-0.25	-0.29	12.38	12.29	12.21	0.33	0.27	0.22	3.20	3.06	3.03
1-25	-0.22	-0.25	-0.30	12.38	12.37	12.26	0.33	0.29	0.21	3.19	3.07	3.03
1-26	-0.22	-0.25	-0.30	12.37	12.33	12.23	0.33	0.29	0.23	3.21	3.08	3.03
1-27	-0.22	-0.26	-0.30	12.38	12.33	12.24	0.34	0.29	0.23	3.22	3.05	3.03
1-28	-0.23	-0.26	-0.30	12.37	12.34	12.21	0.33	0.28	0.21	3.20	3.06	3.04
1-29	-0.23	-0.26	-0.30	12.33	12.31	12.20	0.32	0.27	0.21	3.19	3.06	3.03
1-30	-0.23	-0.27	-0.30	12.38	12.30	12.20	0.34	0.28	0.23	3.20	3.08	3.04
1-31	-0.22	-0.26	-0.30	12.25	12.19	12.13	0.31	0.26	0.22	3.15	3.03	3.03
1-32	-0.23	-0.27	-0.31	12.39	12.30	12.22	0.33	0.28	0.23	3.20	3.06	3.06
1-33	-0.23	-0.27	-0.31	12.37	12.31	12.19	0.33	0.28	0.22	3.19	3.05	3.02
1-34	-0.24	-0.27	-0.31	12.36	12.33	12.22	0.34	0.28	0.22	3.21	3.07	3.03
1-35	-0.14	-0.17	-0.27	12.20	12.11	12.04	0.33	0.24	0.19	3.15	3.01	3.00
1-36	-0.10	-0.13	-0.30	12.34	12.29	12.18	0.33	0.27	0.21	3.21	3.08	3.02
Mean	-0.21	-0.24	-0.29	12.34	12.29	12.19	0.33	0.28	0.22	3.20	3.06	3.03
Max	-0.10	-0.13	-0.27	12.41	12.37	12.26	0.34	0.29	0.23	3.23	3.08	3.06
Min	-0.24	-0.27	-0.31	12.20	12.11	12.04	0.31	0.24	0.19	3.15	3.01	3.00

Table 3.14: $\overline{\eta}$, H_{rms}, Skewness, and Kurtosis for Free Surface Test 2

	Setup, $\overline{\eta}$*(cm)*			H_{rms}*(cm)*			*Skewness s*			*Kurtosis K*		
Run	*Gage 1*	*Gage 2*	*Gage 3*	*Gage 1*	*Gage 2*	*Gage 3*	*Gage 1*	*Gage 2*	*Gage 3*	*Gage 1*	*Gage 2*	*Gage 3*
2-1	-0.35	-0.32	-0.34	16.23	16.17	15.95	0.52	0.58	0.59	3.52	3.56	3.56
2-2	-0.36	-0.32	-0.31	16.11	16.10	15.86	0.53	0.60	0.60	3.52	3.60	3.60
2-3	-0.36	-0.31	-0.28	16.10	16.06	15.82	0.53	0.59	0.60	3.50	3.57	3.58
2-4	-0.38	-0.31	-0.27	16.43	16.26	16.00	0.54	0.60	0.62	3.46	3.56	3.58
2-5	-0.37	-0.30	-0.27	16.71	16.52	16.20	0.56	0.62	0.64	3.54	3.57	3.59
2-6	-0.38	-0.31	-0.26	16.94	16.78	16.48	0.52	0.62	0.65	3.45	3.56	3.60
2-7	-0.38	-0.32	-0.27	17.10	17.04	16.79	0.53	0.61	0.64	3.53	3.60	3.66
2-8	-0.39	-0.32	-0.28	17.20	17.19	16.93	0.53	0.62	0.64	3.56	3.61	3.63
2-9	-0.40	-0.32	-0.27	17.21	17.21	16.93	0.52	0.61	0.62	3.53	3.60	3.61
2-10	-0.26	-0.14	-0.08	17.28	17.19	17.07	0.52	0.62	0.64	3.51	3.60	3.64
2-11	-0.27	-0.14	-0.07	17.25	17.17	17.06	0.51	0.59	0.60	3.53	3.55	3.56
2-12	-0.27	-0.14	0.16	17.12	17.05	16.97	0.52	0.58	0.61	3.54	3.59	3.63
2-13	-0.27	-0.15	0.16	16.86	16.77	16.74	0.51	0.59	0.62	3.54	3.60	3.65
2-14	-0.29	-0.16	0.14	16.79	16.58	16.48	0.51	0.59	0.60	3.48	3.54	3.56
2-15	-0.28	-0.16	0.14	16.95	16.63	16.53	0.52	0.61	0.63	3.48	3.55	3.59
2-16	-0.28	-0.15	0.15	17.06	16.70	16.56	0.52	0.60	0.63	3.47	3.54	3.59
2-17	-0.27	-0.14	0.10	17.08	16.72	16.59	0.53	0.61	0.64	3.50	3.58	3.64
Mean	-0.32	-0.24	-0.11	16.85	16.71	16.53	0.52	0.60	0.62	3.51	3.58	3.60
Max	-0.26	-0.14	0.16	17.28	17.21	17.07	0.56	0.62	0.65	3.56	3.61	3.66
Min	-0.40	-0.32	-0.34	16.10	16.10	15.82	0.51	0.58	0.59	3.45	3.54	3.56

Table 3.15: $\overline{\eta}$, H_{rms}, Skewness, and Kurtosis for Velocity Test 2

	Setup, $\overline{\eta}$*(cm)*			H_{rms}*(cm)*			*Skewness s*			*Kurtosis K*		
Run	*Gage 1*	*Gage 2*	*Gage 3*	*Gage 1*	*Gage 2*	*Gage 3*	*Gage 1*	*Gage 2*	*Gage 3*	*Gage 1*	*Gage 2*	*Gage 3*
2-18	-0.15	-0.16	-0.17	16.69	16.23	16.14	0.54	0.60	0.62	3.50	3.53	3.56
2-19	-0.16	-0.17	-0.19	16.71	16.28	16.14	0.56	0.60	0.62	3.60	3.61	3.65
2-20	-0.16	-0.18	-0.20	16.72	16.28	16.14	0.54	0.59	0.61	3.57	3.57	3.60
2-21	-0.17	-0.19	-0.20	16.83	16.38	16.25	0.55	0.60	0.63	3.57	3.55	3.59
2-22	-0.15	-0.17	-0.19	16.82	16.35	16.23	0.56	0.59	0.61	3.64	3.59	3.64
2-23	-0.16	-0.17	-0.18	16.76	16.32	16.21	0.55	0.60	0.62	3.61	3.56	3.61
2-24	-0.16	-0.17	-0.18	16.87	16.37	16.24	0.57	0.60	0.62	3.65	3.58	3.63
2-25	-0.16	-0.17	-0.18	16.79	16.35	16.23	0.55	0.60	0.64	3.60	3.58	3.64
2-26	-0.16	-0.17	-0.18	16.79	16.34	16.20	0.55	0.60	0.62	3.58	3.57	3.61
2-27	-0.16	-0.17	-0.17	16.88	16.43	16.29	0.54	0.62	0.64	3.55	3.60	3.64
2-28	-0.15	-0.16	-0.17	16.78	16.39	16.24	0.55	0.60	0.62	3.58	3.59	3.63
2-29	-0.15	-0.16	-0.16	16.79	16.36	16.25	0.56	0.59	0.62	3.57	3.56	3.61
2-30	-0.16	-0.16	-0.17	16.85	16.43	16.28	0.54	0.61	0.62	3.57	3.58	3.61
2-31	-0.15	-0.16	-0.16	16.87	16.38	16.25	0.55	0.60	0.63	3.58	3.55	3.62
2-32	-0.15	-0.15	-0.16	16.84	16.36	16.23	0.55	0.59	0.61	3.61	3.59	3.62
2-33	-0.15	-0.15	-0.15	16.81	16.40	16.26	0.55	0.60	0.62	3.60	3.57	3.60
2-34	-0.15	-0.15	-0.15	16.89	16.43	16.30	0.56	0.61	0.63	3.58	3.55	3.59
2-35	-0.23	-0.27	-0.42	16.76	16.34	16.21	0.58	0.58	0.59	3.80	3.71	3.78
2-36	-0.22	-0.26	-0.43	16.86	16.48	16.30	0.60	0.61	0.62	3.87	3.79	3.84
Mean	-0.16	-0.18	-0.19	16.81	16.36	16.23	0.56	0.60	0.62	3.61	3.59	3.64
Max	-0.15	-0.15	-0.15	16.89	16.48	16.30	0.60	0.62	0.64	3.87	3.79	3.84
Min	-0.23	-0.27	-0.43	16.69	16.23	16.14	0.54	0.58	0.59	3.50	3.53	3.56

Table 3.16: $\overline{\eta}$, H_{rms}, Skewness, and Kurtosis for Free Surface Test 3

	Setup, $\overline{\eta}$*(cm)*			H_{rms}*(cm)*			*Skewness s*			*Kurtosis K*		
Run	*Gage 1*	*Gage 2*	*Gage 3*	*Gage 1*	*Gage 2*	*Gage 3*	*Gage 1*	*Gage 2*	*Gage 3*	*Gage 1*	*Gage 2*	*Gage 3*
3-1	-0.22	-0.29	-0.27	18.35	18.09	18.22	0.43	0.50	0.53	2.99	3.19	3.26
3-2	-0.23	-0.30	-0.28	18.40	18.12	18.26	0.44	0.51	0.55	3.02	3.25	3.31
3-3	-0.24	-0.31	-0.29	18.40	18.10	18.25	0.43	0.51	0.54	3.01	3.23	3.30
3-4	-0.25	-0.32	-0.29	18.40	18.17	18.30	0.43	0.51	0.54	2.99	3.23	3.29
3-5	-0.26	-0.32	-0.29	18.39	18.14	18.30	0.42	0.50	0.53	2.96	3.20	3.28
3-6	-0.26	-0.33	-0.30	18.43	18.19	18.35	0.42	0.50	0.53	2.99	3.23	3.28
3-7	-0.27	-0.33	-0.29	18.40	18.16	18.32	0.42	0.50	0.54	2.98	3.23	3.32
3-8	-0.27	-0.33	-0.30	18.38	18.19	18.33	0.42	0.51	0.54	2.98	3.22	3.29
3-9	-0.22	-0.29	-0.26	18.38	18.14	18.26	0.43	0.51	0.53	2.99	3.26	3.29
3-10	-0.23	-0.29	-0.26	18.35	18.09	18.23	0.42	0.49	0.53	2.95	3.18	3.27
3-11	-0.24	-0.29	-0.26	18.37	18.15	18.29	0.42	0.50	0.52	2.95	3.21	3.27
3-12	-0.23	-0.29	-0.26	18.40	18.16	18.31	0.41	0.49	0.52	2.95	3.19	3.29
3-13	-0.23	-0.28	-0.25	18.43	18.19	18.31	0.41	0.50	0.53	2.97	3.20	3.26
3-14	-0.23	-0.28	-0.25	18.40	18.18	18.30	0.42	0.52	0.53	2.97	3.23	3.28
3-15	-0.23	-0.28	-0.24	18.41	18.16	18.30	0.42	0.50	0.53	2.97	3.24	3.29
3-16	-0.22	-0.28	-0.24	18.47	18.22	18.36	0.42	0.51	0.54	2.99	3.27	3.33
3-17	-0.23	-0.28	-0.24	18.42	18.20	18.34	0.42	0.50	0.54	2.97	3.23	3.31
Mean	-0.24	-0.30	-0.27	18.40	18.16	18.30	0.42	0.50	0.53	2.98	3.22	3.29
Max	-0.22	-0.28	-0.24	18.47	18.22	18.36	0.44	0.52	0.55	3.02	3.27	3.33
Min	-0.27	-0.33	-0.30	18.35	18.09	18.22	0.41	0.49	0.52	2.95	3.18	3.26

Table 3.17: $\overline{\eta}$, H_{rms}, Skewness, and Kurtosis for Velocity Test 3

	Setup, $\overline{\eta}$*(cm)*			H_{rms}*(cm)*			*Skewness s*			*Kurtosis K*		
Run	*Gage 1*	*Gage 2*	*Gage 3*	*Gage 1*	*Gage 2*	*Gage 3*	*Gage 1*	*Gage 2*	*Gage 3*	*Gage 1*	*Gage 2*	*Gage 3*
3-18	-0.60	-0.37	-0.40	18.27	17.95	17.75	0.40	0.46	0.47	2.97	3.16	3.20
3-19	-0.60	-0.38	-0.40	18.24	17.90	17.72	0.40	0.46	0.47	2.98	3.15	3.22
3-20	-0.60	-0.38	-0.39	18.26	17.95	17.71	0.40	0.46	0.46	2.96	3.16	3.18
3-21	-0.60	-0.38	-0.39	18.30	17.96	17.77	0.39	0.45	0.47	2.96	3.15	3.21
3-22	-0.61	-0.40	-0.40	18.28	17.98	17.77	0.39	0.45	0.47	2.96	3.14	3.18
3-23	-0.61	-0.40	-0.42	18.28	18.02	17.78	0.39	0.47	0.48	2.97	3.17	3.21
3-24	-0.62	-0.40	-0.42	18.27	17.95	17.77	0.40	0.46	0.48	2.97	3.14	3.20
3-25	-0.63	-0.40	-0.42	18.26	17.96	17.75	0.40	0.46	0.47	2.98	3.14	3.17
3-26	-0.63	-0.40	-0.42	18.25	17.97	17.75	0.40	0.46	0.47	2.97	3.16	3.19
3-27	-0.64	-0.41	-0.44	18.30	17.97	17.77	0.40	0.47	0.47	3.00	3.17	3.21
3-28	-0.64	-0.42	-0.44	18.31	17.99	17.78	0.40	0.46	0.47	2.97	3.17	3.21
3-29	-0.65	-0.43	-0.45	18.27	18.00	17.80	0.38	0.45	0.47	2.95	3.14	3.20
3-30	-0.65	-0.43	-0.45	18.28	18.01	17.82	0.39	0.45	0.47	2.96	3.15	3.21
3-31	-0.66	-0.44	-0.46	18.31	18.01	17.81	0.39	0.46	0.47	2.95	3.16	3.20
3-32	-0.66	-0.44	-0.46	18.28	18.01	17.83	0.39	0.46	0.47	2.95	3.16	3.20
3-33	-0.67	-0.45	-0.47	18.29	18.07	17.86	0.39	0.46	0.47	2.96	3.15	3.22
3-34	-0.66	-0.45	-0.47	18.30	18.03	17.82	0.39	0.45	0.46	2.96	3.12	3.17
3-35	-0.32	-0.36	-0.58	18.10	17.93	18.24	0.38	0.44	0.40	3.09	3.27	3.45
3-36	-0.33	-0.37	-0.58	18.08	17.92	18.19	0.37	0.45	0.45	3.05	3.28	3.34
Mean	-0.60	-0.41	-0.45	18.25	17.97	17.83	0.39	0.46	0.47	2.98	3.16	3.22
Max	-0.32	-0.36	-0.39	18.31	18.07	18.24	0.40	0.47	0.48	3.09	3.28	3.45
Min	-0.67	-0.45	-0.58	18.08	17.92	17.71	0.37	0.44	0.40	2.95	3.14	3.17

Chapter 4

FREE SURFACE ELEVATIONS

The wave setup $\overline{\eta}$, the standard derivation σ, the skewness s, and the kurtosis K for each of the measured time series of the free surface elevation, η, of the 325 s duration sampled at the rate of 20 Hz are computed under the assumption of equivalency of probabilistic and time averaging. These time series include the effects of reflected waves. The root-mean-square wave height H_{rms} is obtained using equation (2.8). The normalized free surface elevation, $\eta_* = (\eta - \overline{\eta})/\sigma$, is then calculated using the measured values of $\overline{\eta}$ and σ. For each of the time series of η_*, the probability density function, $f(\eta_*)$, is computed using 20 bins in the range determined by the measured maximum and minimum values of η_*.

4.1 Probability Density Functions for Gages 1–3 for Tests 1–3

Figure 4.1 shows the measured probability density functions at wave gages 1–3 for the 17 runs in free surface tests 1–3. The exponential gamma distribution, $f(\eta_*)$, given by equation (2.1) is also plotted in Figure 4.1 for the measured minimum and maximum values of s for each test. The ordinate for the figures plotted for $f(\eta_*)$ is the normalized free surface elevation η_* varying vertically. Figure 4.1 is another indicator of the degree of repeatability for the 17 runs in each test, as the different runs for each test set are virtually indistinguishable. It is noted that separate figures for each wave gage indicate slightly better repeatability. The exponential gamma distribution changes little for the measured range of s for each test and is in good

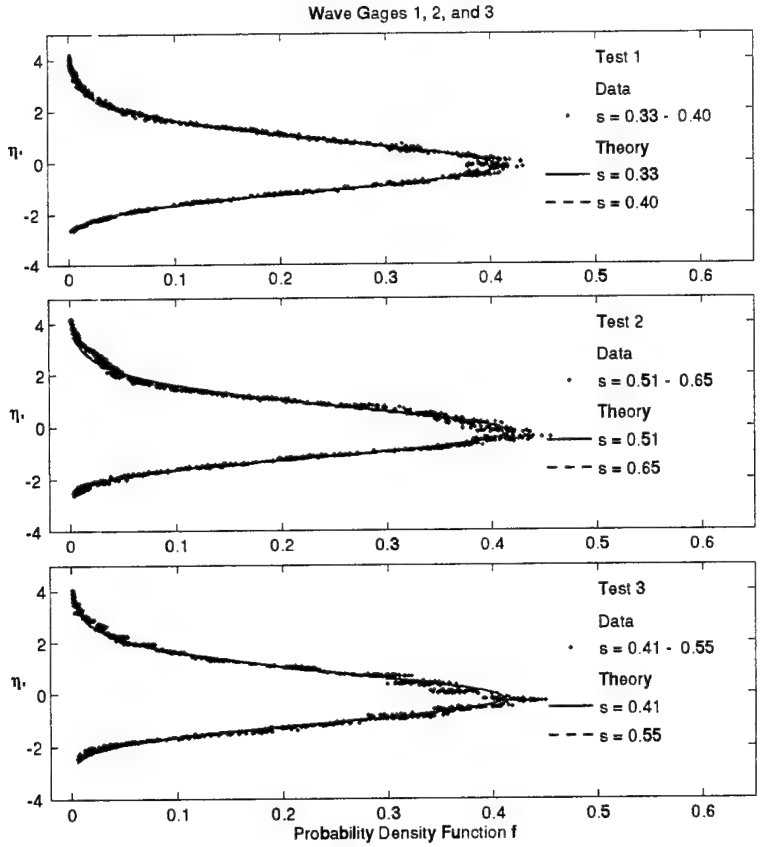

Figure 4.1: Measured and Computed Probability Distributions for 17 Runs at Wave Gages 1–3 for Test Sets 1–3

agreement with the measured distributions except for the scatter of data points at the peak of $f(\eta_*)$.

4.2 Spacial Variations of Statistical Values in Free Surface Elevations

The measured cross-shore variations of $\overline{\eta}$, $H_{\rm rms}/\overline{h}$, and s for tests 1–3 are shown in Figures 4.2 – 4.4, where the horizontal coordinate $x = 0$ at the still water depth $d = 75$ cm. The mean water depth $\overline{h}$ is given by $\overline{h} = (\overline{\eta} - z_b)$ where the bottom elevation z_b corresponding to the 1:16 slope is indicated by the solid line in these figures to show that the wave setup $\overline{\eta}$ becomes tangential to the 1:16

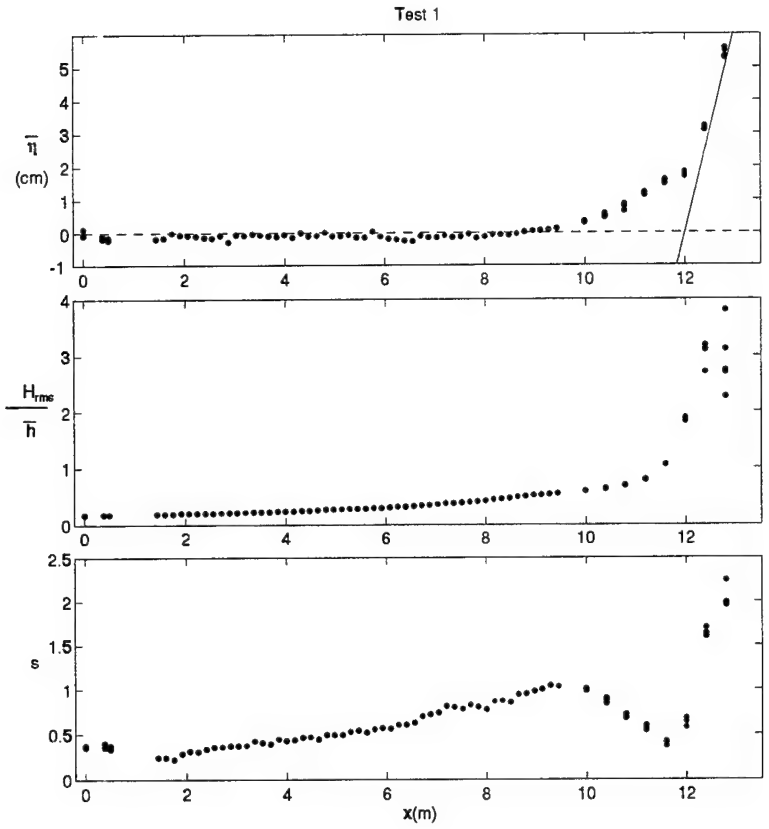

Figure 4.2: Measured Cross-Shore Variations of $\overline{\eta}$, $H_{\rm rms}/\overline{h}$, and s for Test 1

slope. The present data analysis is limited to the region of $\overline{h} \gtrsim 0.4$ cm because the statistical analysis becomes less reliable in the region of extremely small depth affected by infrequent wave uprush and downrush. The values of $\overline{\eta}$, $H_{\rm rms}/\overline{h}$ and s at the locations of wave gages 1–3 are plotted for all 17 runs in each test. The data from the repeated measurements at the locations of the gage wells are plotted individually without averaging to indicate that the visible scatter of data points is limited to the swash zone.

The measured values of $H_{\rm rms}/\overline{h}$ in Figures 4.2 – 4.4 show a gradual increase and then rise rapidly near the still water shoreline. The gradual landward increase of $H_{\rm rms}/\overline{h}$ is mostly caused by the landward decrease of $\overline{h}$ where the measured values

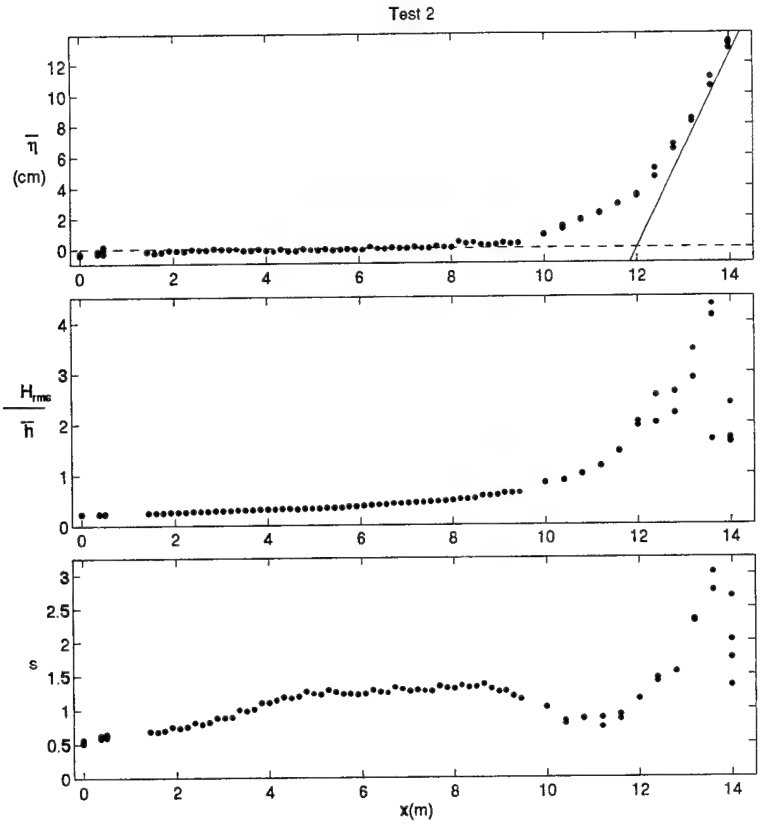

Figure 4.3: Measured Cross-Shore Variations of $\overline{\eta}$, $H_{\text{rms}}/\overline{h}$, and s for Test 2

of H_{rms} are approximately constant in the shoaling zone and decrease gradually in the surf and swash zones. The measured values of $H_{\text{rms}}/\overline{h}$ on the 1:16 slope do not approach constant in the inner surf zone, unlike the field data on gently sloping concave beaches obtained by Thornton and Guza (1982, 1983). The measured values of $H_{\text{rms}}/\overline{h}$ approach the intuitive upper limit of $H_{\text{rms}}/\overline{h} = \sqrt{8}$ in the swash zone predicted by equation (2.7) with (2.8), although, the exact upper limit is difficult to pinpoint because of the rapid increase and scatter of $H_{\text{rms}}/\overline{h}$ as $\overline{h}$ approaches zero. This implies that the landward decrease of H_{rms} is more gradual than that of $\overline{h}$ in the swash zone.

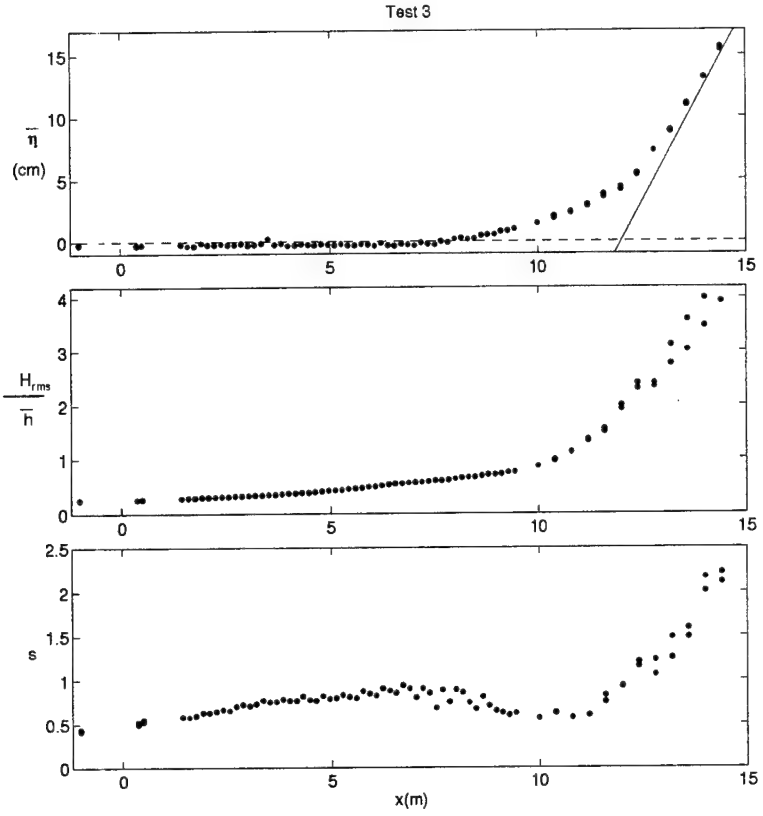

Figure 4.4: Measured Cross-Shore Variations of $\overline{\eta}$, $H_{\text{rms}}/\overline{h}$, and s for Test 3

Figures 4.2 – 4.4 show that the skewness s increases landward and then decreases toward the still water shoreline as expected from available data [e.g., Mase and Kobayashi (1991); Raubenheimer *et al.* (1995)]. However, the skewness increases again in the swash zone and approaches the upper limit of $s = 2$ corresponding to the exponential distribution given by equation (2.6). This upper limit of $s = 2$ may not be very accurate but implies that the probability distribution of the free surface elevation is strongly affected by the bottom elevation. It is also noted that the detailed cross-shore variations of s are noticeably different for the three tests whose incident wave characteristics are listed in Table 3.4. Complete listings of the data points plotted in these figures can be found in Tables A.1 – A.3 in Appendix

A.

4.3 Measured and Theoretical Probability Density Functions

The measured probability density function of η_* in the region of $d \leq 66$ cm was compared individually with the exponential gamma distribution given by equation (2.1) together with the measured value of s. The agreement was good in the shoaling and surf zones, and fair in the swash zone. Figures 4.5 – 4.7 show the degree of the overall agreement for tests 1–3, respectively. The region of $d \leq 66$ cm

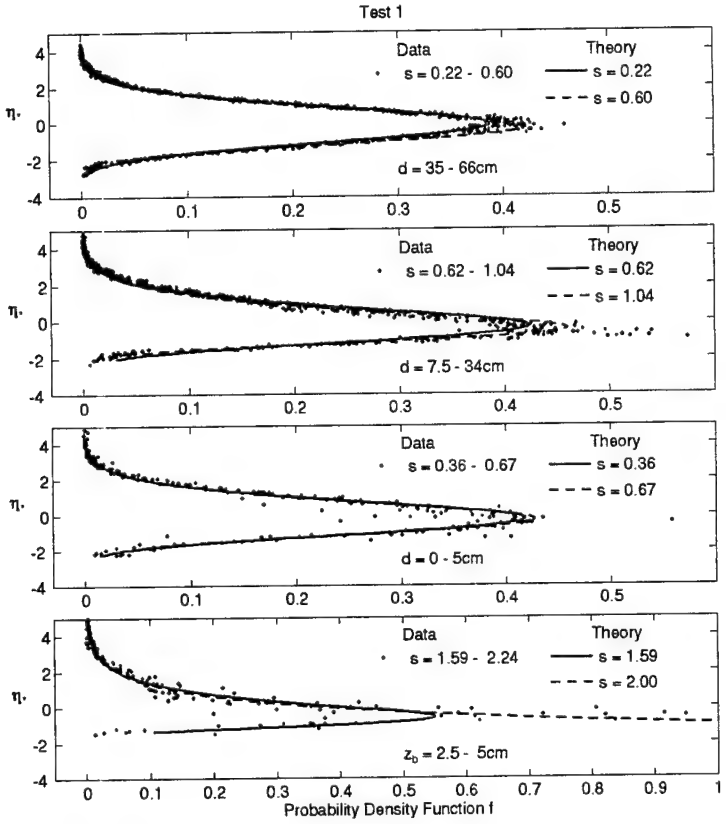

Figure 4.5: Measured and Computed Probability Distributions in Four Zones for Test 1

is separated into four zones for each test on the basis of the cross-shore variations

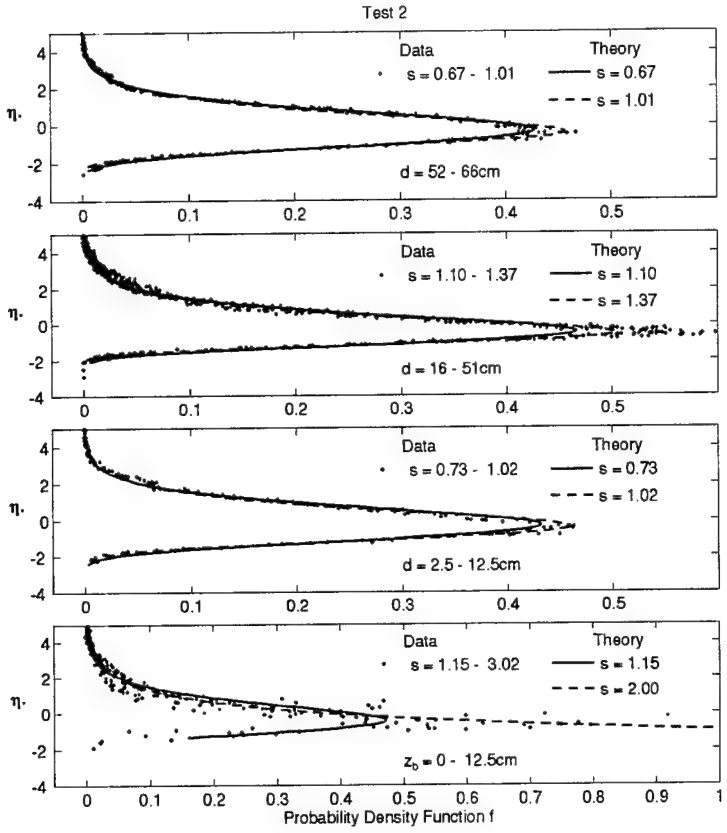

Figure 4.6: Measured and Computed Probability Distributions in Four Zones for Test 2

of s shown in Figures 4.2 – 4.4. The four zones roughly correspond to the landward increase zone of little wave breaking, the peak zone of intense wave breaking, the trough zone seaward of the still water shoreline, and the rapid increase zone above the still water shoreline. Figures 4.5 – 4.7 indicate the range of the still water depth d or the bottom elevation z_b above SWL for each zone where $d = -z_b$. The measured minimum and maximum values of s in each zone are indicated in these figures. The exponential gamma distributions based on these minimum and maximum values of s are plotted for each zone so that the data points would fall between the two theoretical curves if the agreement were perfect. In the swash zone, the exponential gamma

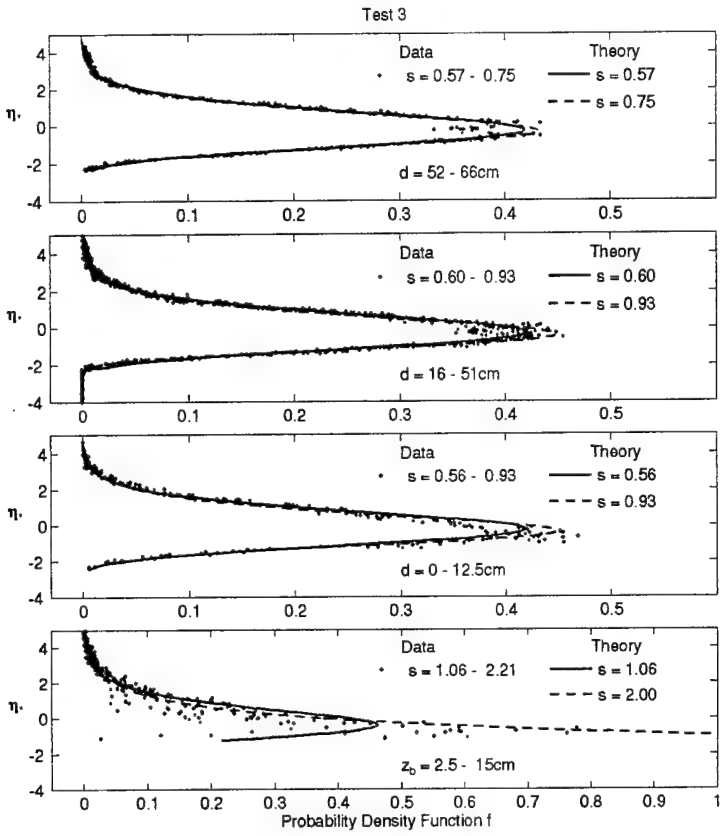

Figure 4.7: Measured and Computed Probability Distributions in Four Zones for Test 3

distribution is limited by the exponential distribution with $s = 2$ given by equation (2.6). In the rapid increase zone above the still water shoreline, the agreement is better for the large values of η_* corresponding to the large free surface elevations. This is partialy because the theoretical distributions for the large values of η_* are not very sensitive to the skewness, s. In addition, the free surface measurements landward of the still water shoreline are less accurate when a thin layer of water remains on the 1:16 slope. Separate figures for each wave gage are plotted in Figures 4.9 – 4.55, and indicate even better agreement. In these figures, each gage position is plotted separately. In the area where $d \leq 12.5$ cm, repeated tests are plotted

together.

Finally, the measured values of the kurtosis K are compared with the theoretical values of K based on equation (2.4) with (2.3) using the corresponding measured values of s. Figure 4.8 shows all the measured values of $(K-3)$ as a function of s

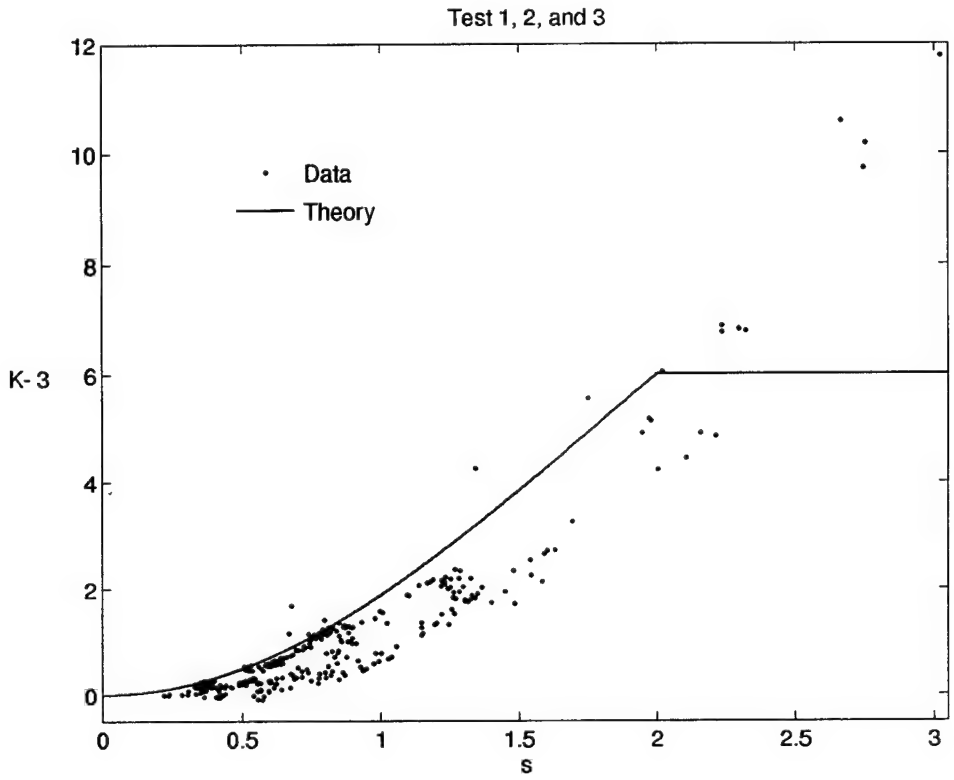

Figure 4.8: Measured and Computed Kurtosis, K, as a Function of Measured Skewness, s

in comparison to the theoretical curve shown in Figure 2.1 where $(K-3)=6$ for $s>2$ is assumed. The relation between K and s based on the exponential gamma distribution tends to overpredict K somewhat for $s<2$ and can not explain the increase of K for $s>2$.

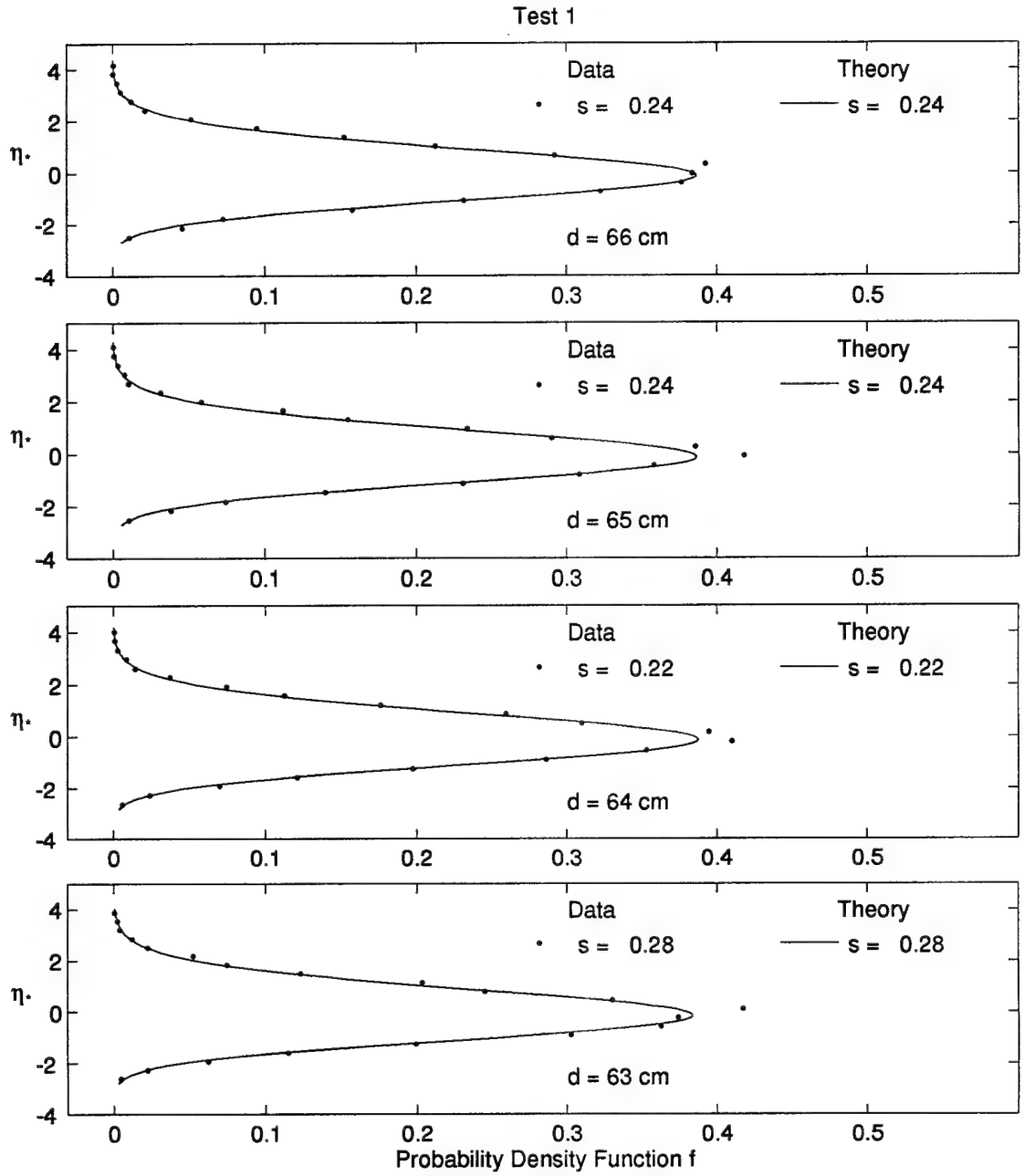

Figure 4.9: Measured and Computed Probability Distributions at Water Depth $d = 66$, 65, 64, and 63cm for Test 1

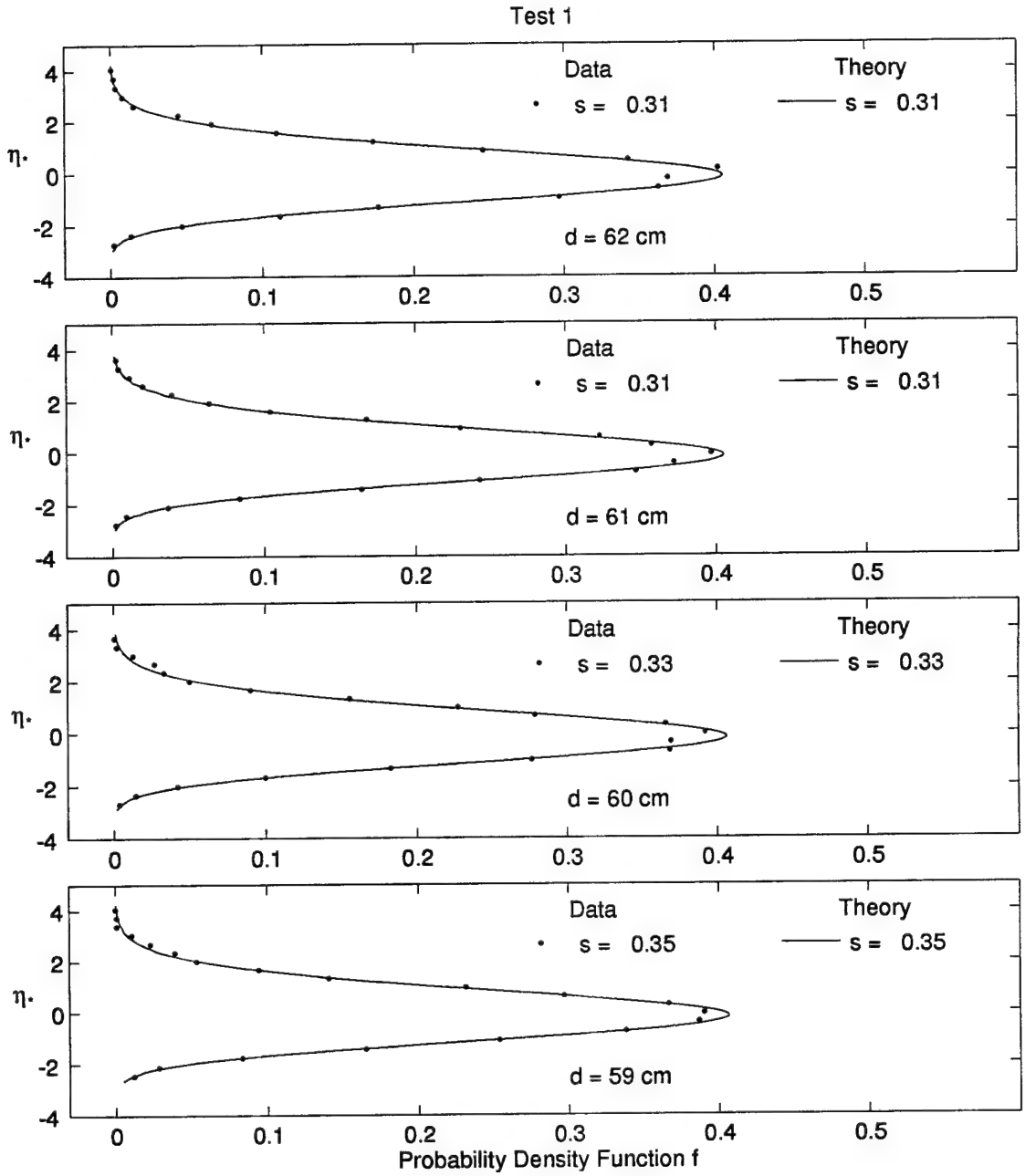

Figure 4.10: Measured and Computed Probability Distributions at Water Depth $d = 62$, 61, 60, and 59cm for Test 1

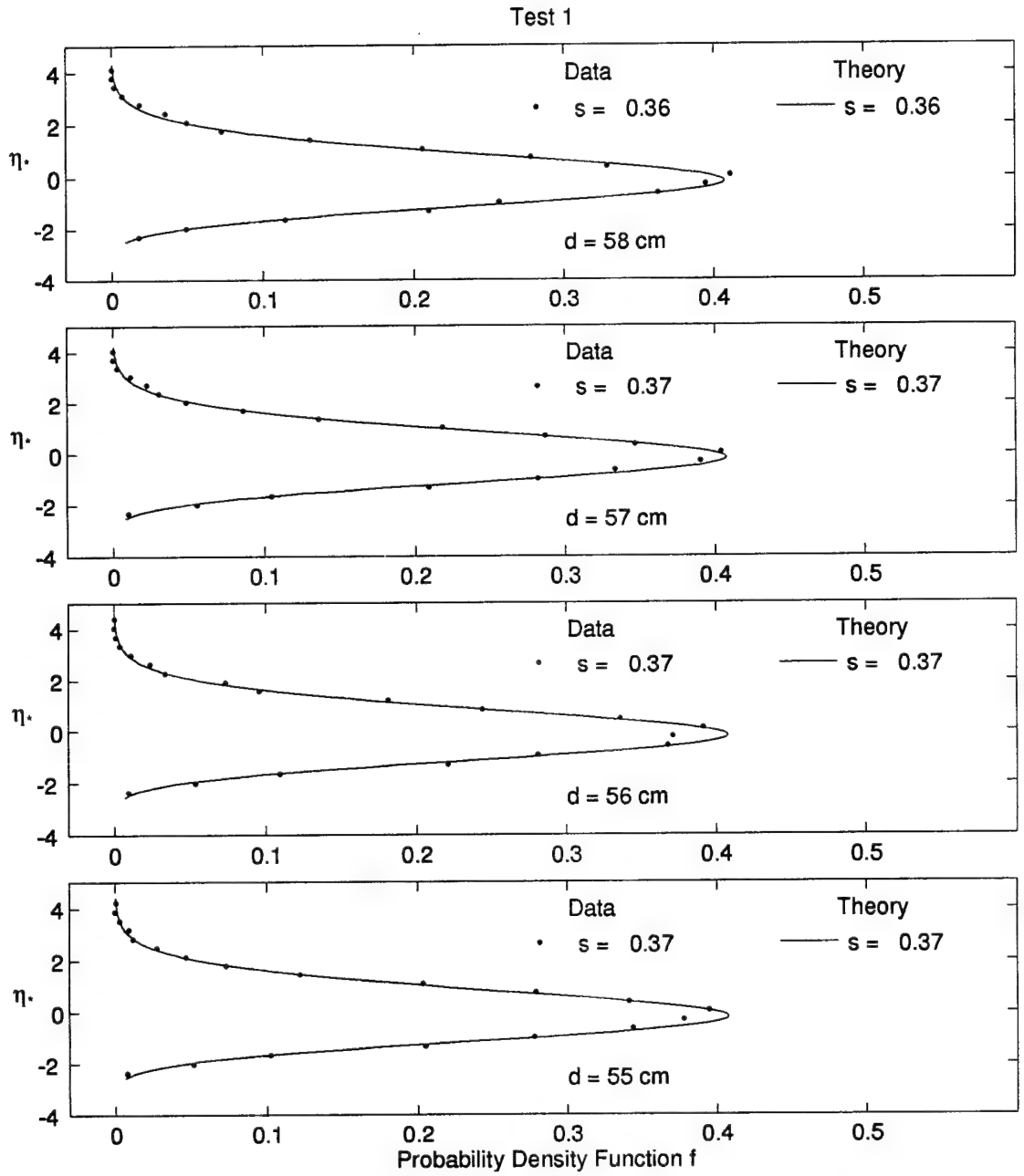

Figure 4.11: Measured and Computed Probability Distributions at Water Depth $d = 58$, 57, 56, and 55cm for Test 1

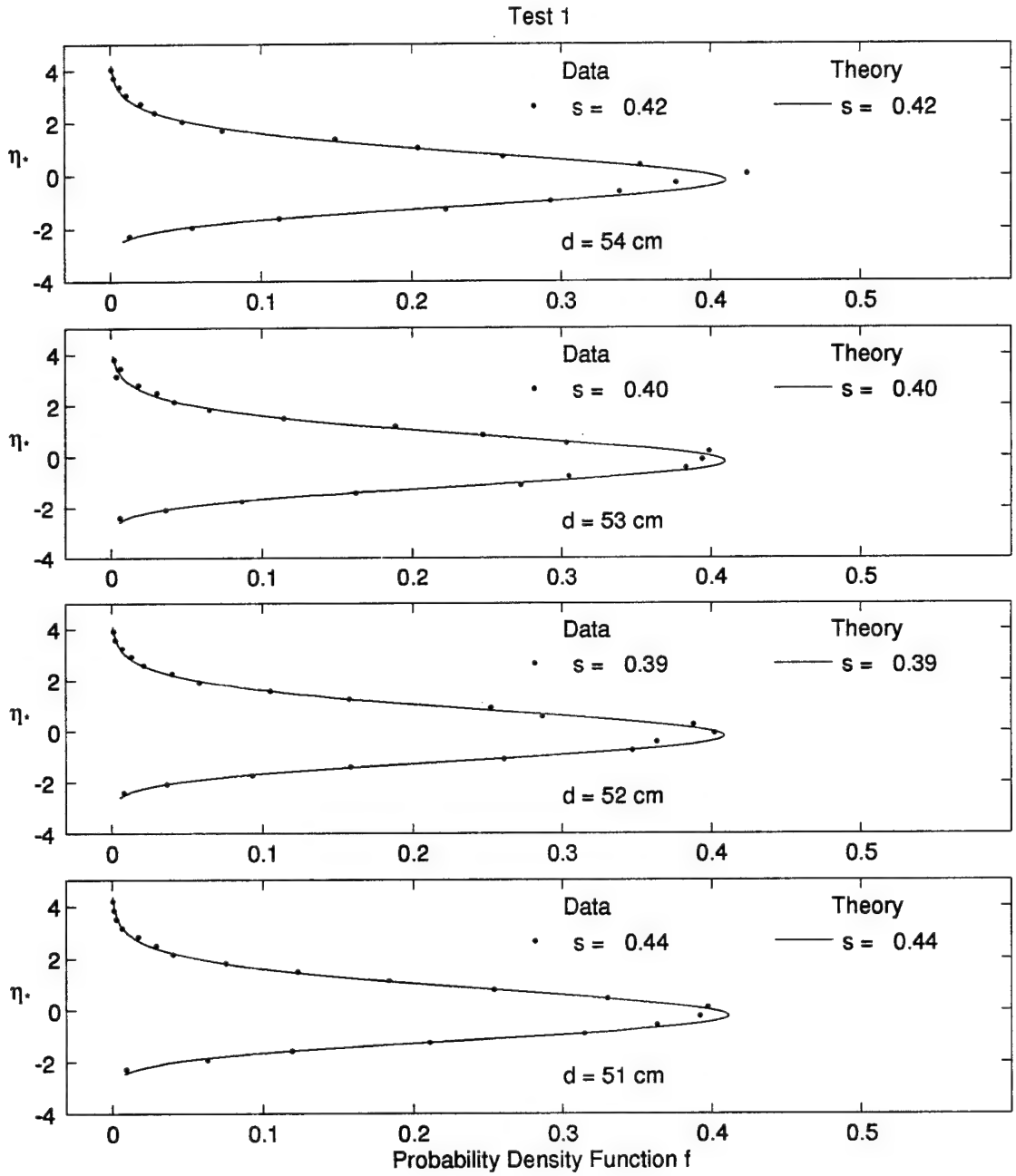

Figure 4.12: Measured and Computed Probability Distributions at Water Depth $d = 54$, 53, 52, and 51cm for Test 1

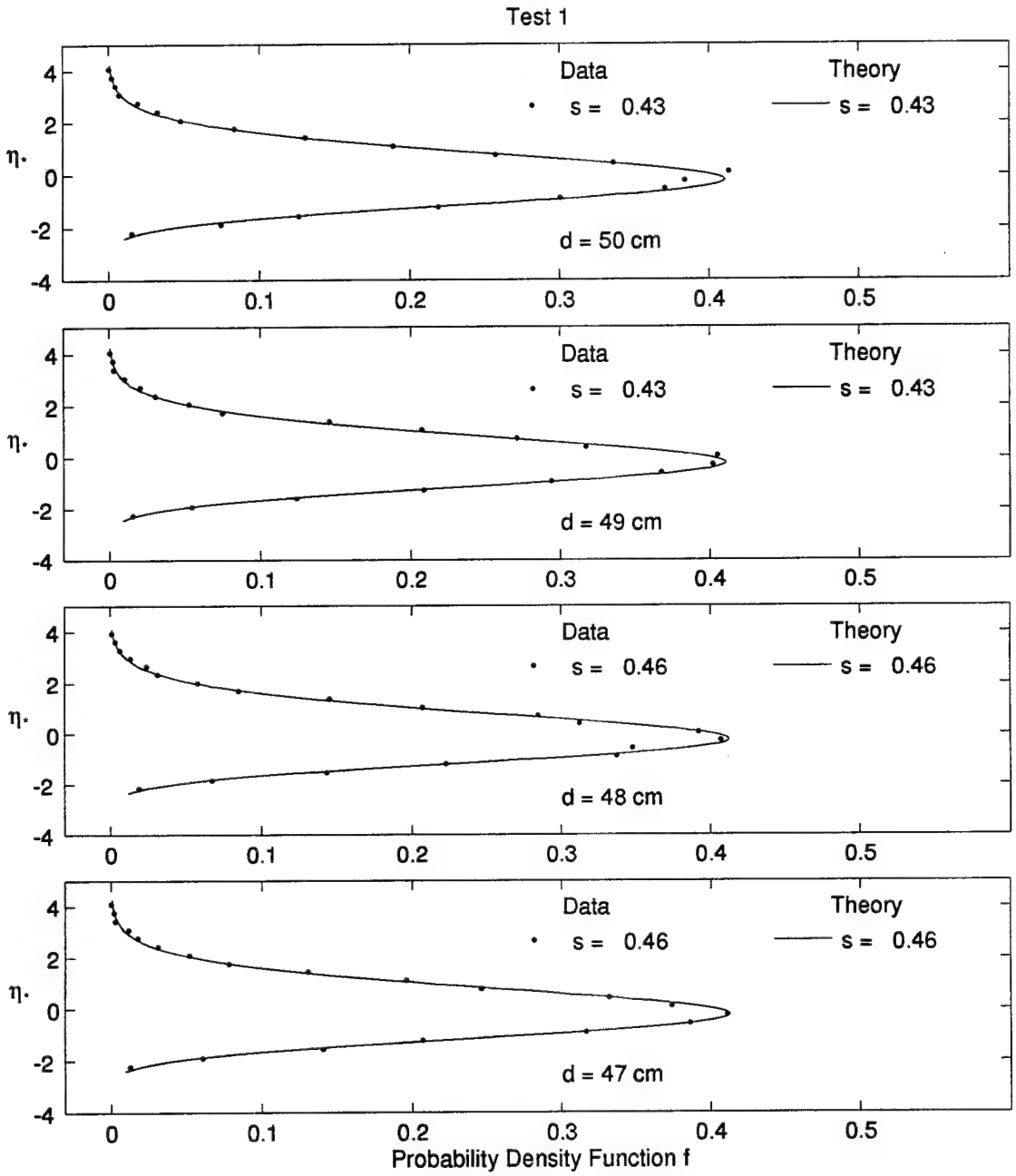

Figure 4.13: Measured and Computed Probability Distributions at Water Depth $d = 50$, 49, 48, and 47cm for Test 1

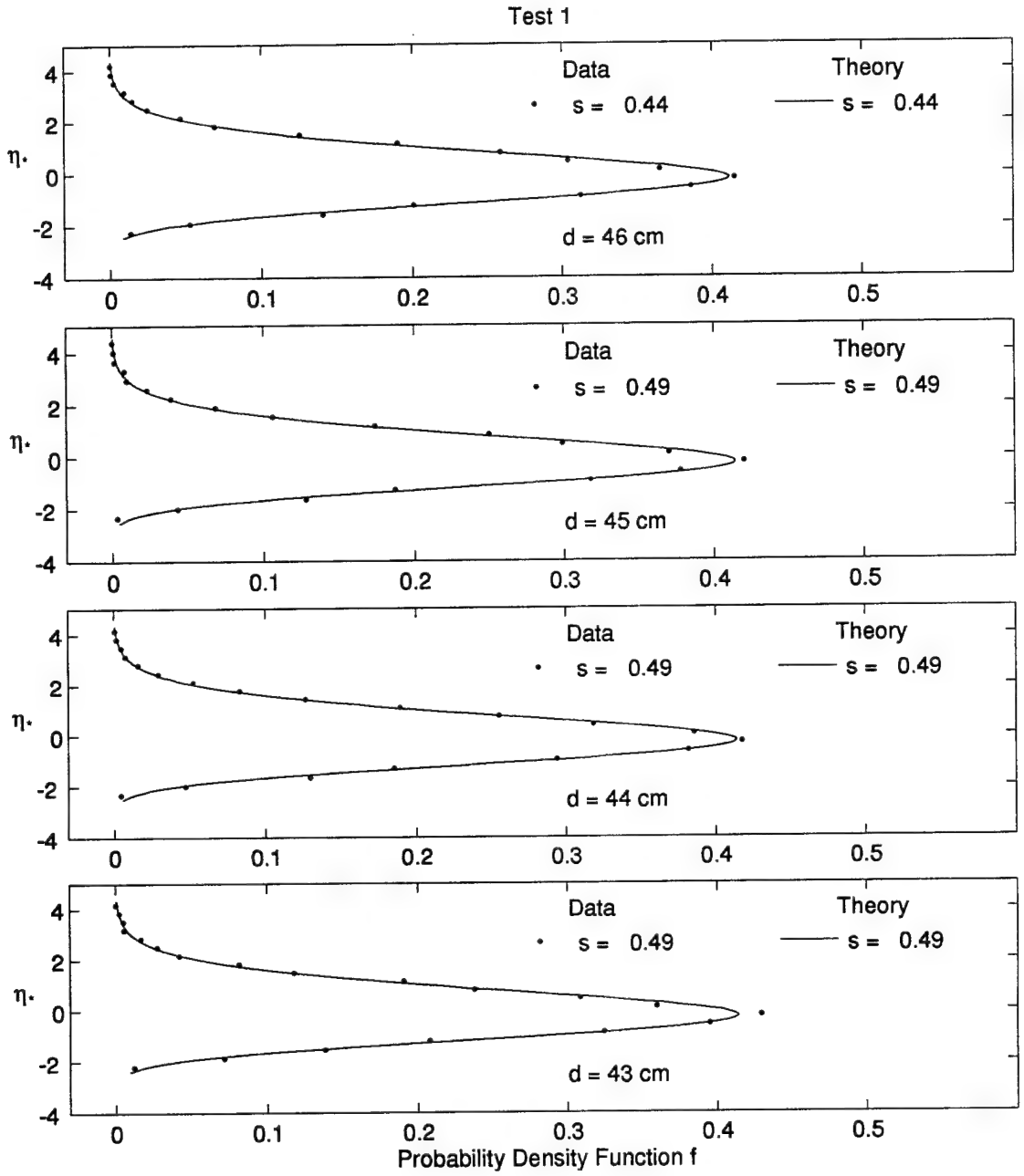

Figure 4.14: Measured and Computed Probability Distributions at Water Depth $d = 46$, 45, 44, and 43cm for Test 1

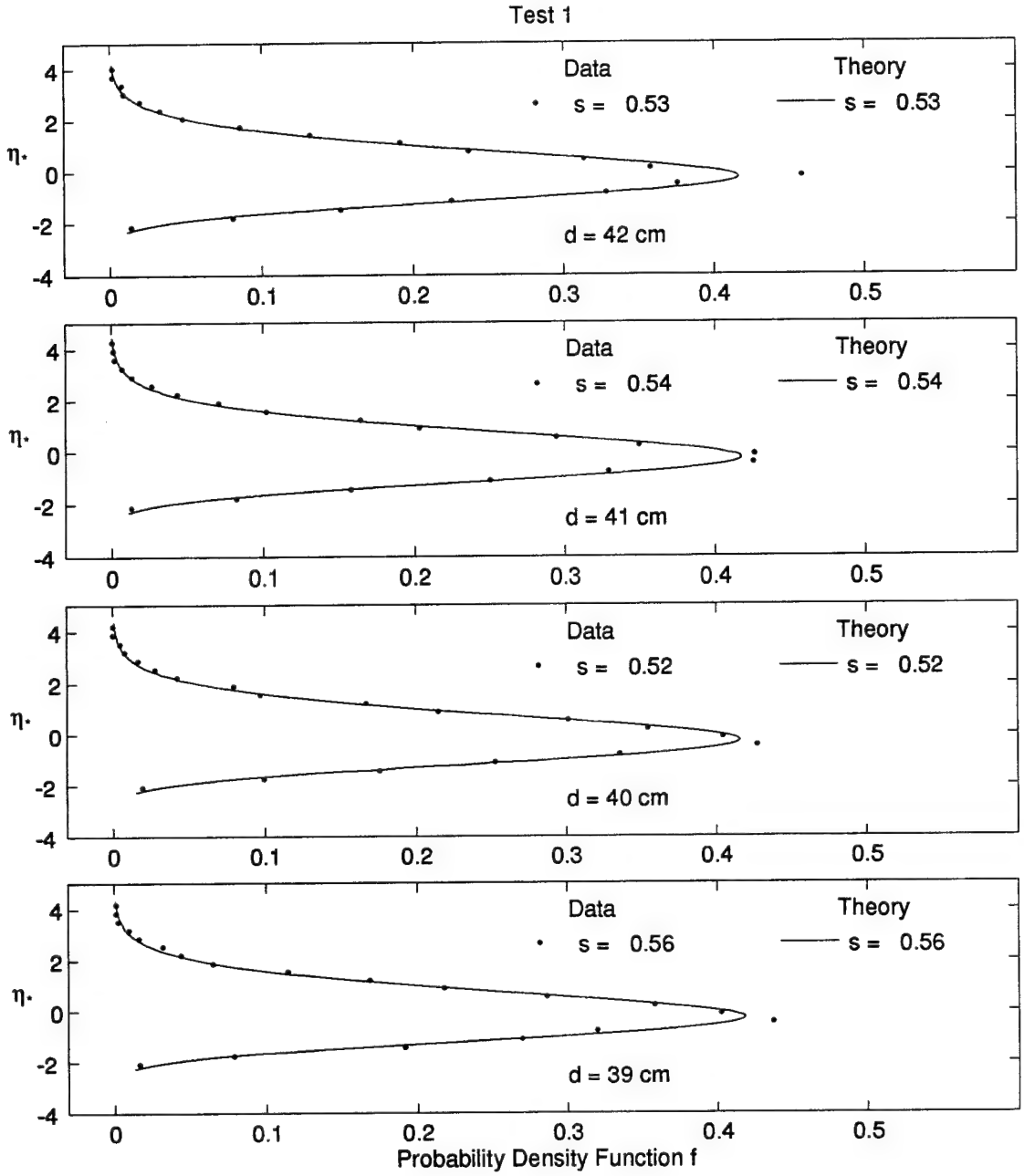

Figure 4.15: Measured and Computed Probability Distributions at Water Depth $d = 42$, 41, 40, and 39cm for Test 1

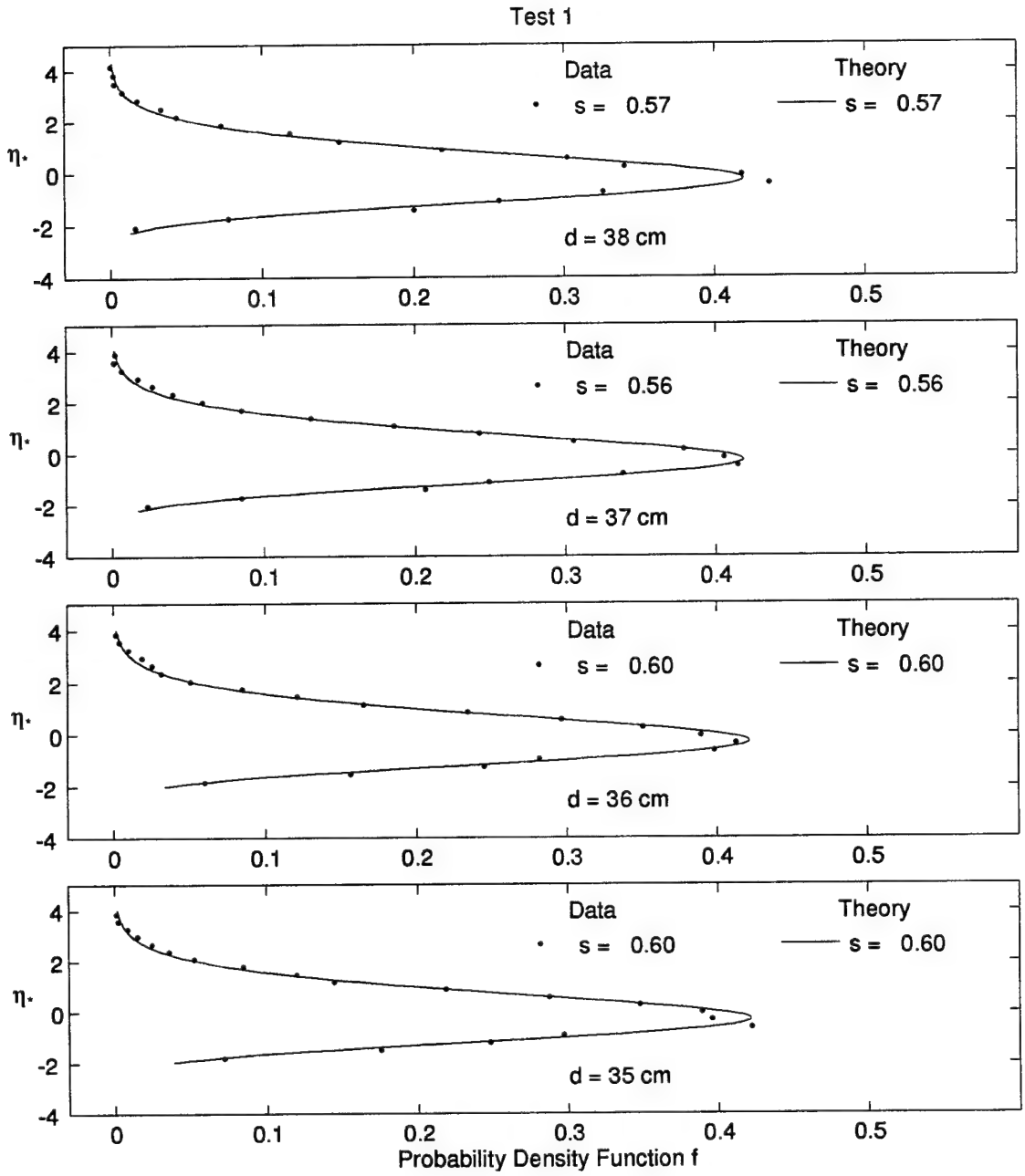

Figure 4.16: Measured and Computed Probability Distributions at Water Depth $d = 38$, 37, 36, and 35cm for Test 1

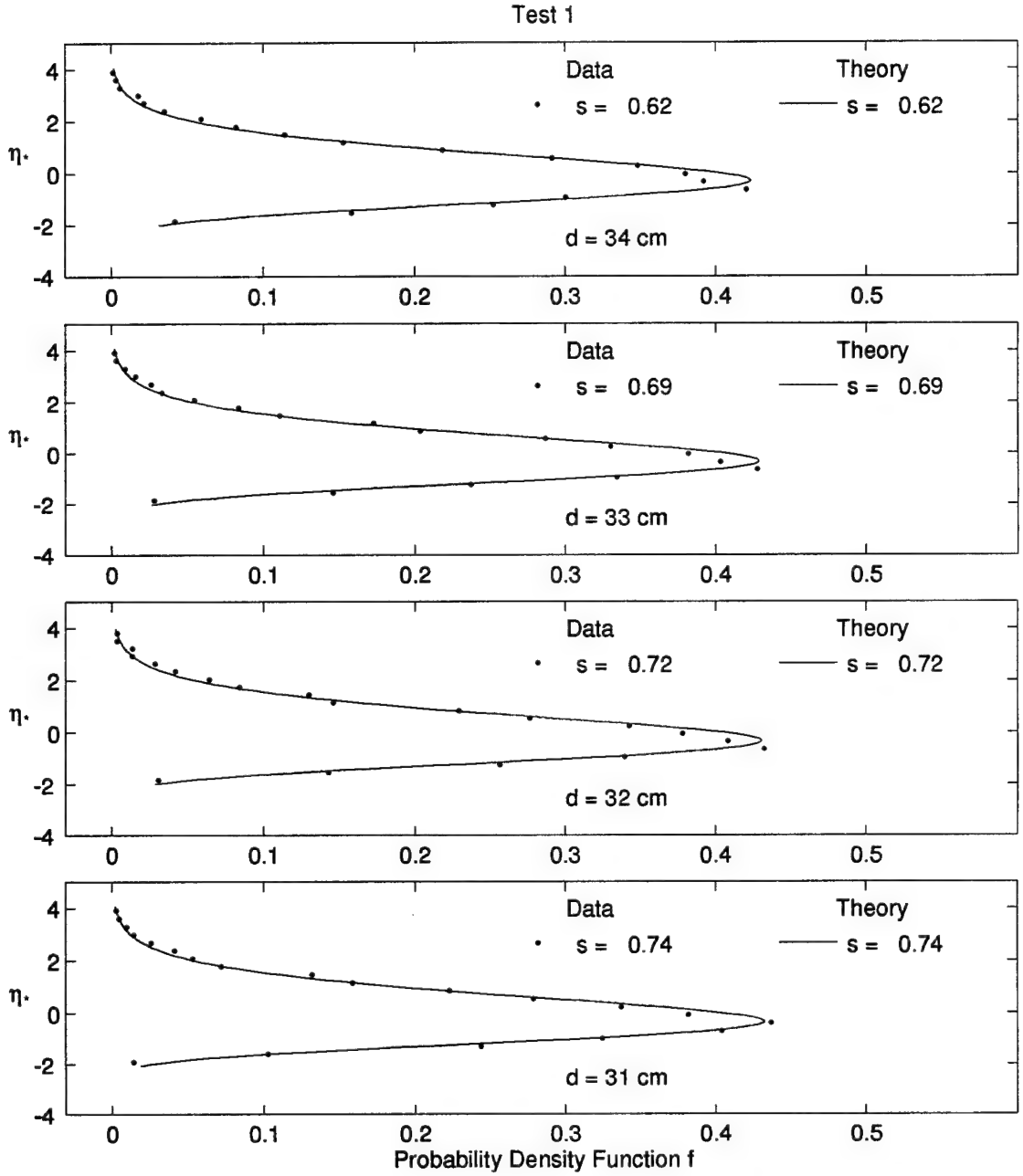

Figure 4.17: Measured and Computed Probability Distributions at Water Depth $d = 34$, 33, 32, and 31cm for Test 1

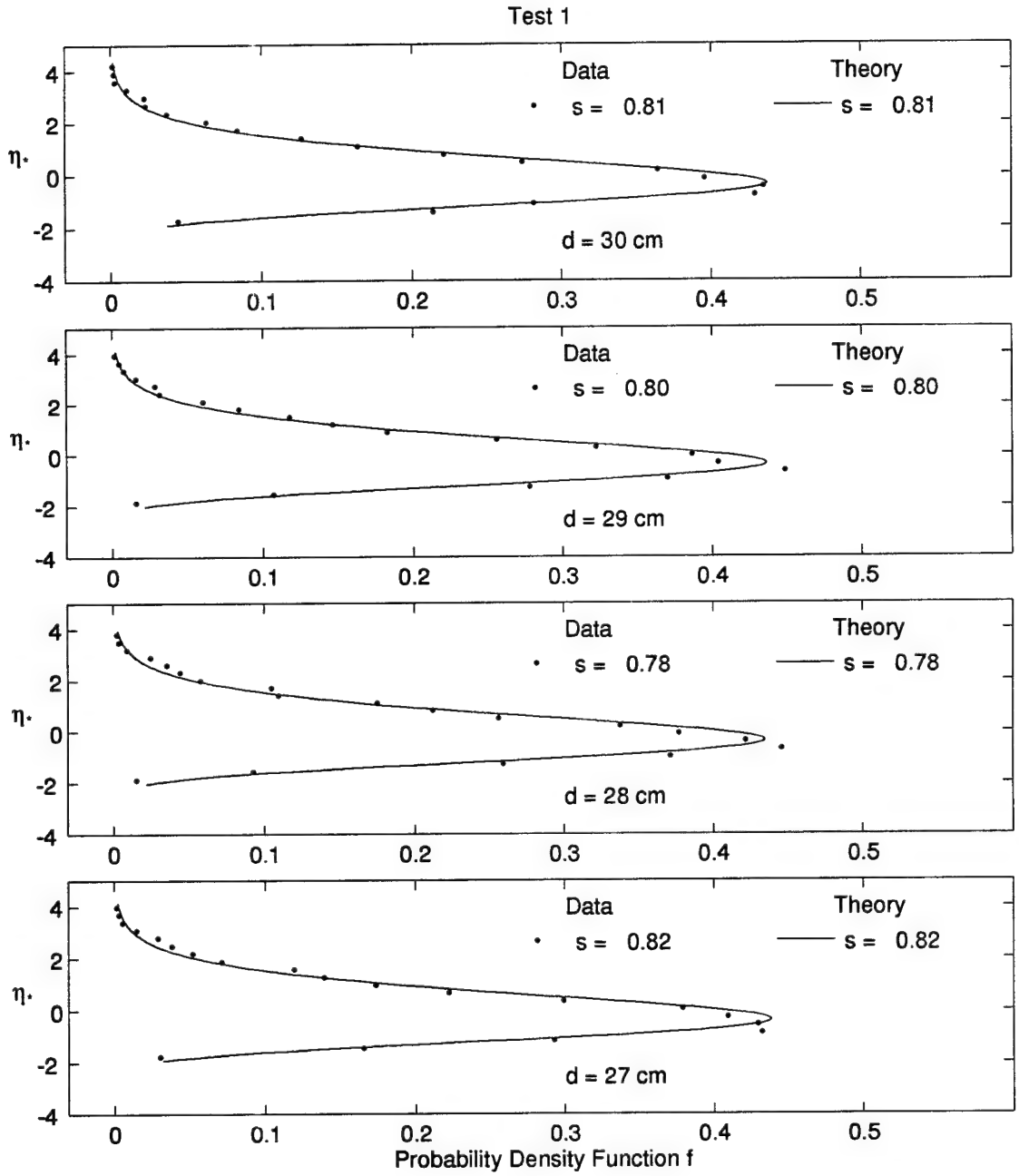

Figure 4.18: Measured and Computed Probability Distributions at Water Depth $d = 30$, 29, 28, and 27cm for Test 1

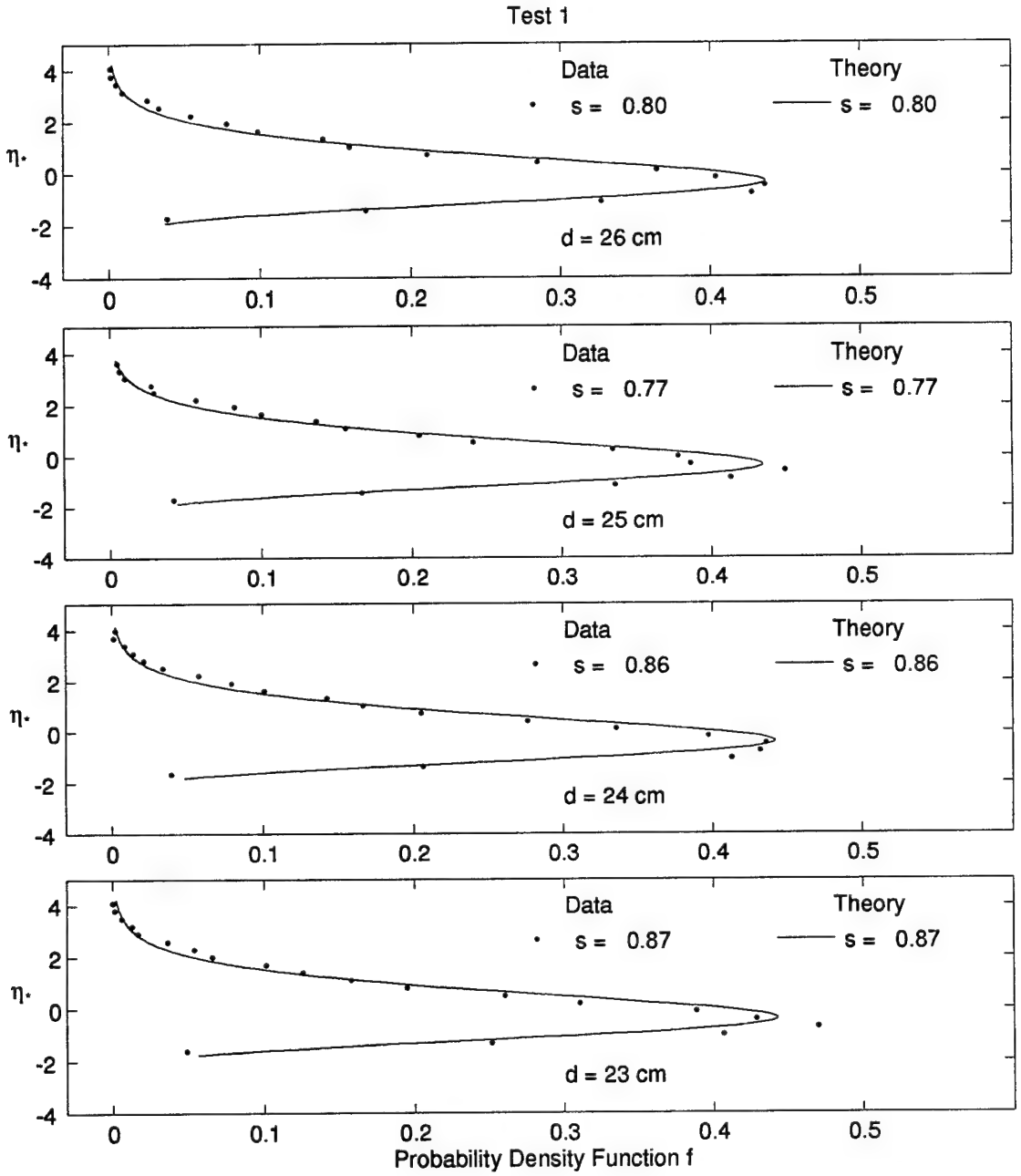

Figure 4.19: Measured and Computed Probability Distributions at Water Depth $d = 26$, 25, 24, and 23cm for Test 1

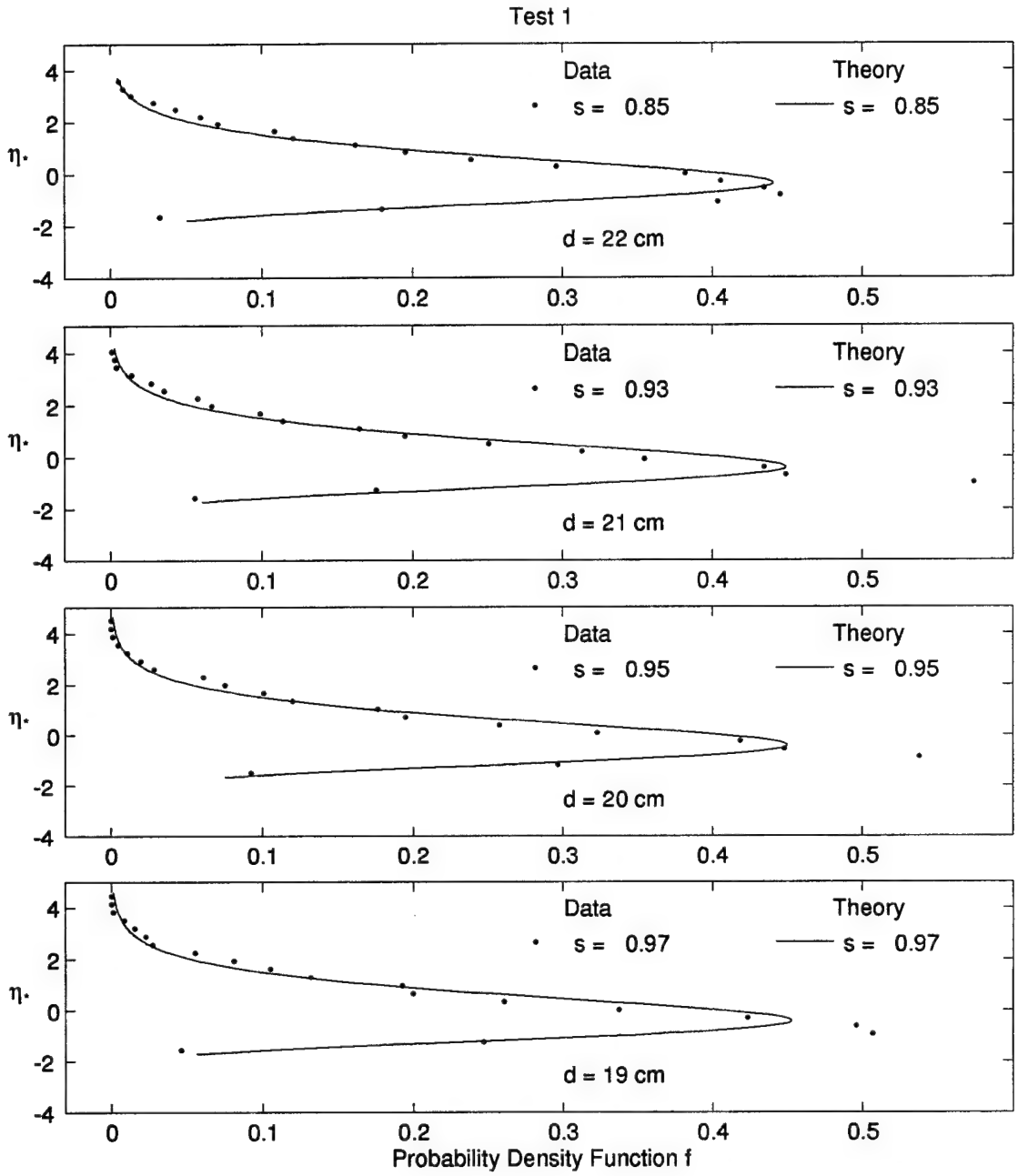

Figure 4.20: Measured and Computed Probability Distributions at Water Depth d = 22, 21, 20, and 19cm for Test 1

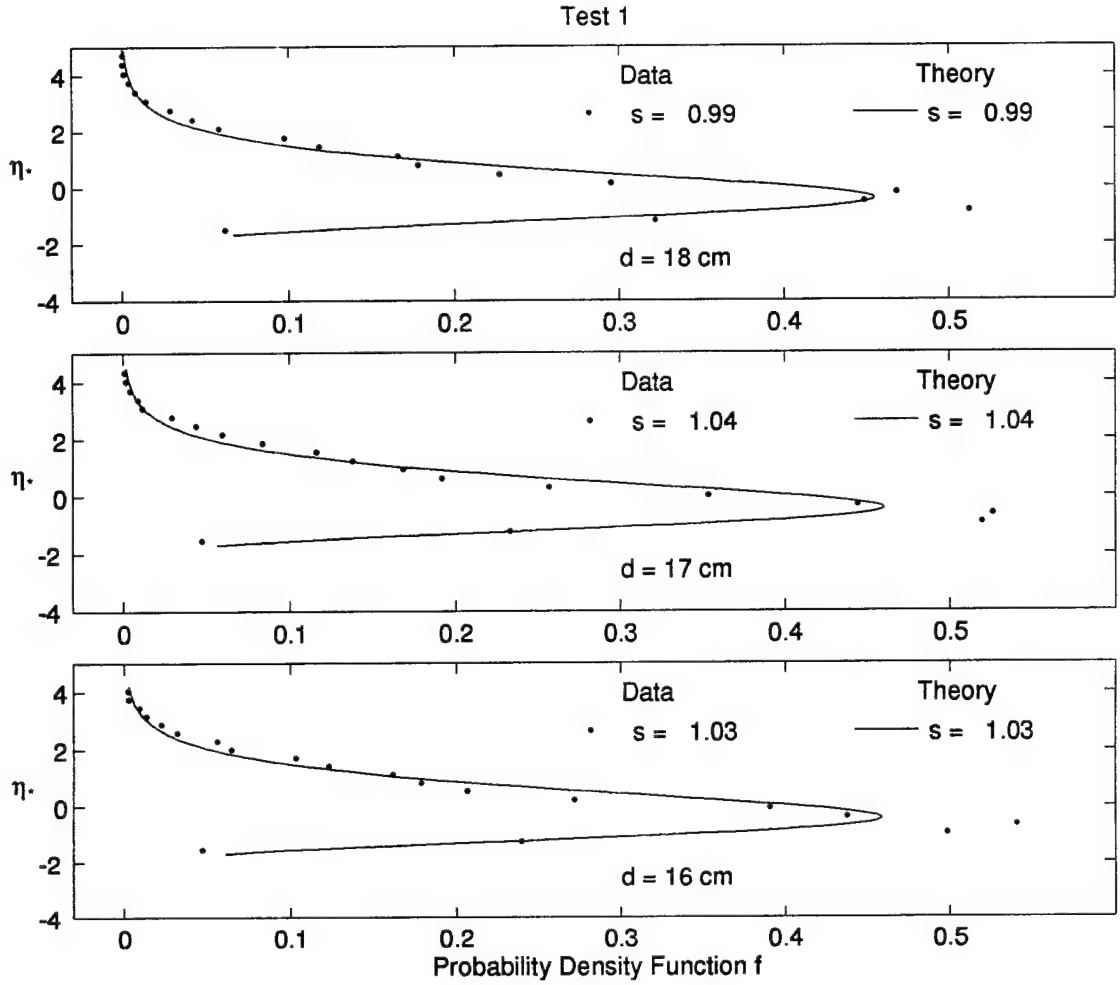

Figure 4.21: Measured and Computed Probability Distributions at Water Depth $d = 18$, 17, and 16cm for Test 1

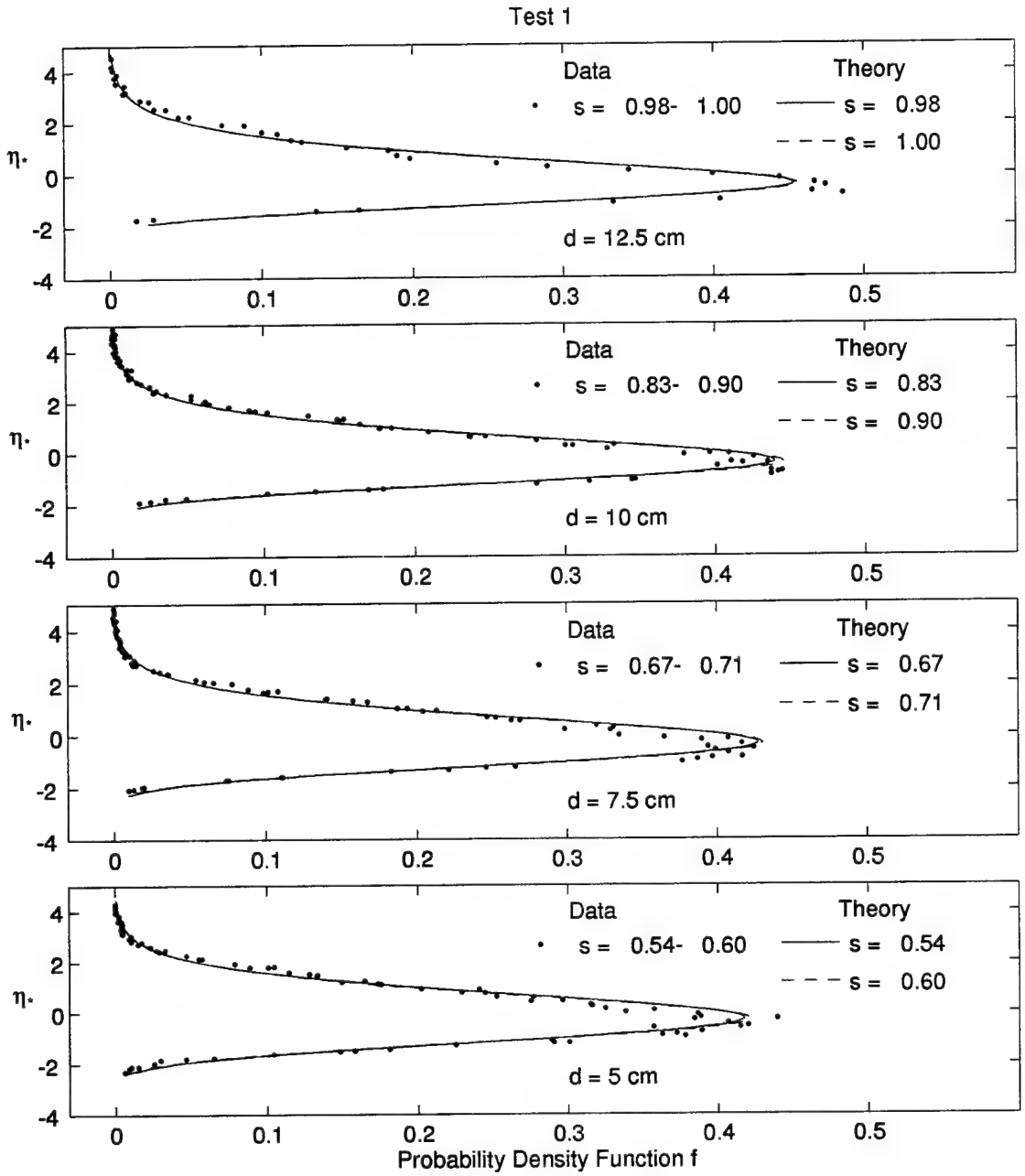

Figure 4.22: Measured and Computed Probability Distributions at Water Depth $d = 12.5$, 10, 7.5, and 5cm for Test 1

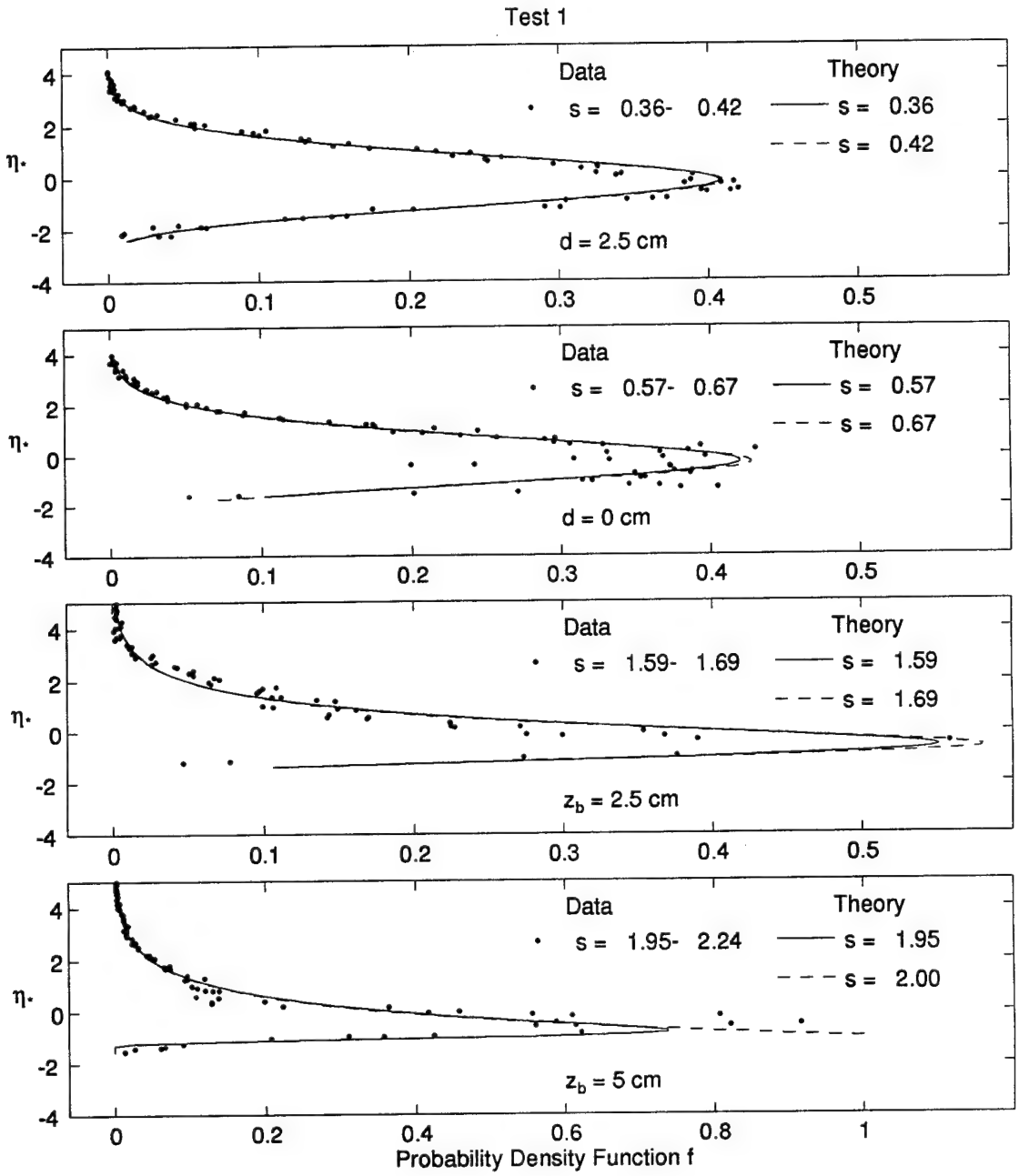

Figure 4.23: Measured and Computed Probability Distributions at Water Depth $d = 2.5$ and 0cm and Bottom Elevation $z_b = 2.5$ and 5cm for Test 1

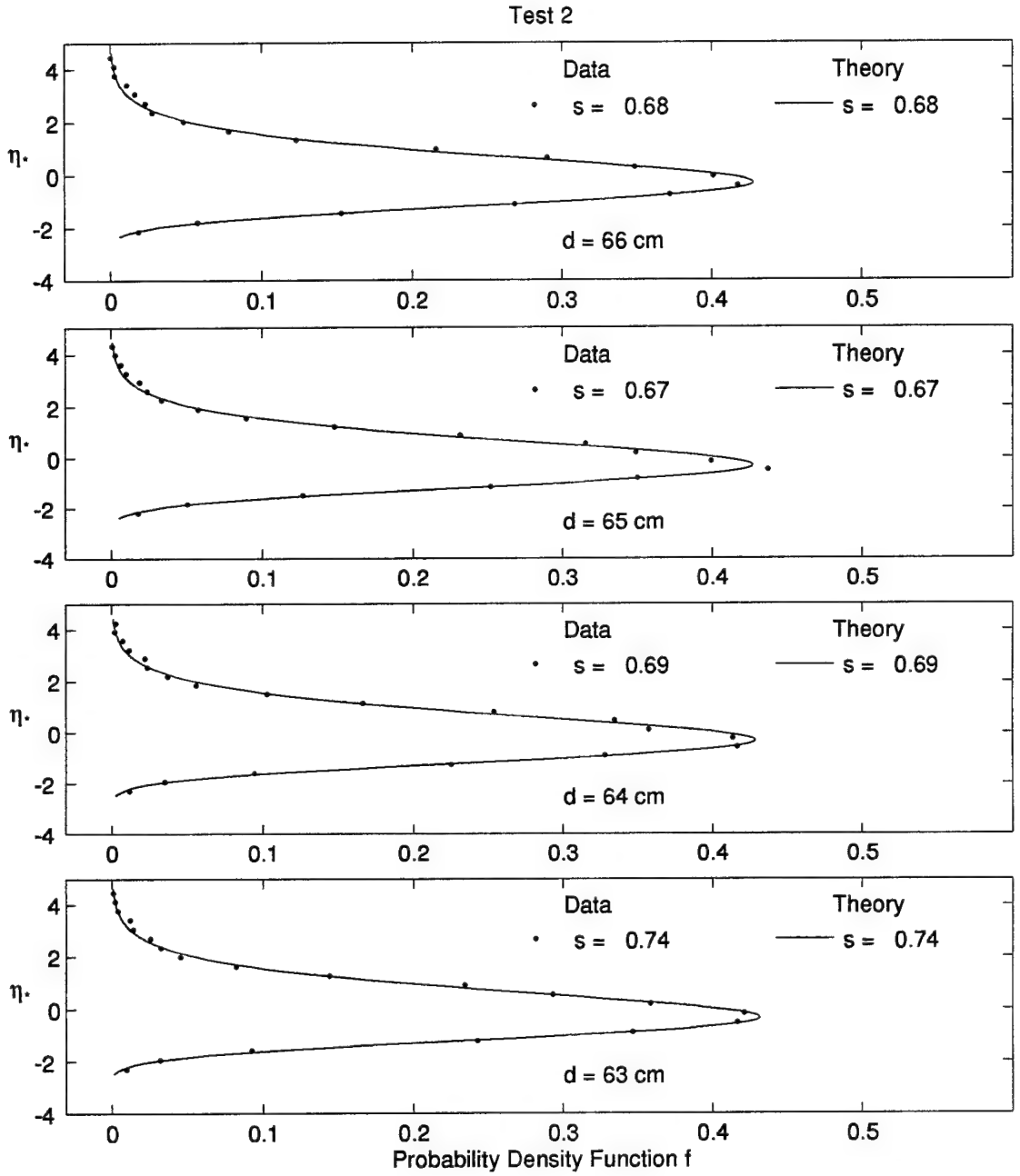

Figure 4.24: Measured and Computed Probability Distributions at Water Depth $d = 66$, 65, 64, and 63cm for Test 2

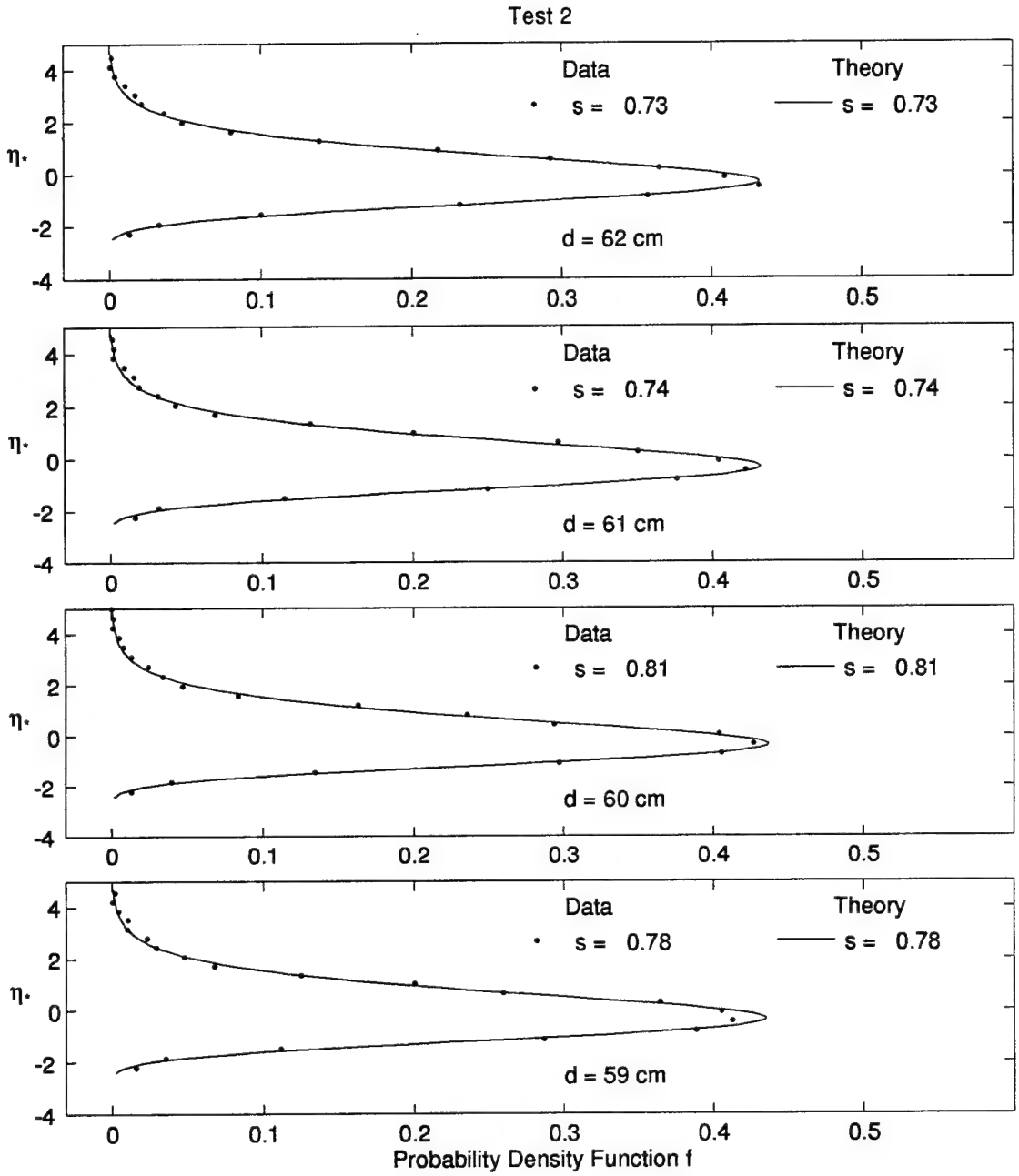

Figure 4.25: Measured and Computed Probability Distributions at Water Depth $d = 62$, 61, 60, and 59cm for Test 2

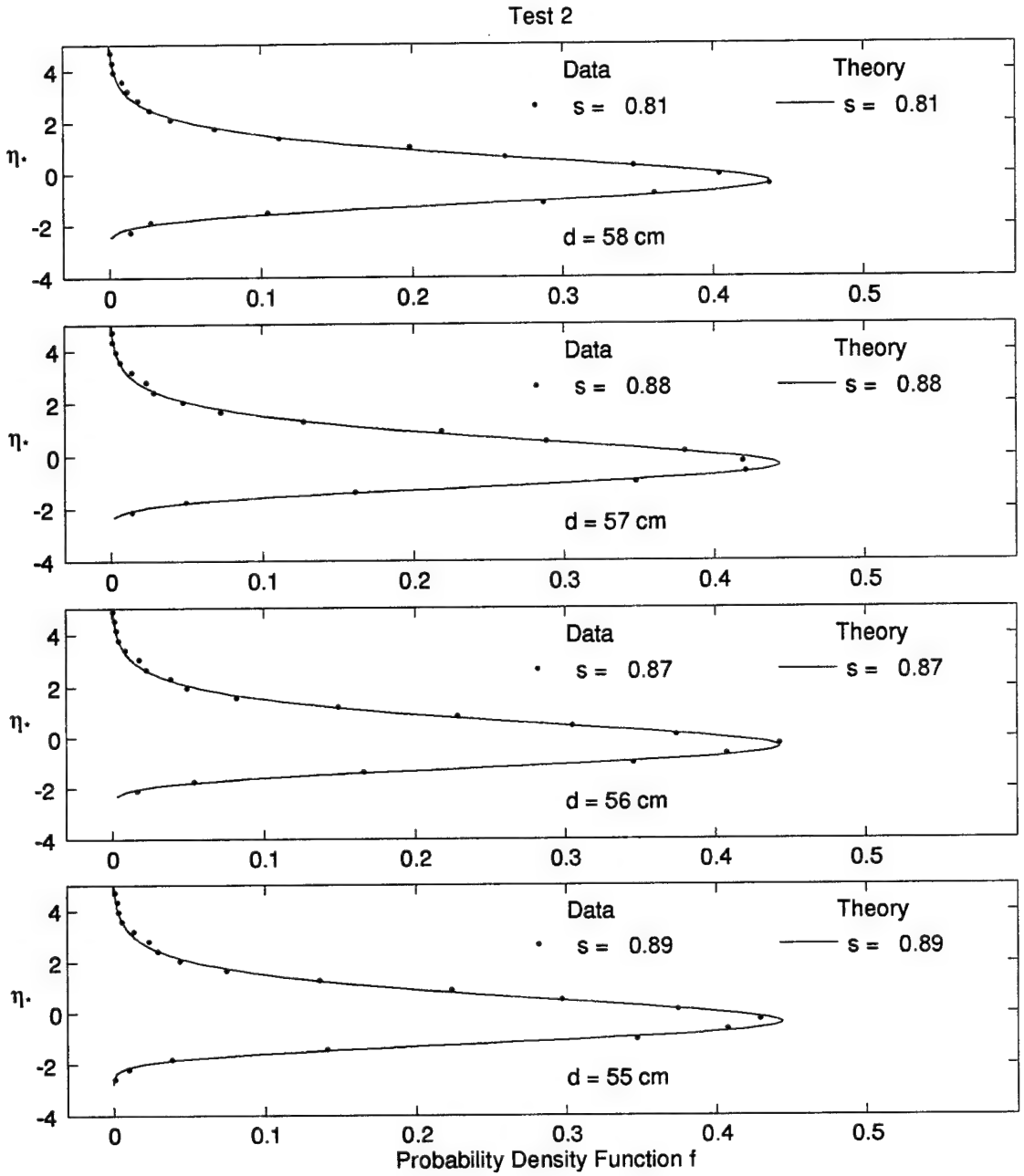

Figure 4.26: Measured and Computed Probability Distributions at Water Depth $d = 58$, 57, 56, and 55cm for Test 2

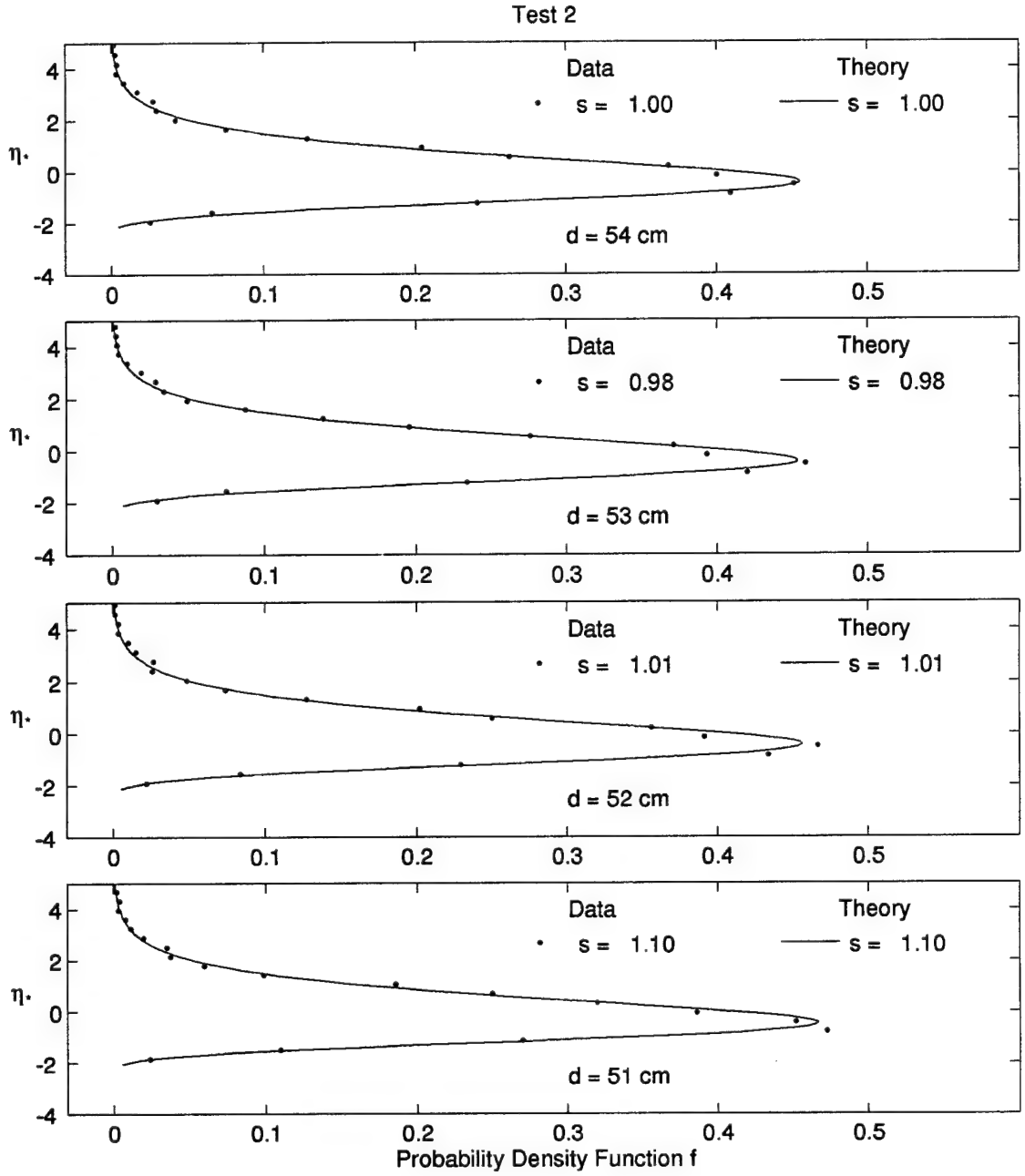

Figure 4.27: Measured and Computed Probability Distributions at Water Depth $d = 54$, 53, 52, and 51cm for Test 2

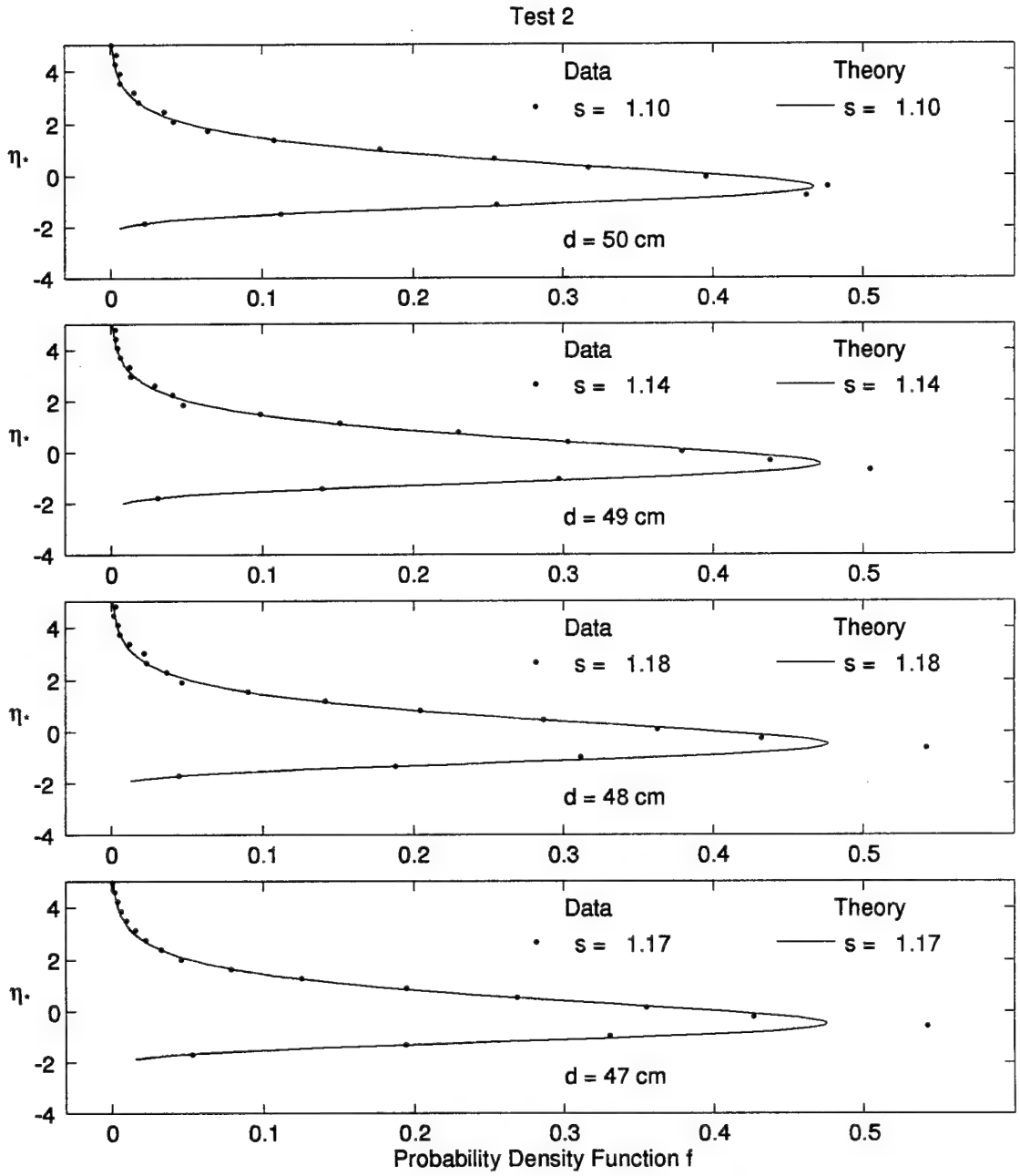

Figure 4.28: Measured and Computed Probability Distributions at Water Depth $d = 50$, 49, 48, and 47cm for Test 2

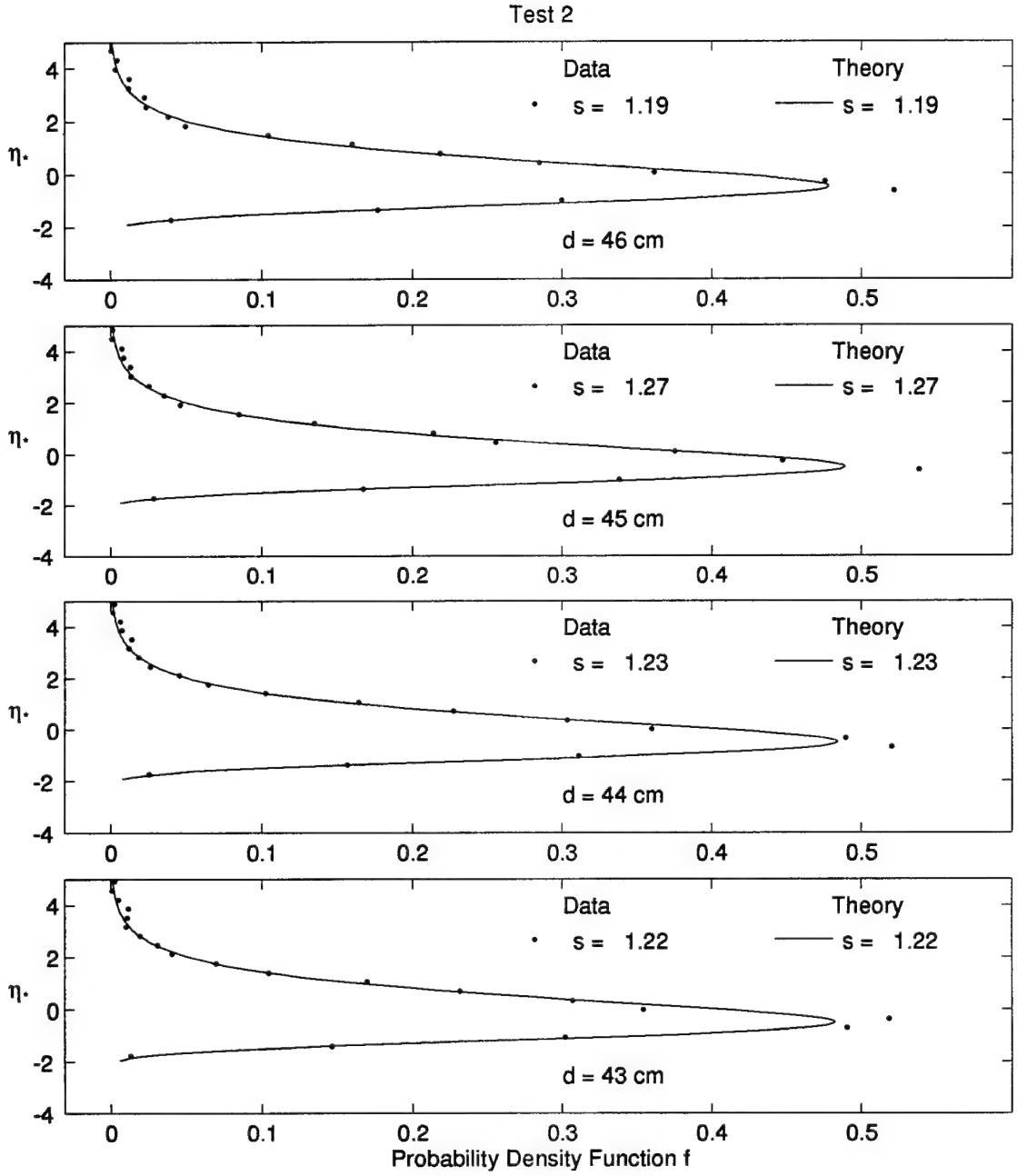

Figure 4.29: Measured and Computed Probability Distributions at Water Depth $d = 46$, 45, 44, and 43cm for Test 2

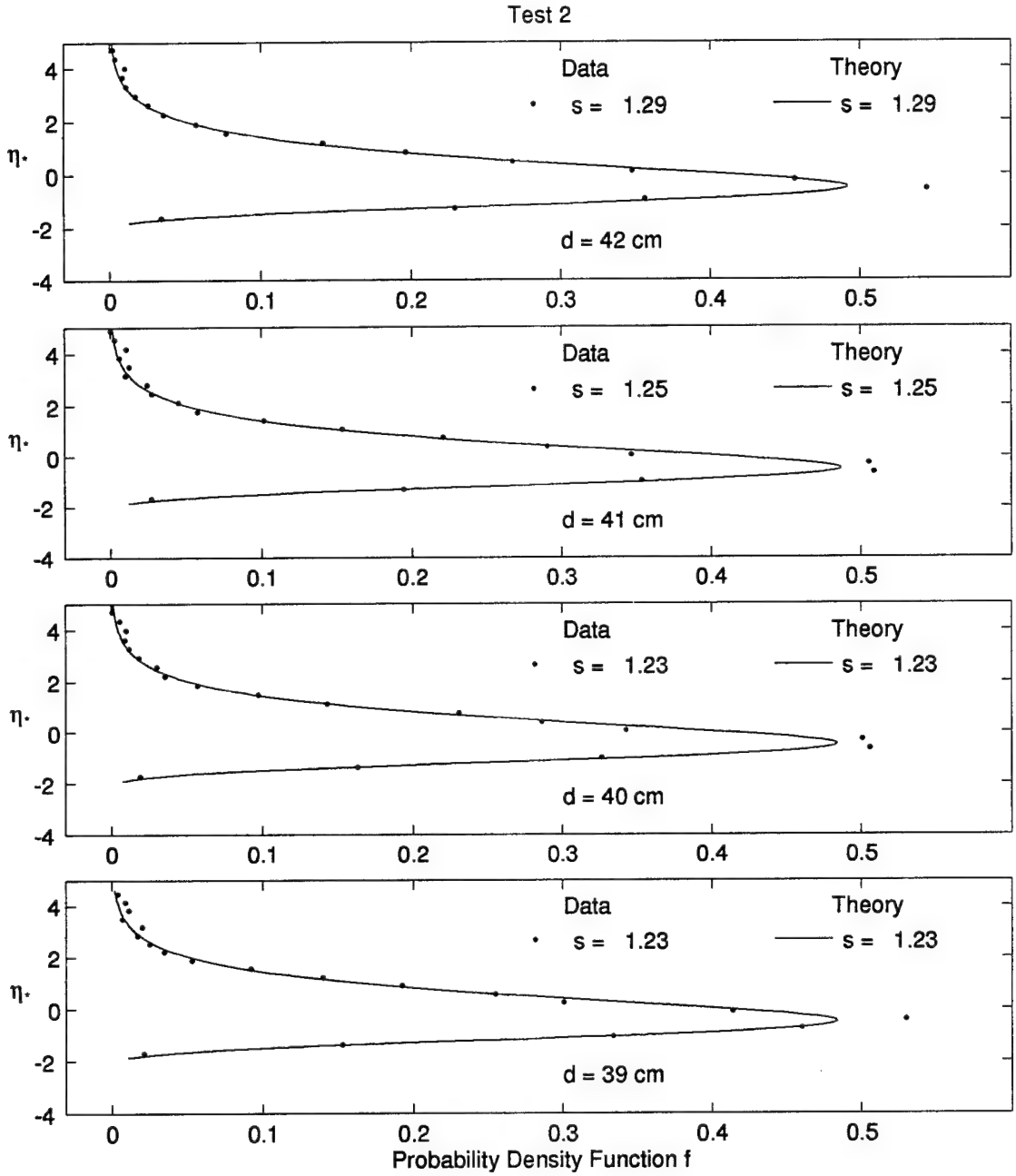

Figure 4.30: Measured and Computed Probability Distributions at Water Depth $d = 42$, 41, 40, and 39cm for Test 2

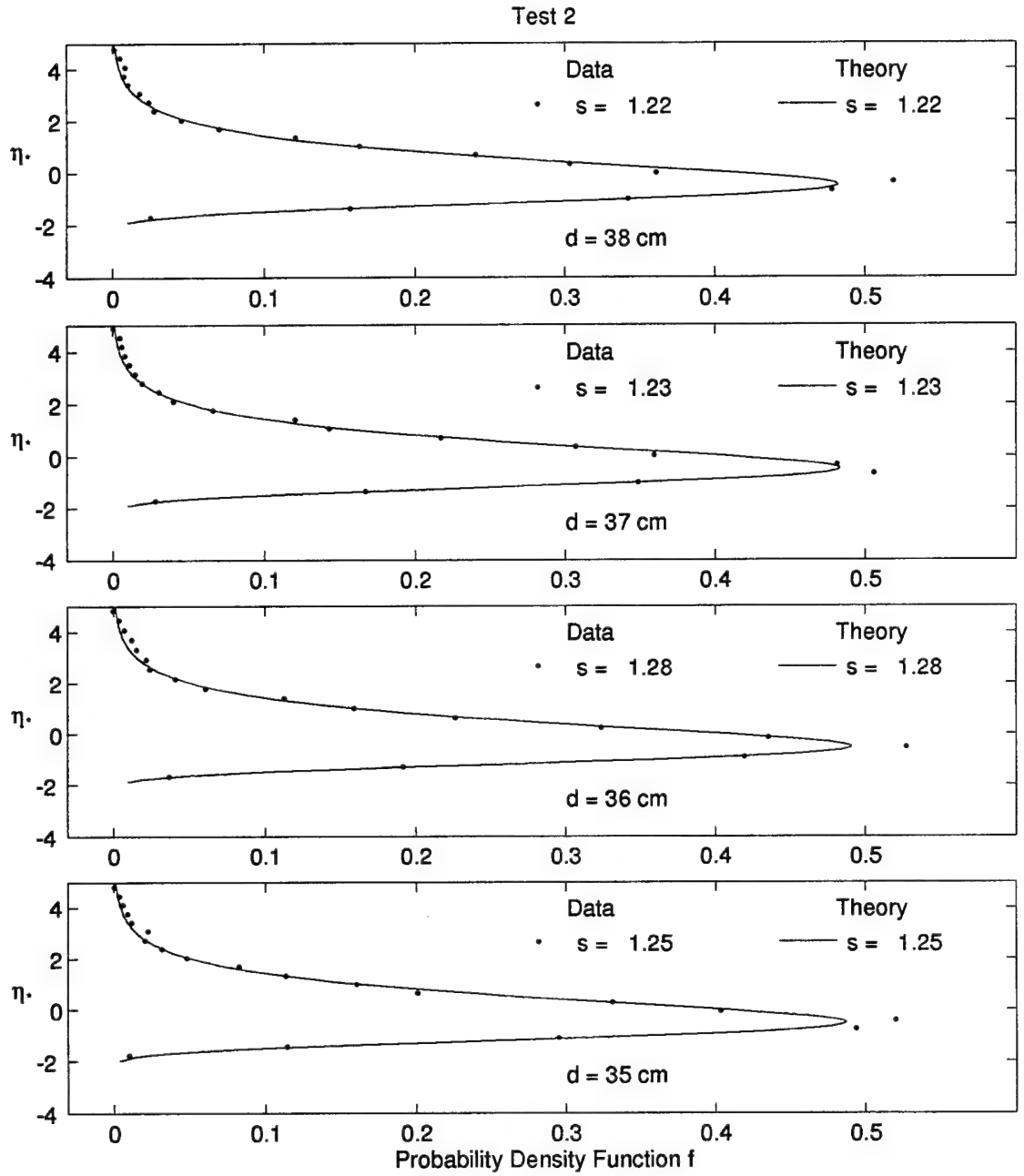

Figure 4.31: Measured and Computed Probability Distributions at Water Depth $d = 38$, 37, 36, and 35cm for Test 2

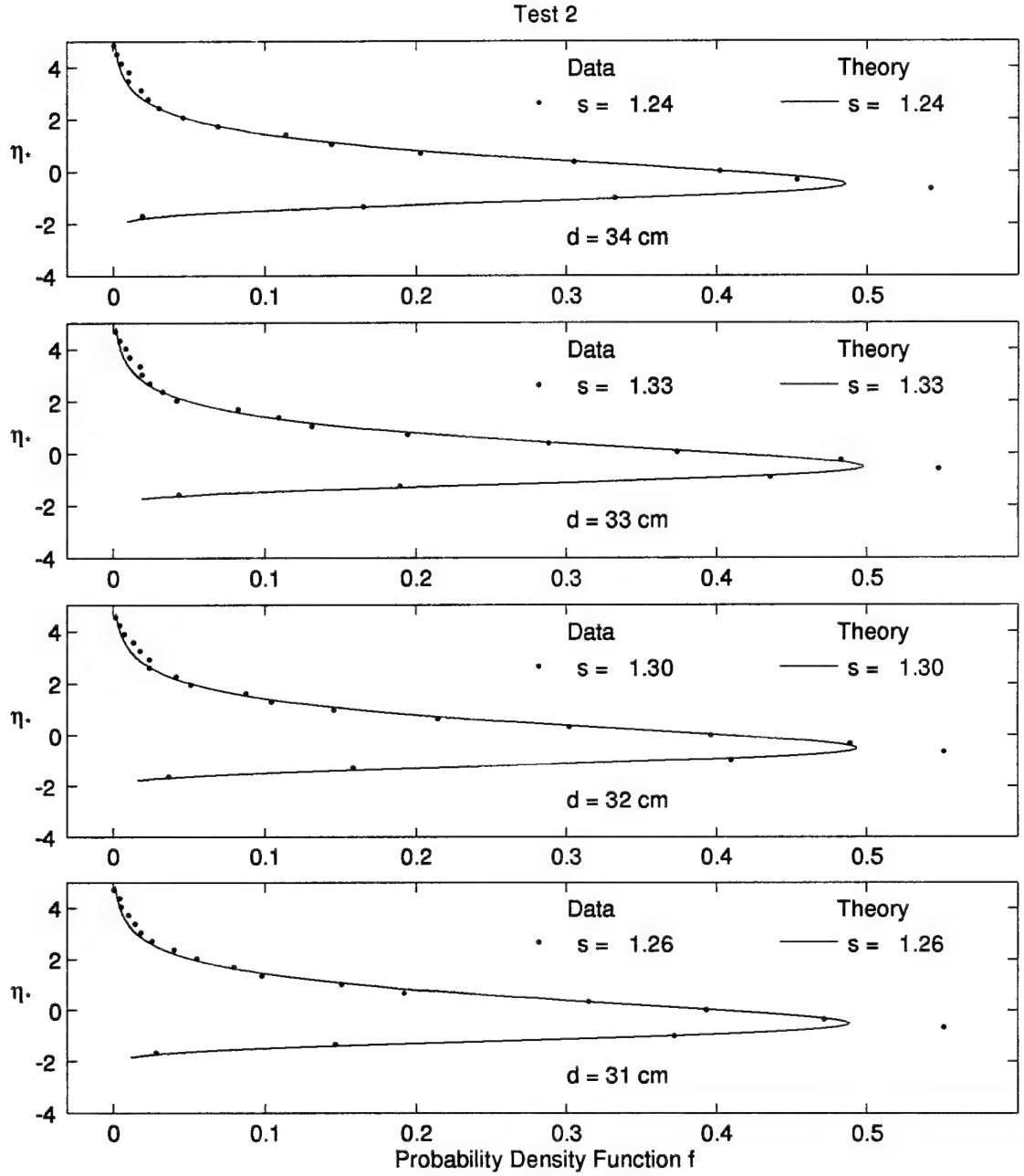

Figure 4.32: Measured and Computed Probability Distributions at Water Depth $d = 34$, 33, 32, and 31cm for Test 2

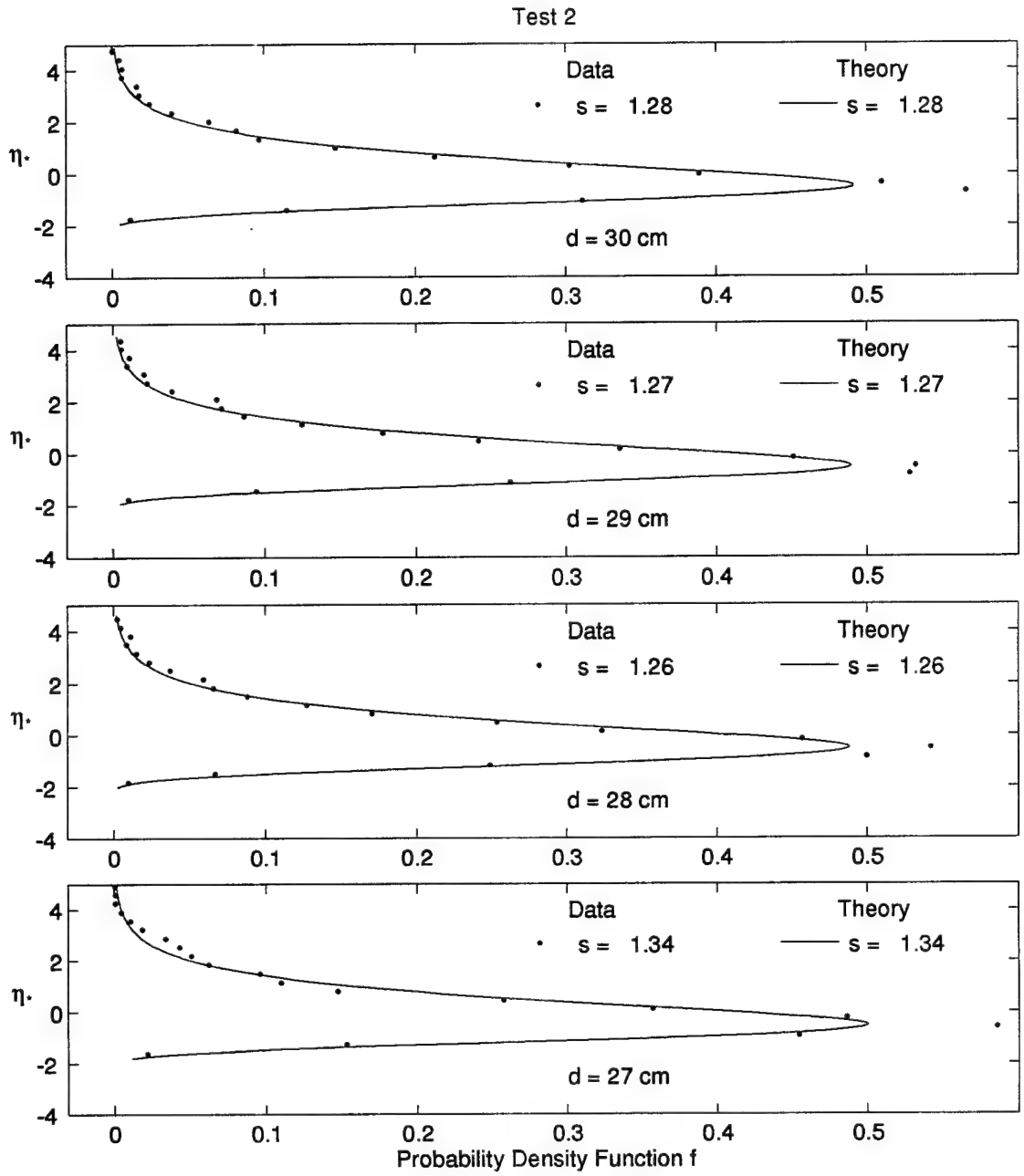

Figure 4.33: Measured and Computed Probability Distributions at Water Depth $d = 30$, 29, 28, and 27cm for Test 2

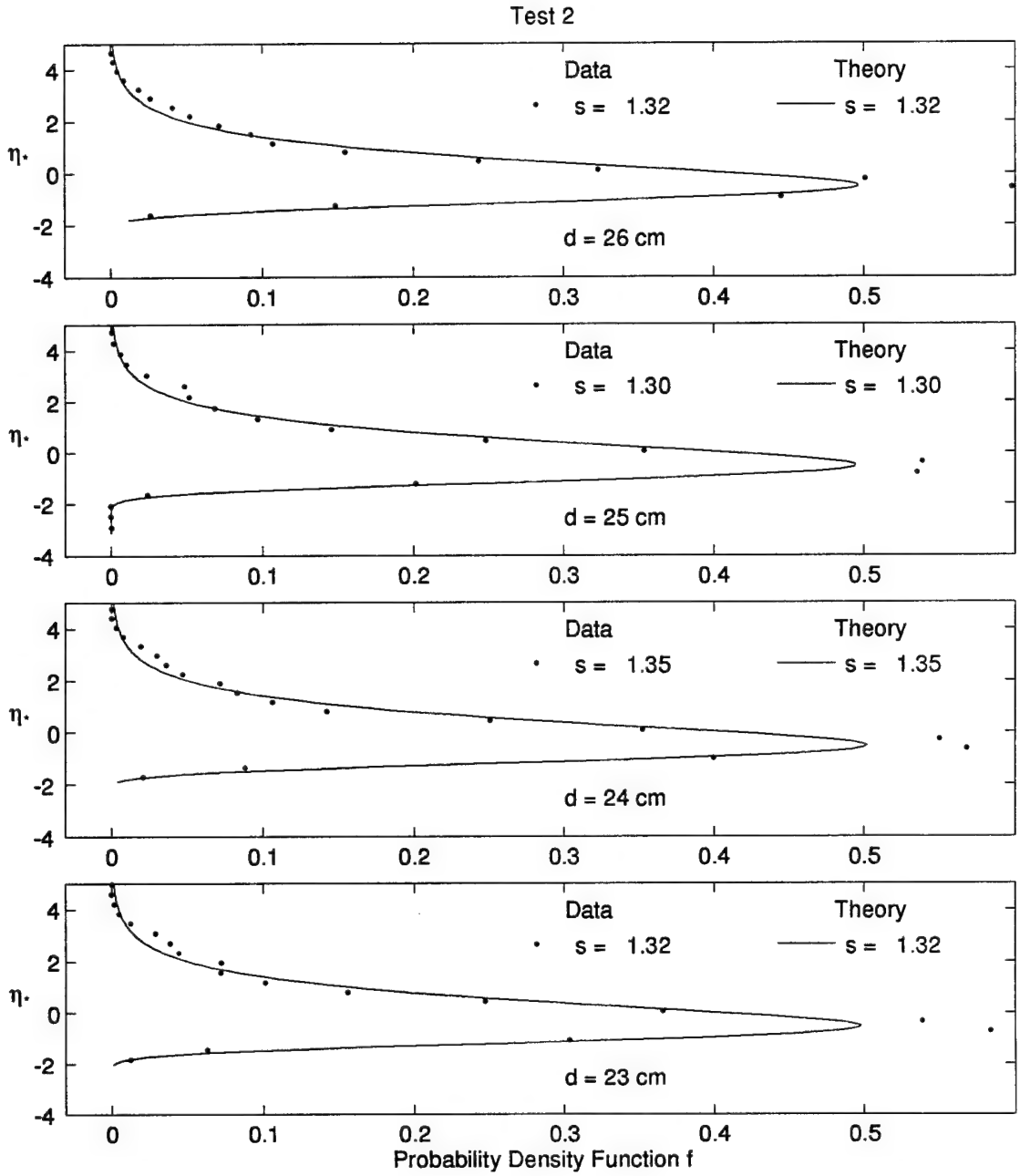

Figure 4.34: Measured and Computed Probability Distributions at Water Depth $d = 26$, 25, 24, and 23cm for Test 2

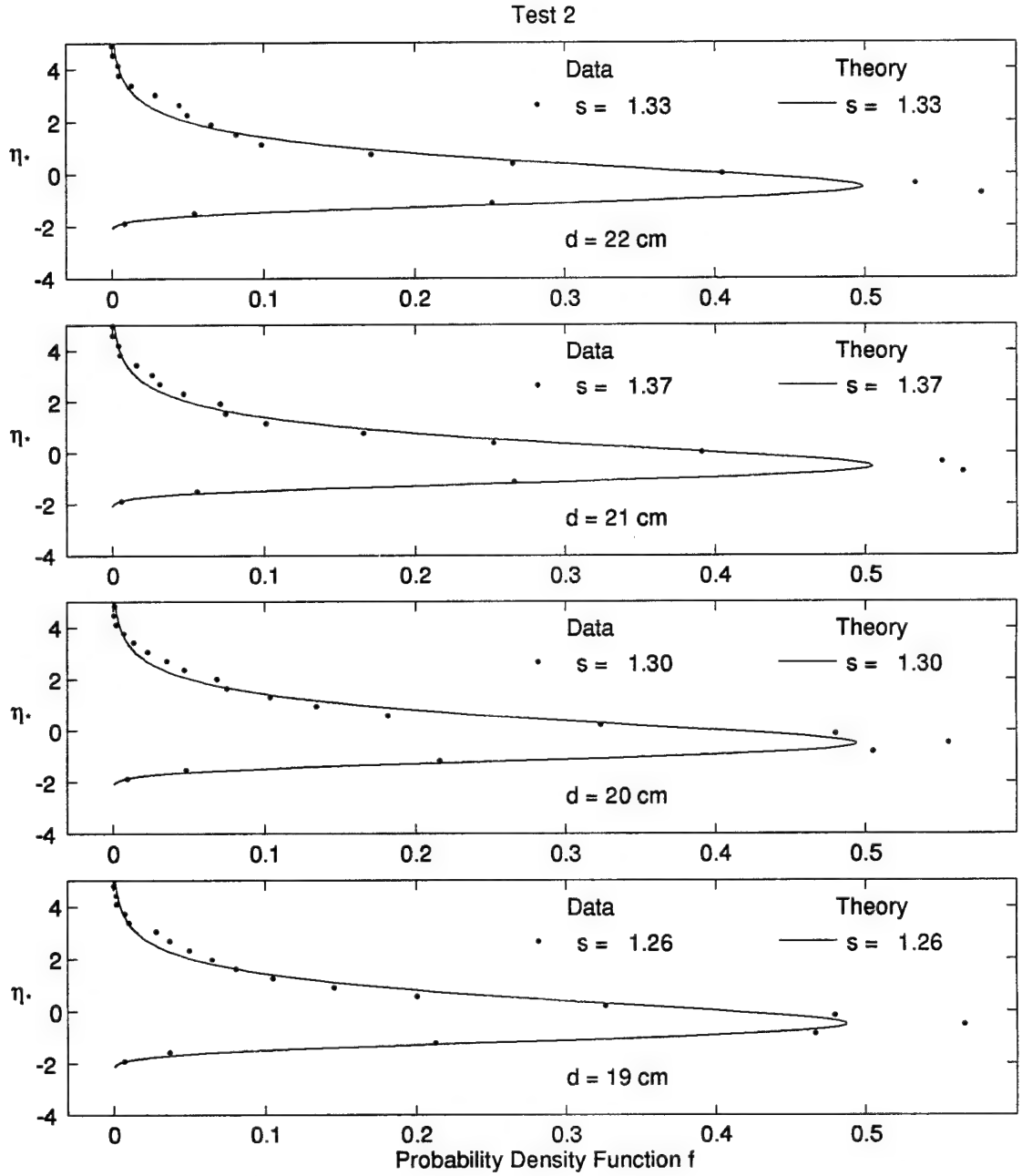

Figure 4.35: Measured and Computed Probability Distributions at Water Depth $d = 22$, 21, 20, and 19cm for Test 2

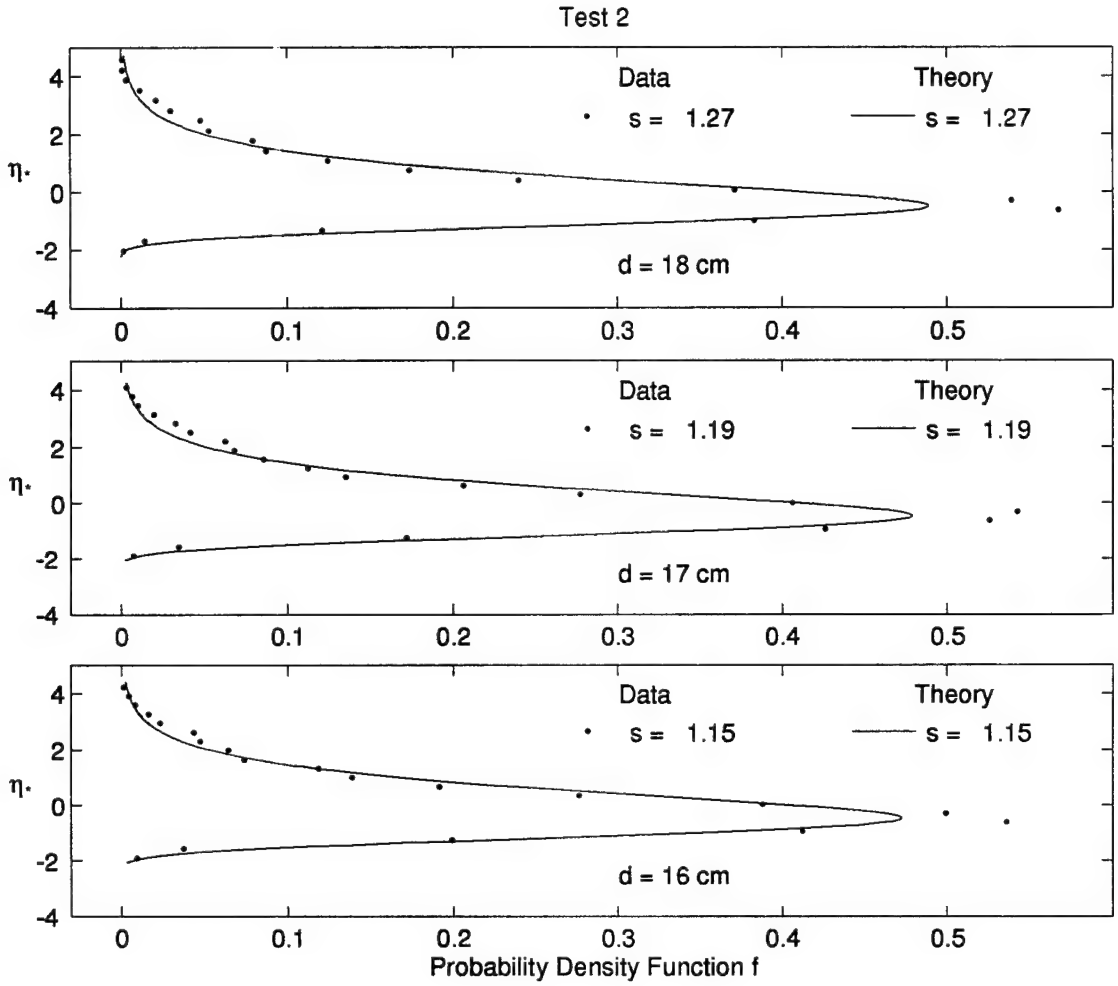

Figure 4.36: Measured and Computed Probability Distributions at Water Depth $d = 18$, 17, and 16cm for Test 2

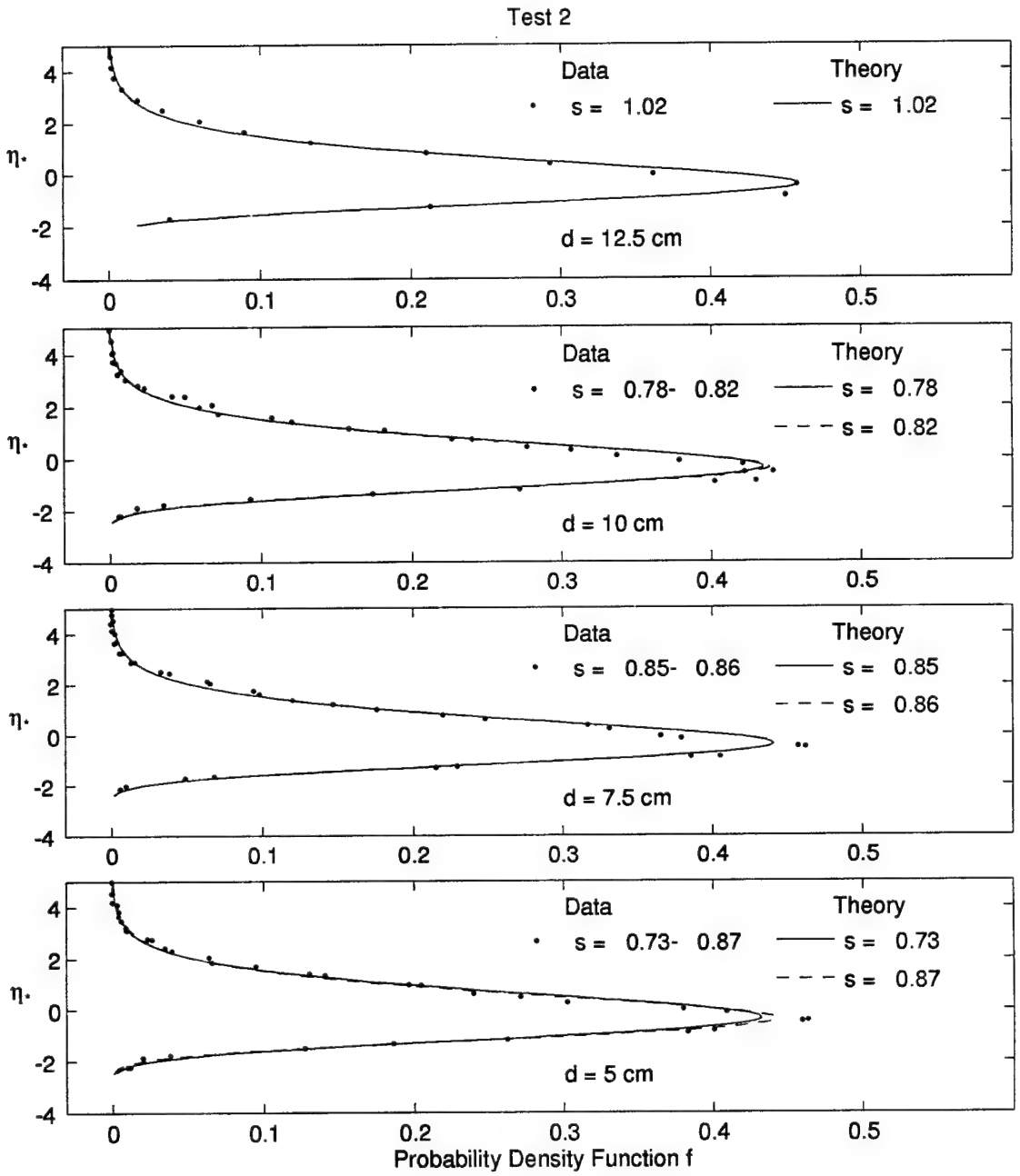

Figure 4.37: Measured and Computed Probability Distributions at Water Depth $d = 12.5$, 10, 7.5, and 5cm for Test 2

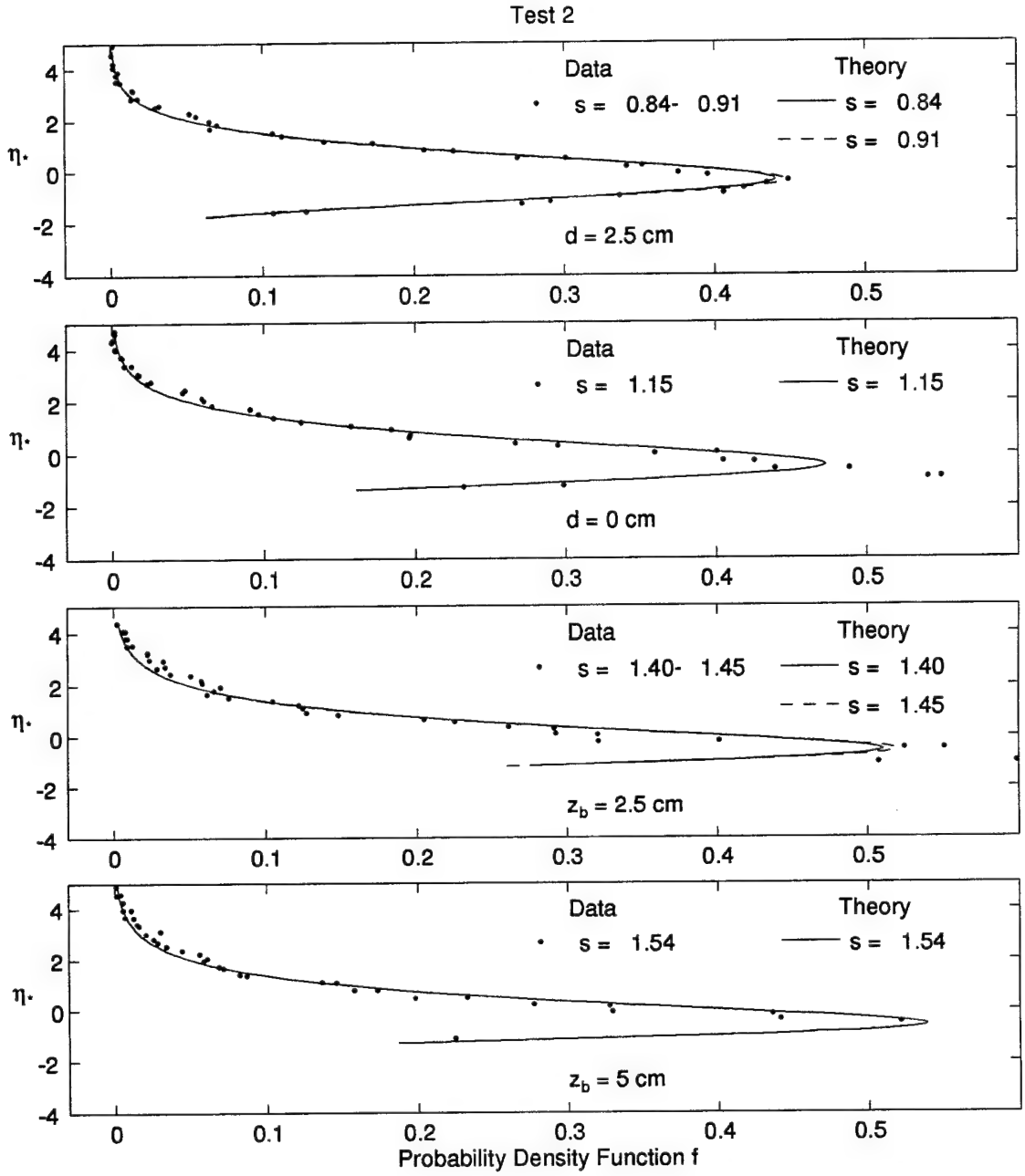

Figure 4.38: Measured and Computed Probability Distributions at Water Depth $d = 2.5$ and 0cm and Bottom Elevation $z_b = 2.5$ and 5cm for Test 2

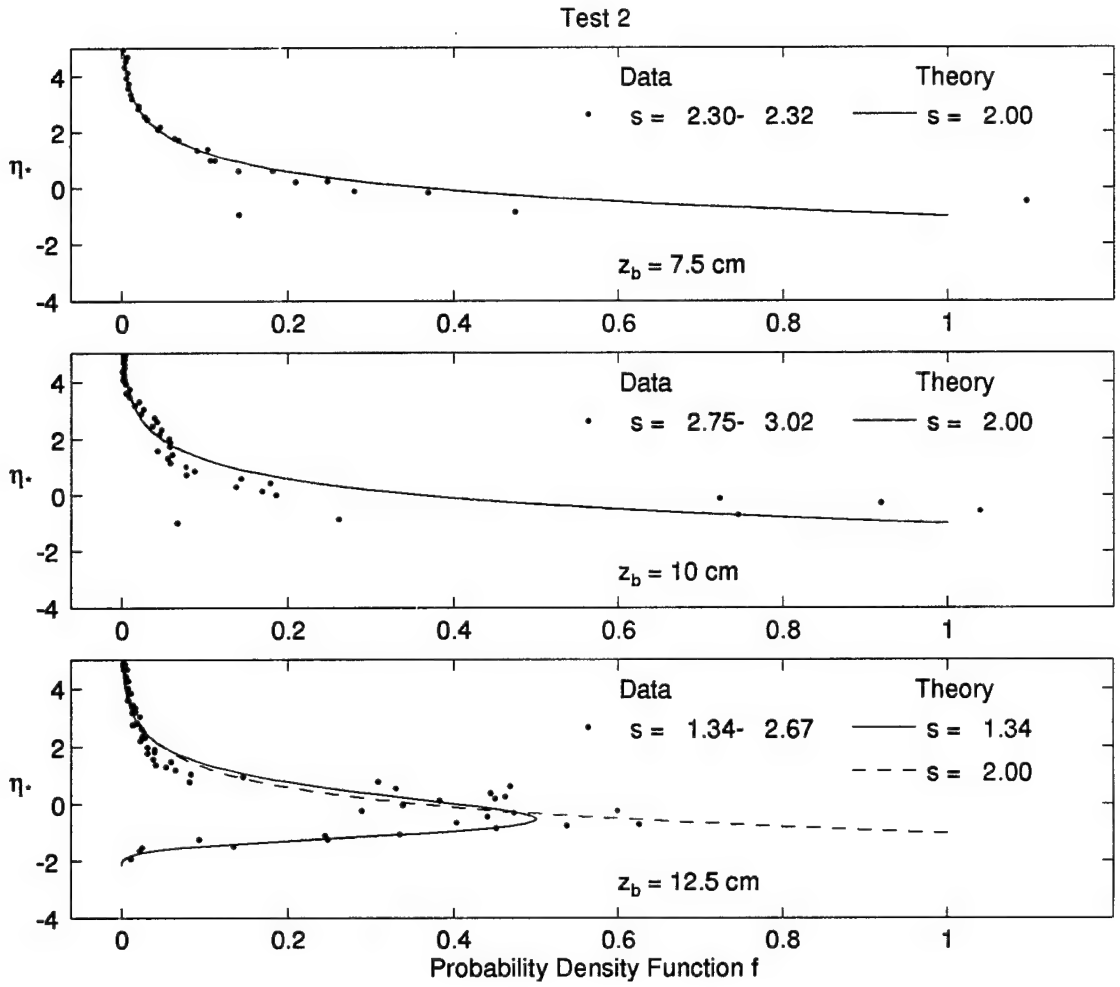

Figure 4.39: Measured and Computed Probability Distributions at Bottom Elevation z_b = 7.5, 10, and 12.5cm for Test 2

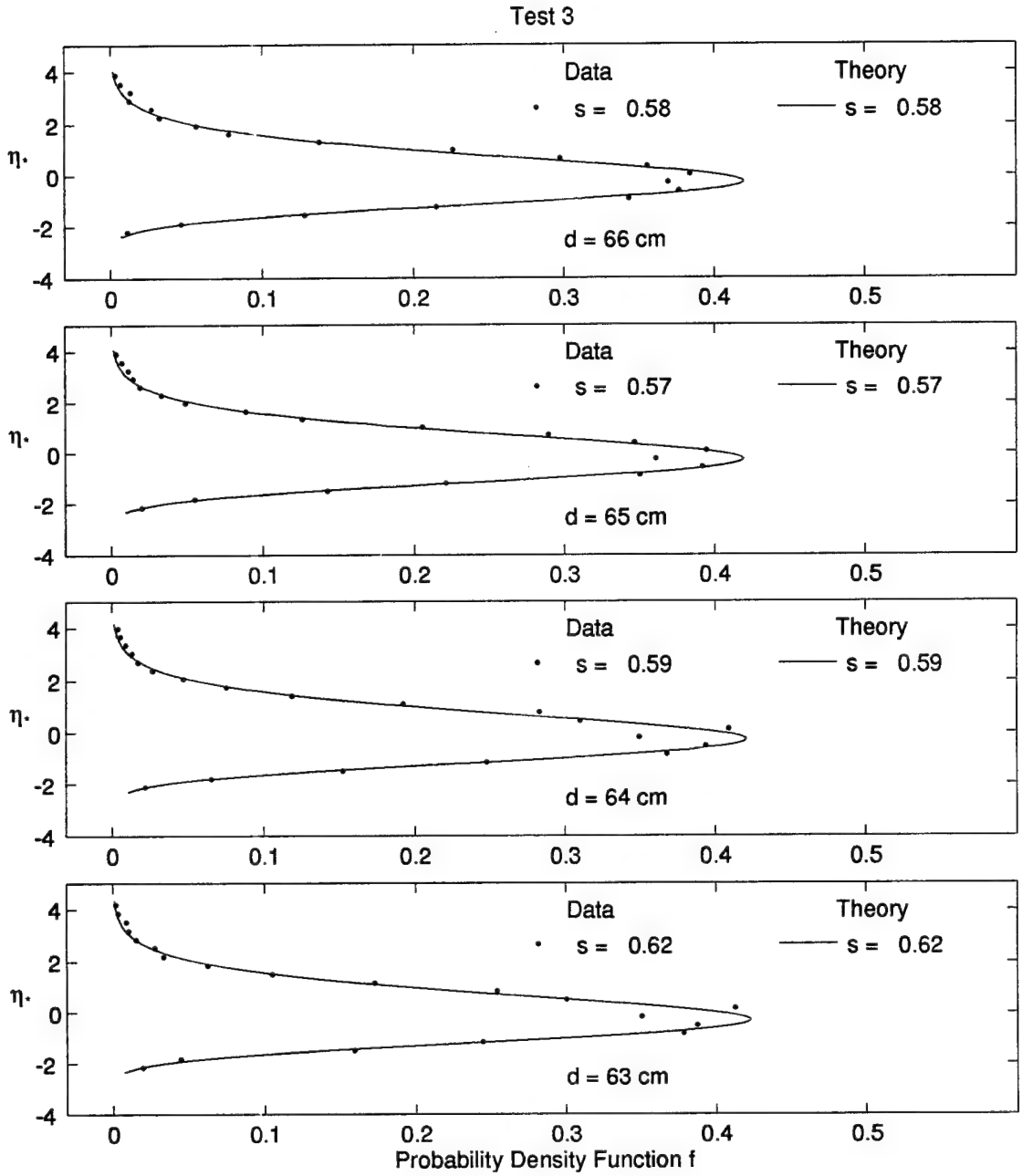

Figure 4.40: Measured and Computed Probability Distributions at Water Depth $d = 66$, 65, 64, and 63cm for Test 3

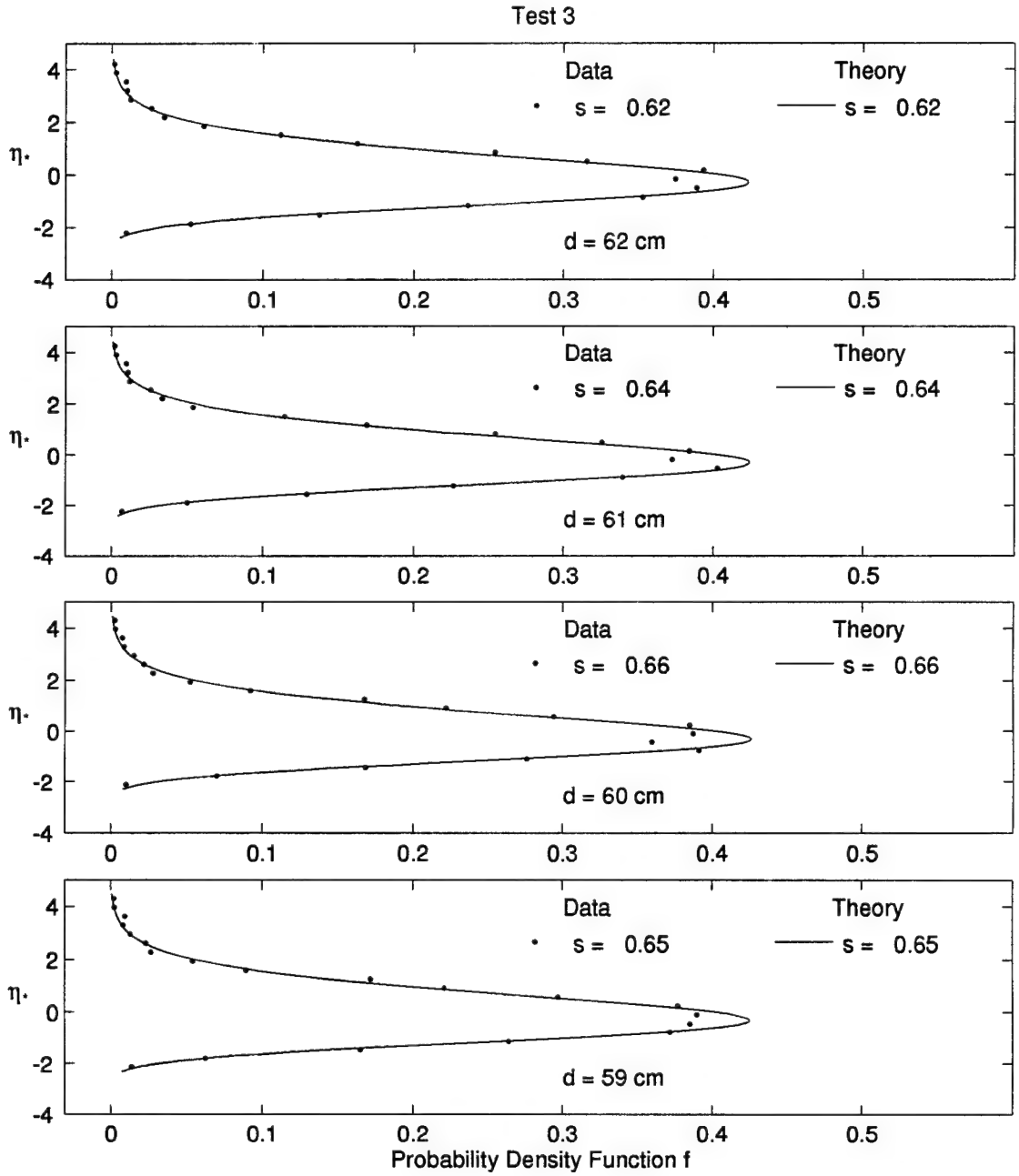

Figure 4.41: Measured and Computed Probability Distributions at Water Depth $d = 62$, 61, 60, and 59cm for Test 3

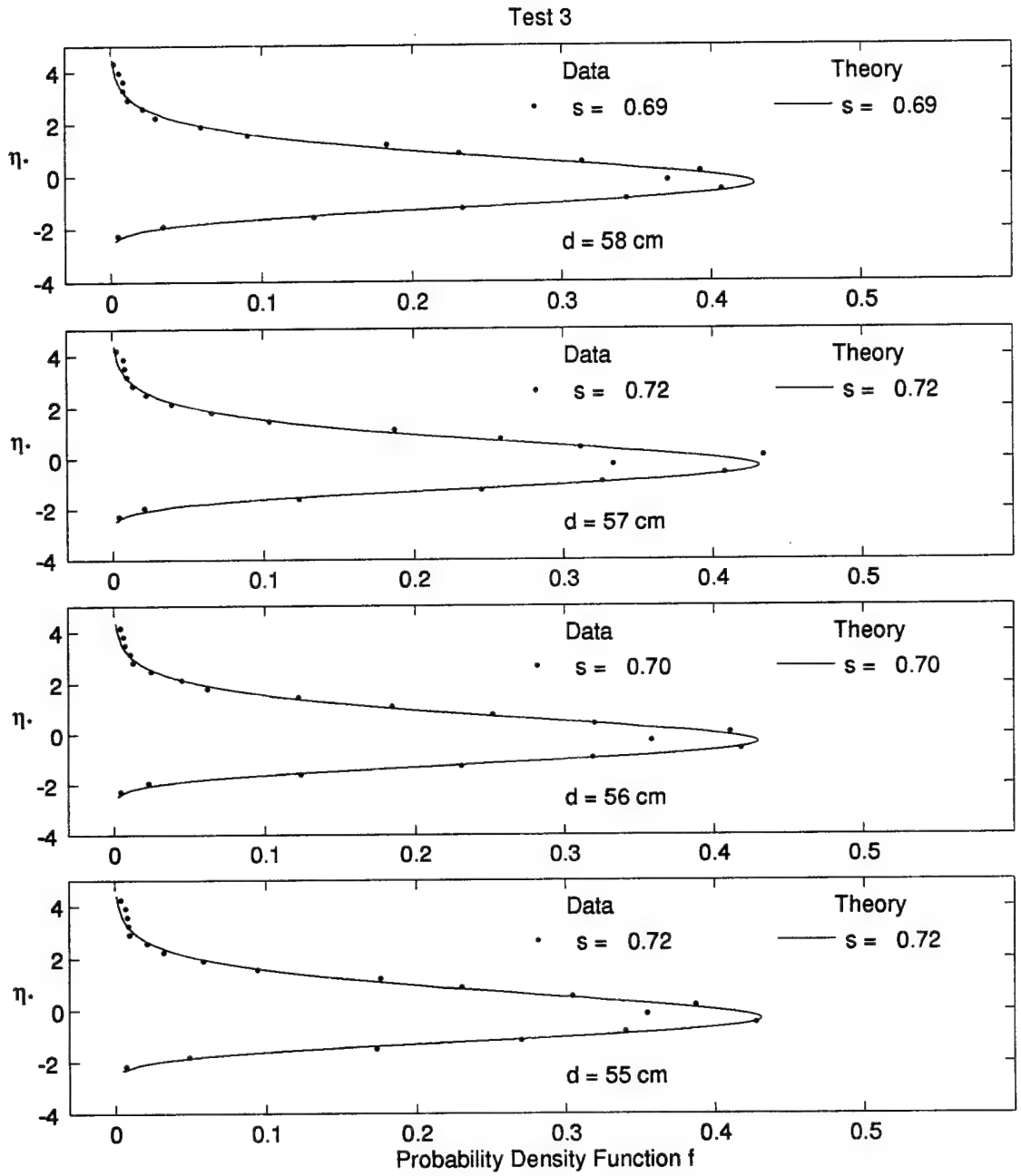

Figure 4.42: Measured and Computed Probability Distributions at Water Depth $d = 58$, 57, 56, and 55cm for Test 3

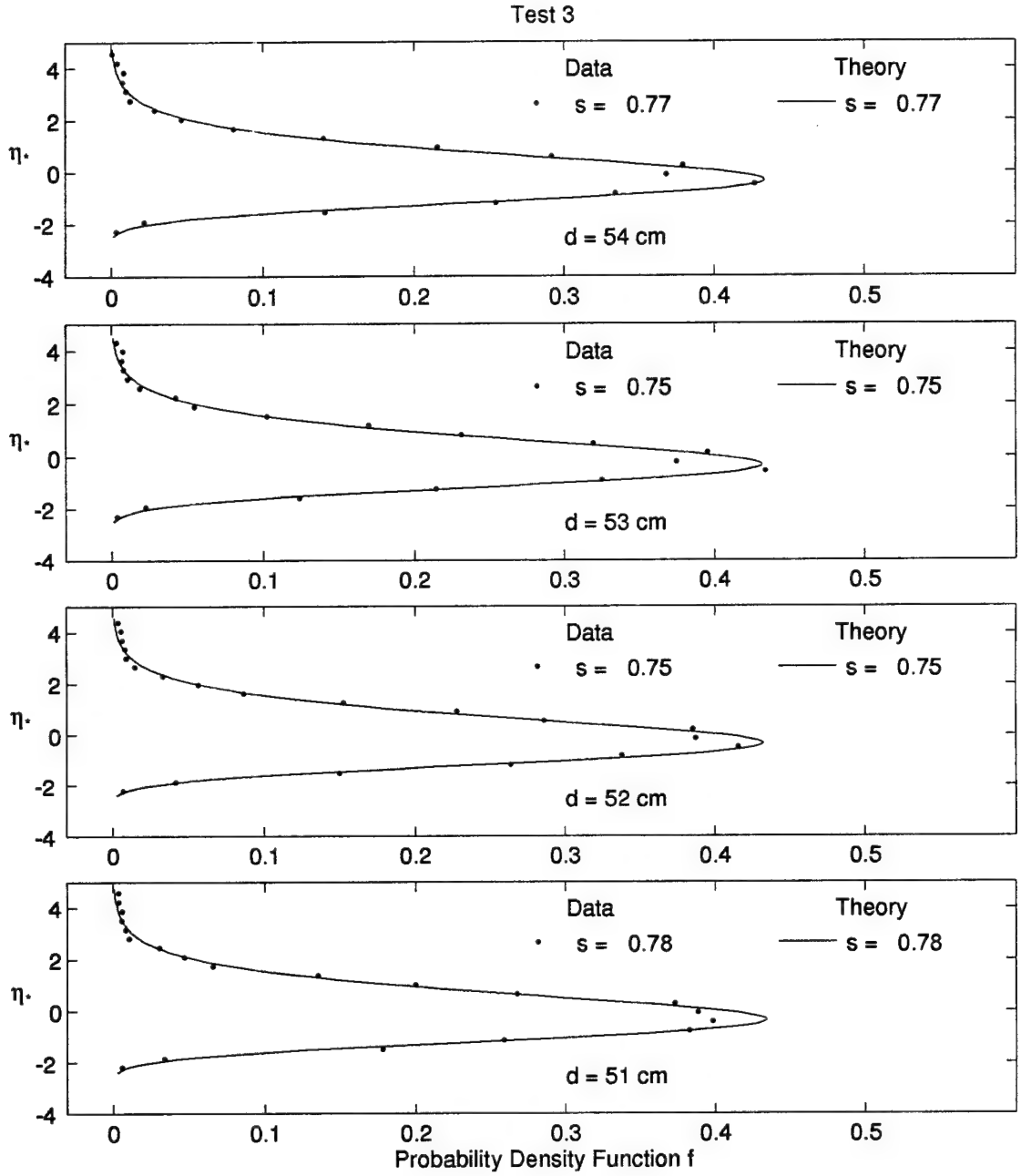

Figure 4.43: Measured and Computed Probability Distributions at Water Depth $d = 54$, 53, 52, and 51cm for Test 3

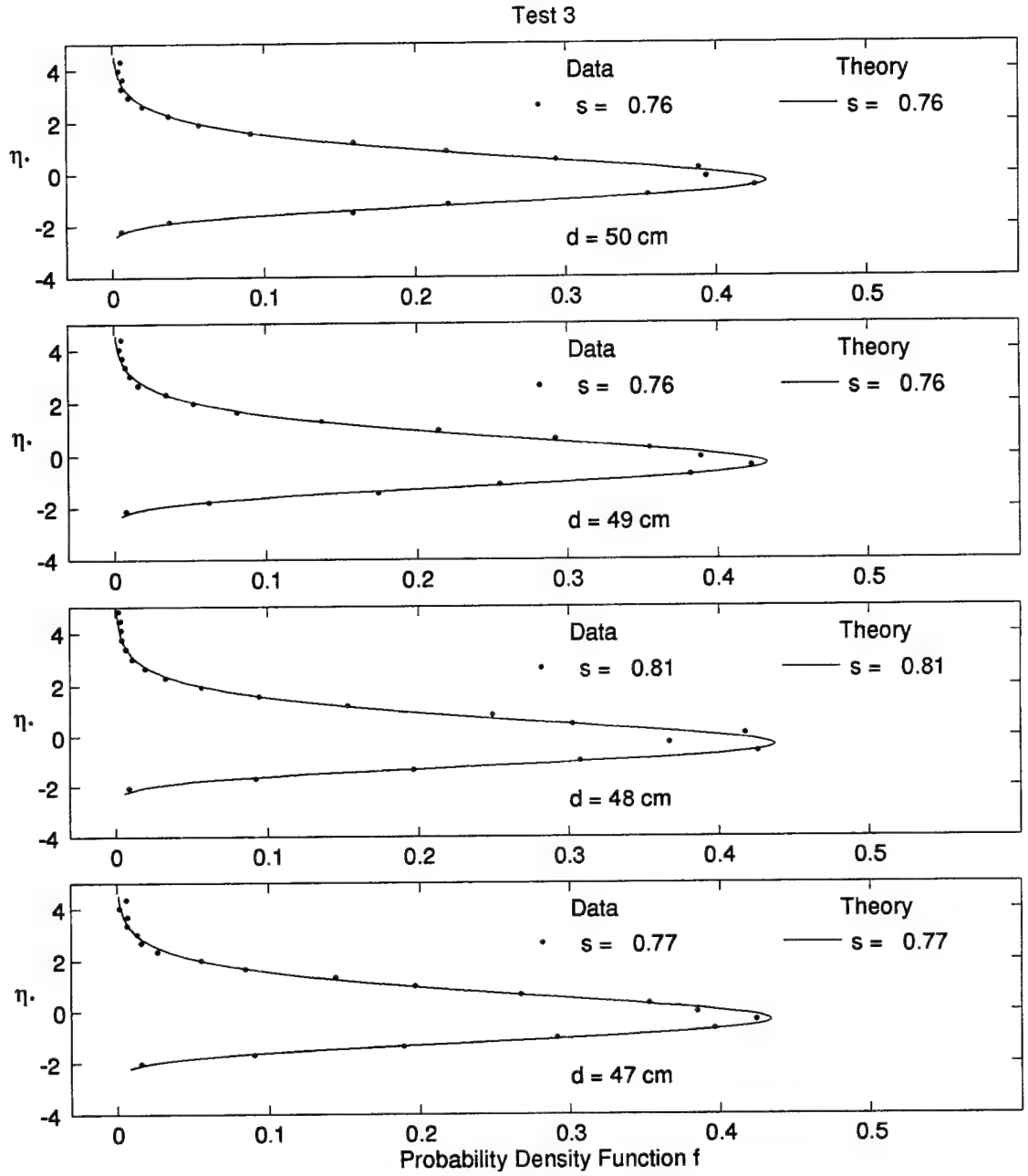

Figure 4.44: Measured and Computed Probability Distributions at Water Depth $d = 50$, 49, 48, and 47cm for Test 3

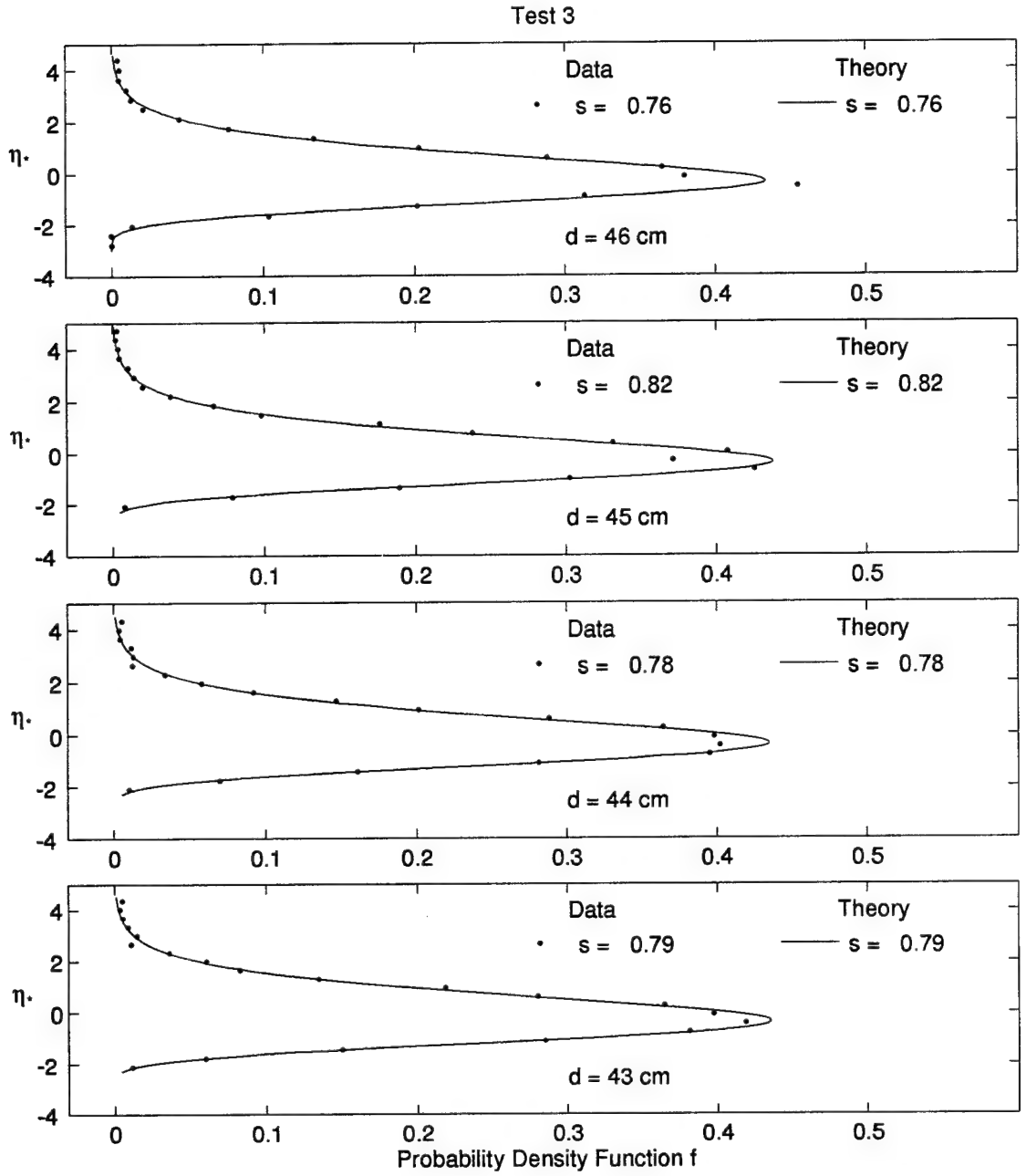

Figure 4.45: Measured and Computed Probability Distributions at Water Depth $d = 46$, 45, 44, and 43cm for Test 3

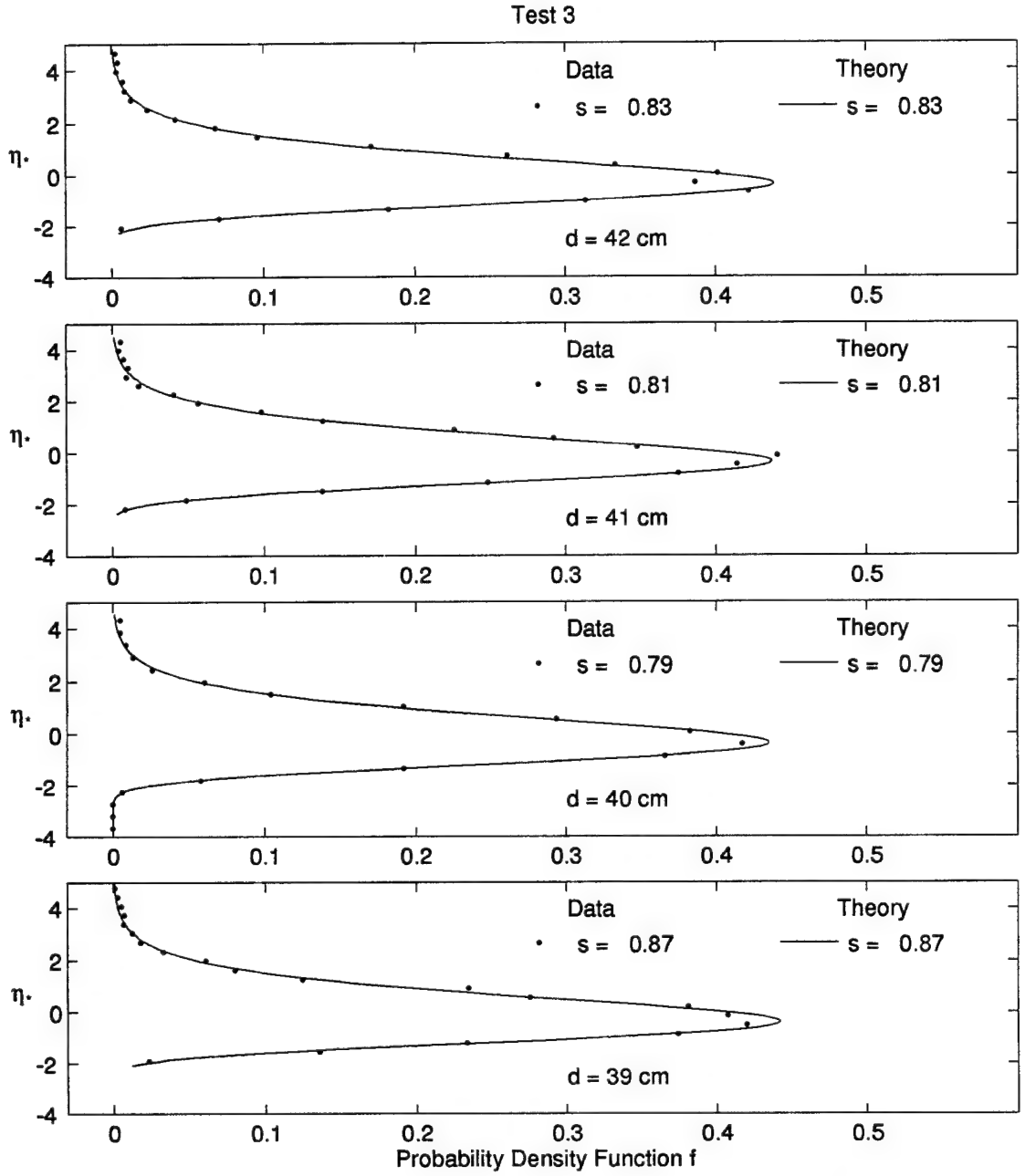

Figure 4.46: Measured and Computed Probability Distributions at Water Depth $d = 42$, 41, 40, and 39cm for Test 3

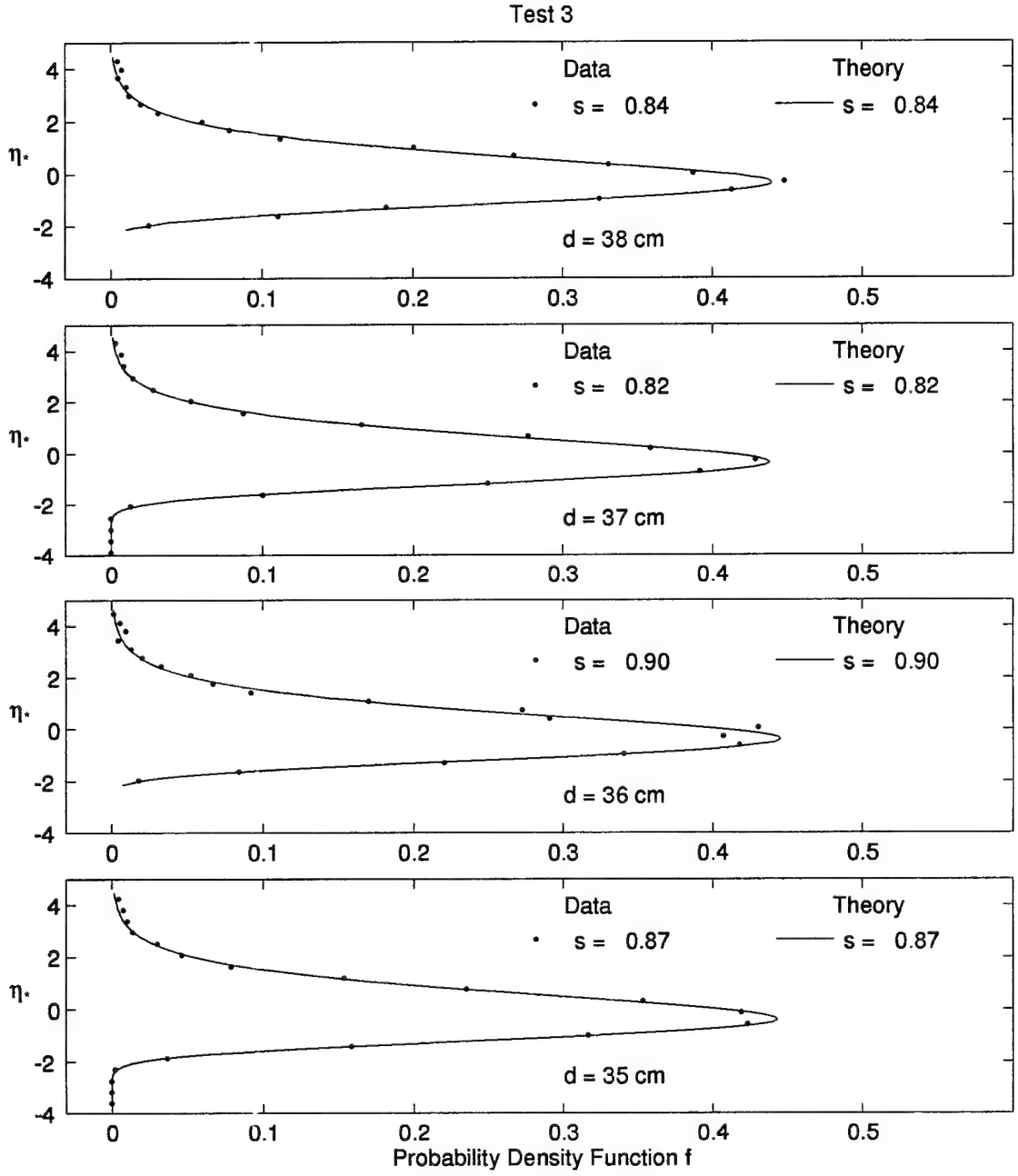

Figure 4.47: Measured and Computed Probability Distributions at Water Depth $d = 38$, 37, 36, and 35cm for Test 3

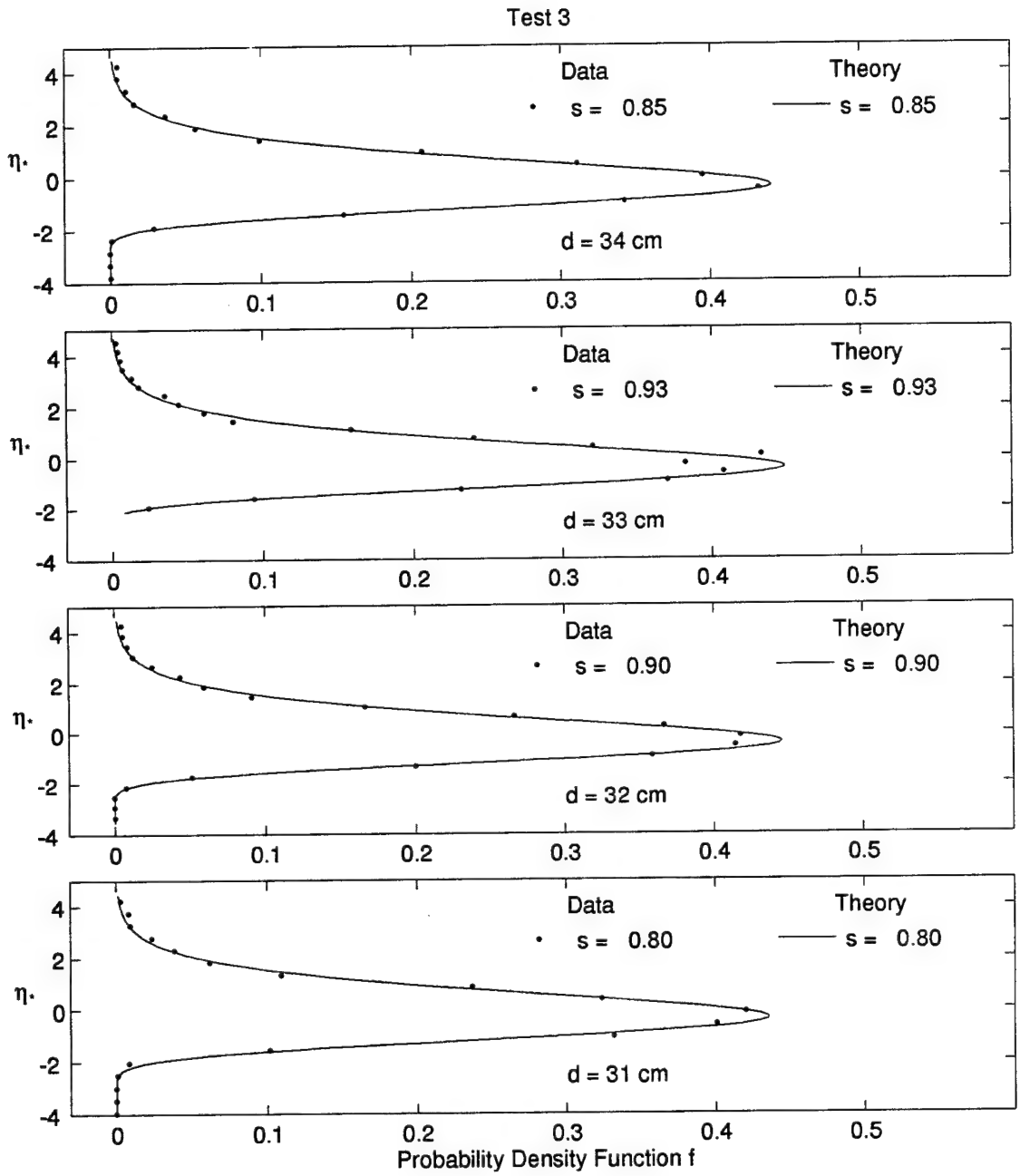

Figure 4.48: Measured and Computed Probability Distributions at Water Depth $d = 34$, 33, 32, and 31cm for Test 3

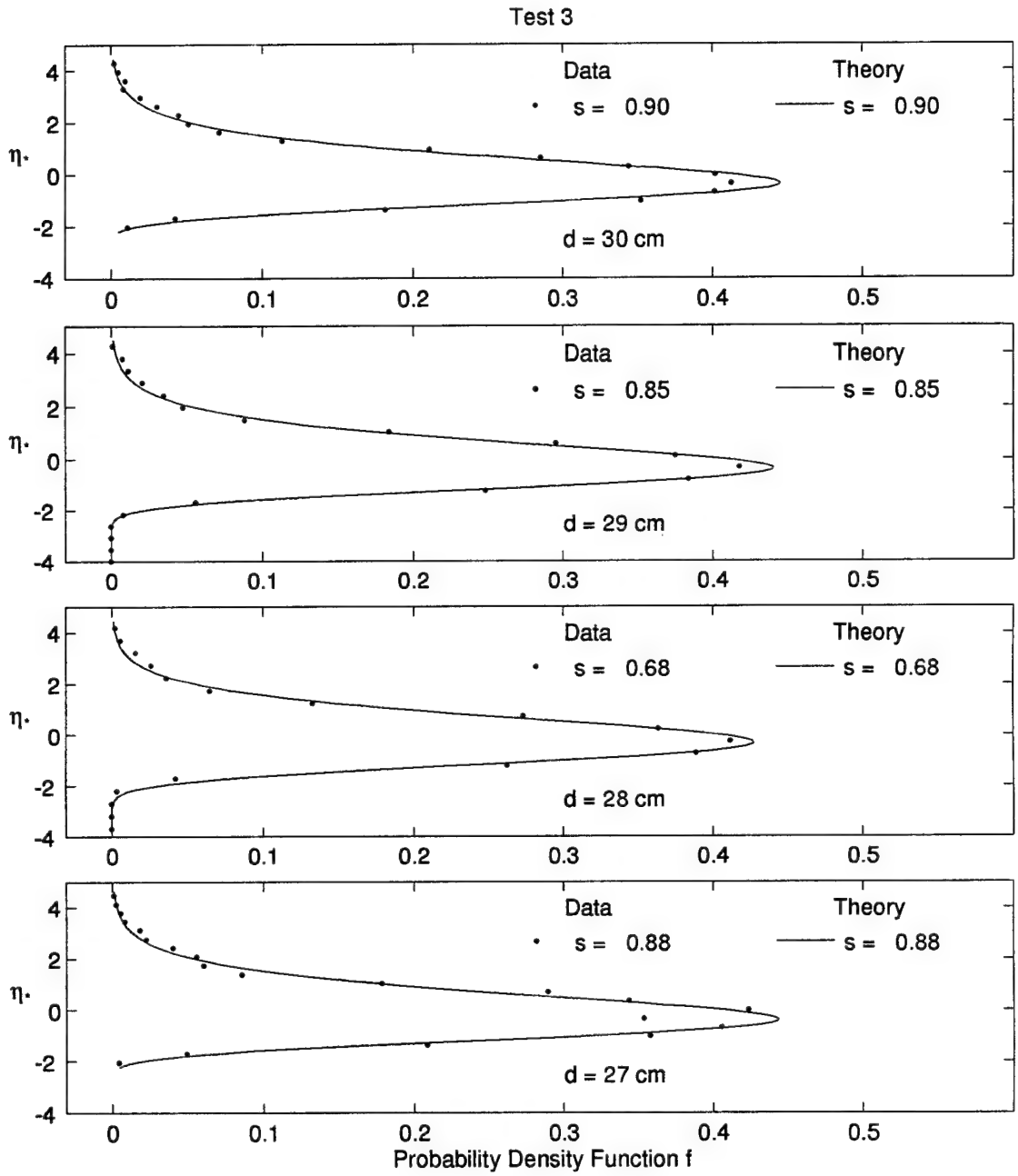

Figure 4.49: Measured and Computed Probability Distributions at Water Depth $d = 30$, 29, 28, and 27cm for Test 3

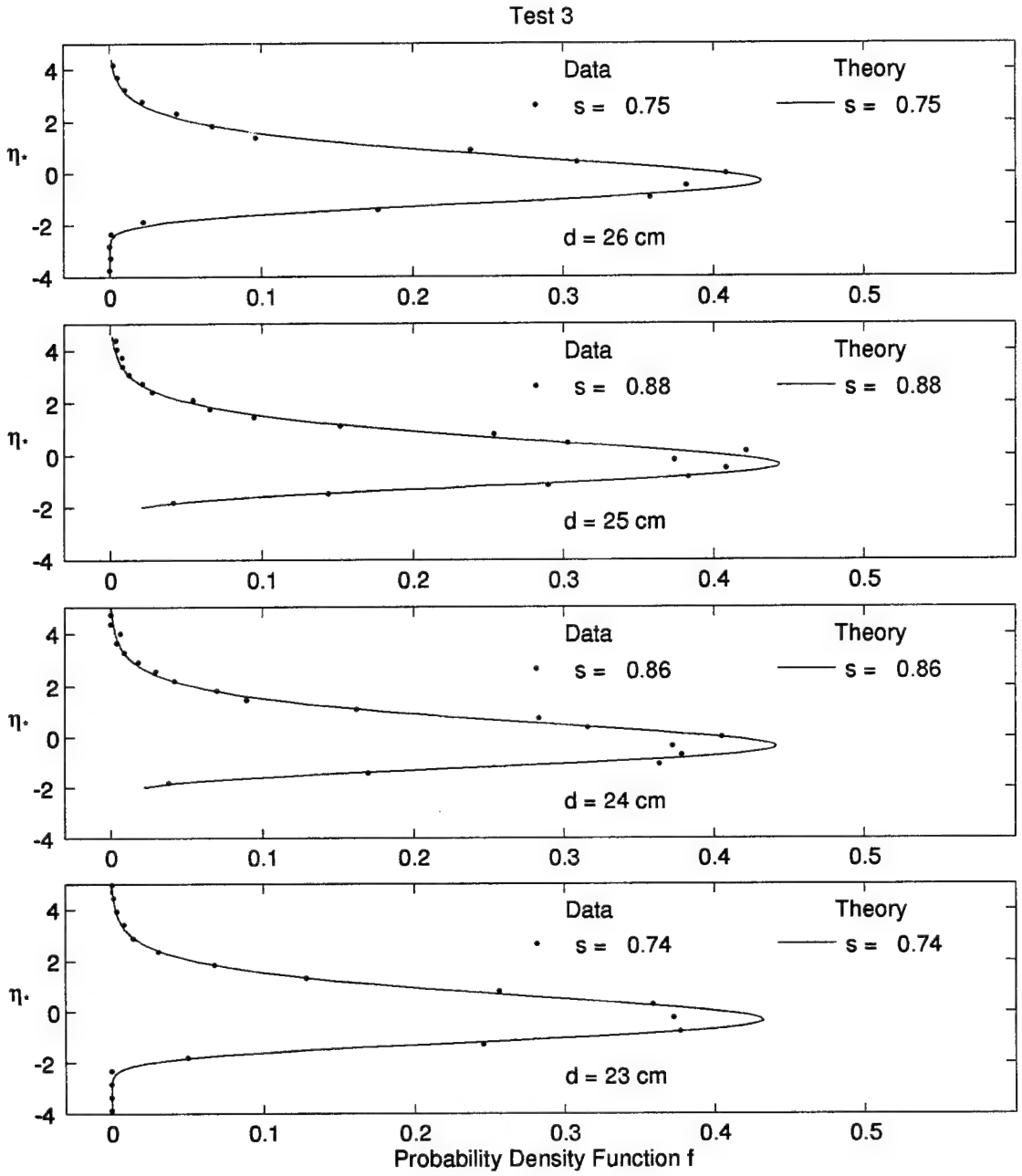

Figure 4.50: Measured and Computed Probability Distributions at Water Depth $d = 26$, 25, 24, and 23cm for Test 3

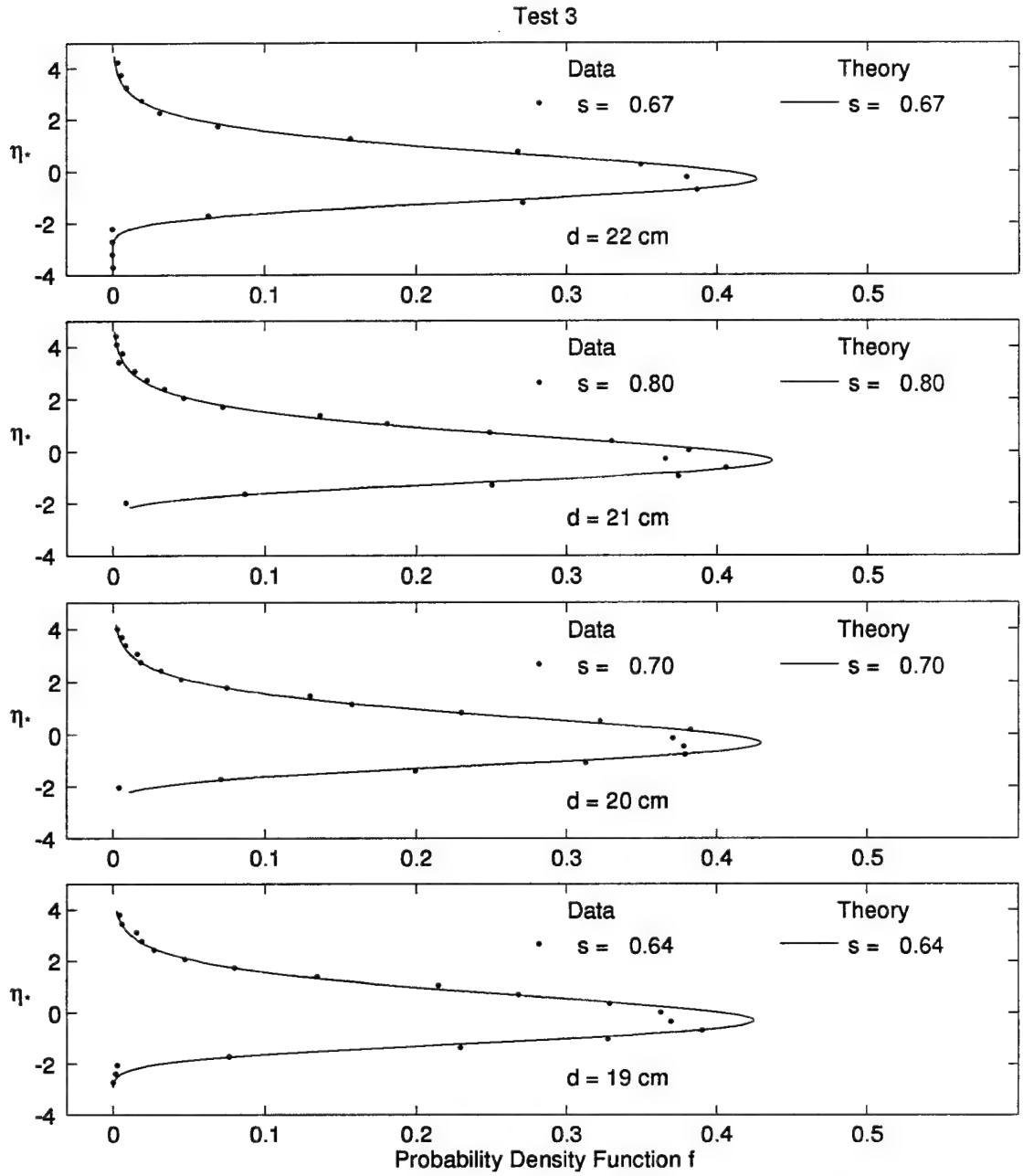

Figure 4.51: Measured and Computed Probability Distributions at Water Depth $d = 22$, 21, 20, and 19cm for Test 3

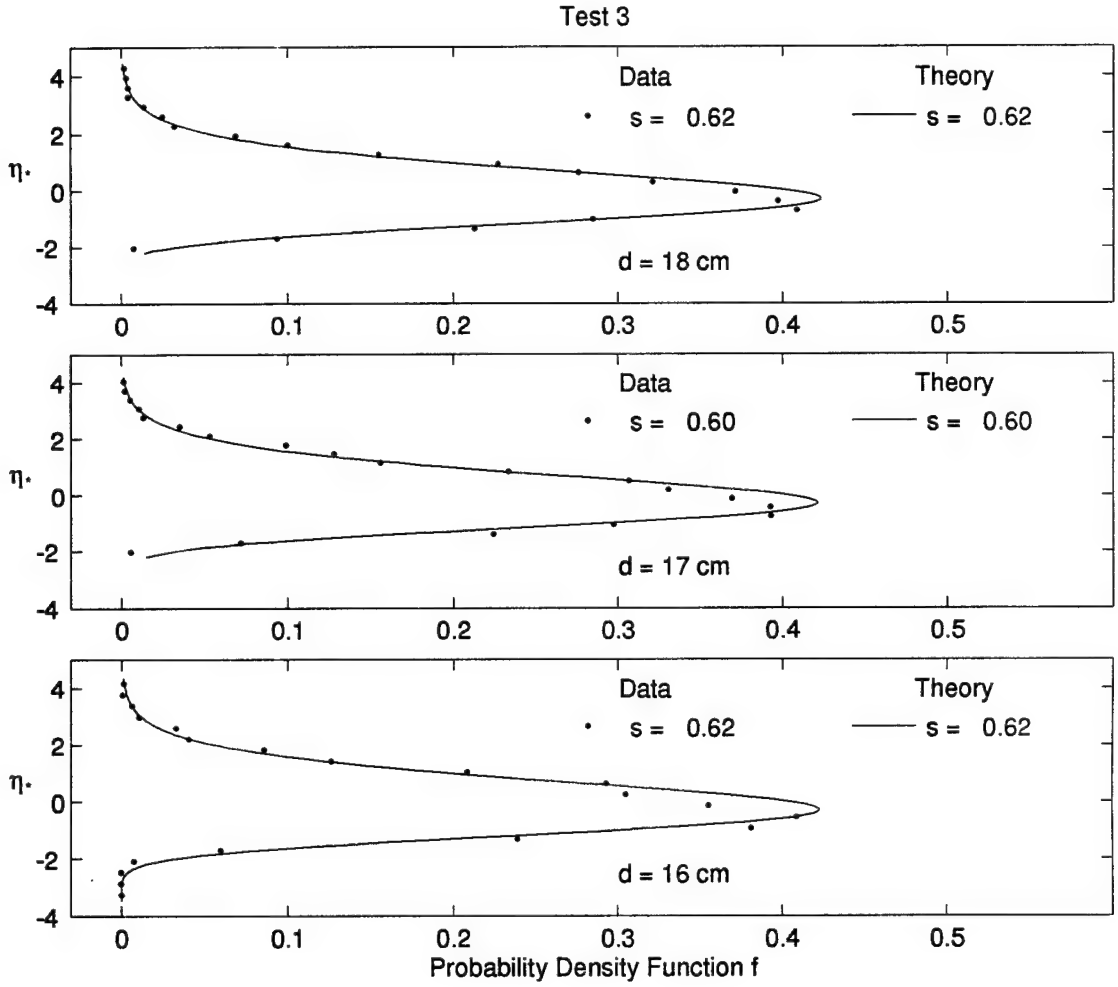

Figure 4.52: Measured and Computed Probability Distributions at Water Depth $d = 18$, 17, and 16cm for Test 3

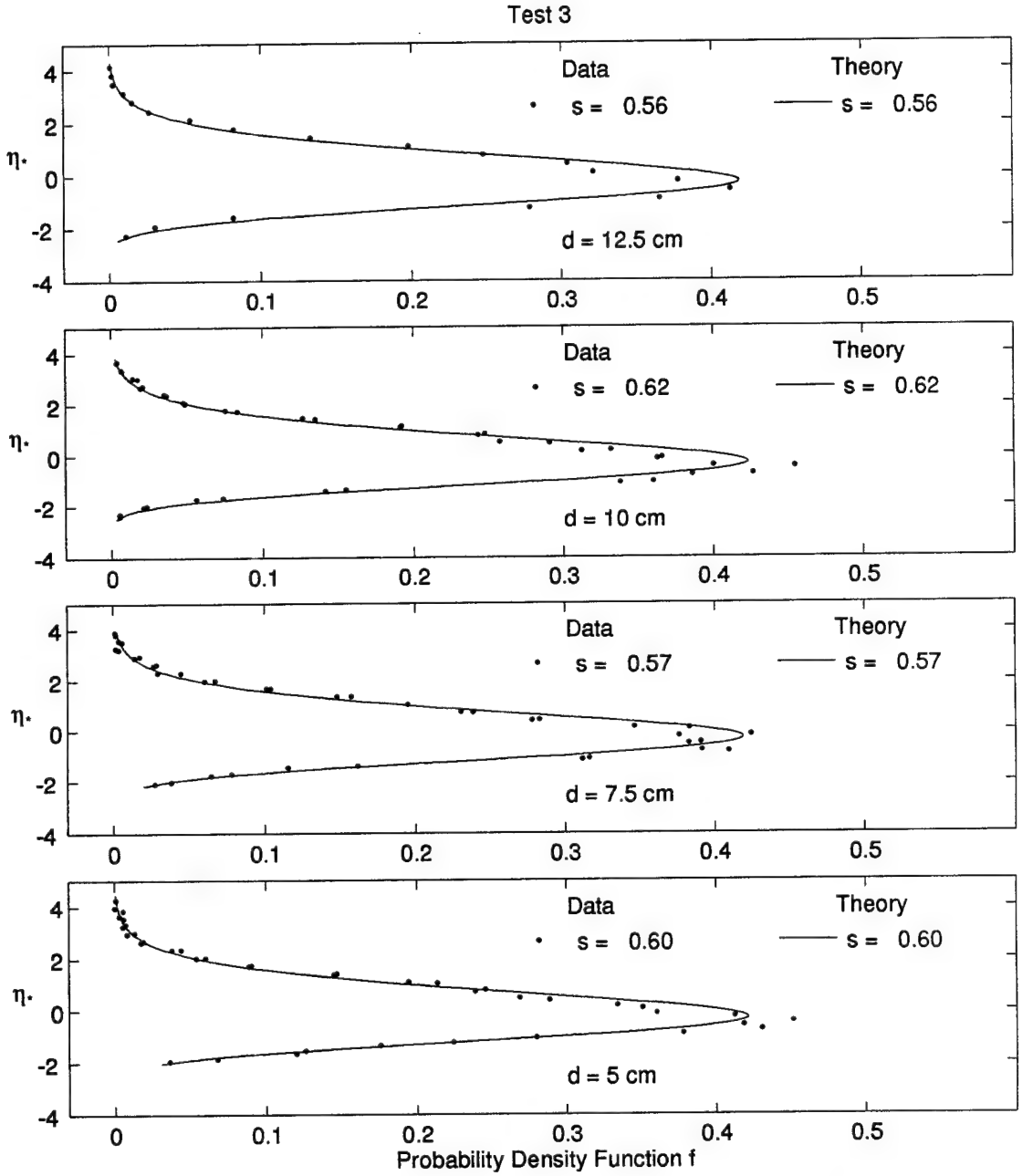

Figure 4.53: Measured and Computed Probability Distributions at Water Depth $d = 12.5$, 10, 7.5, and 5cm for Test 3

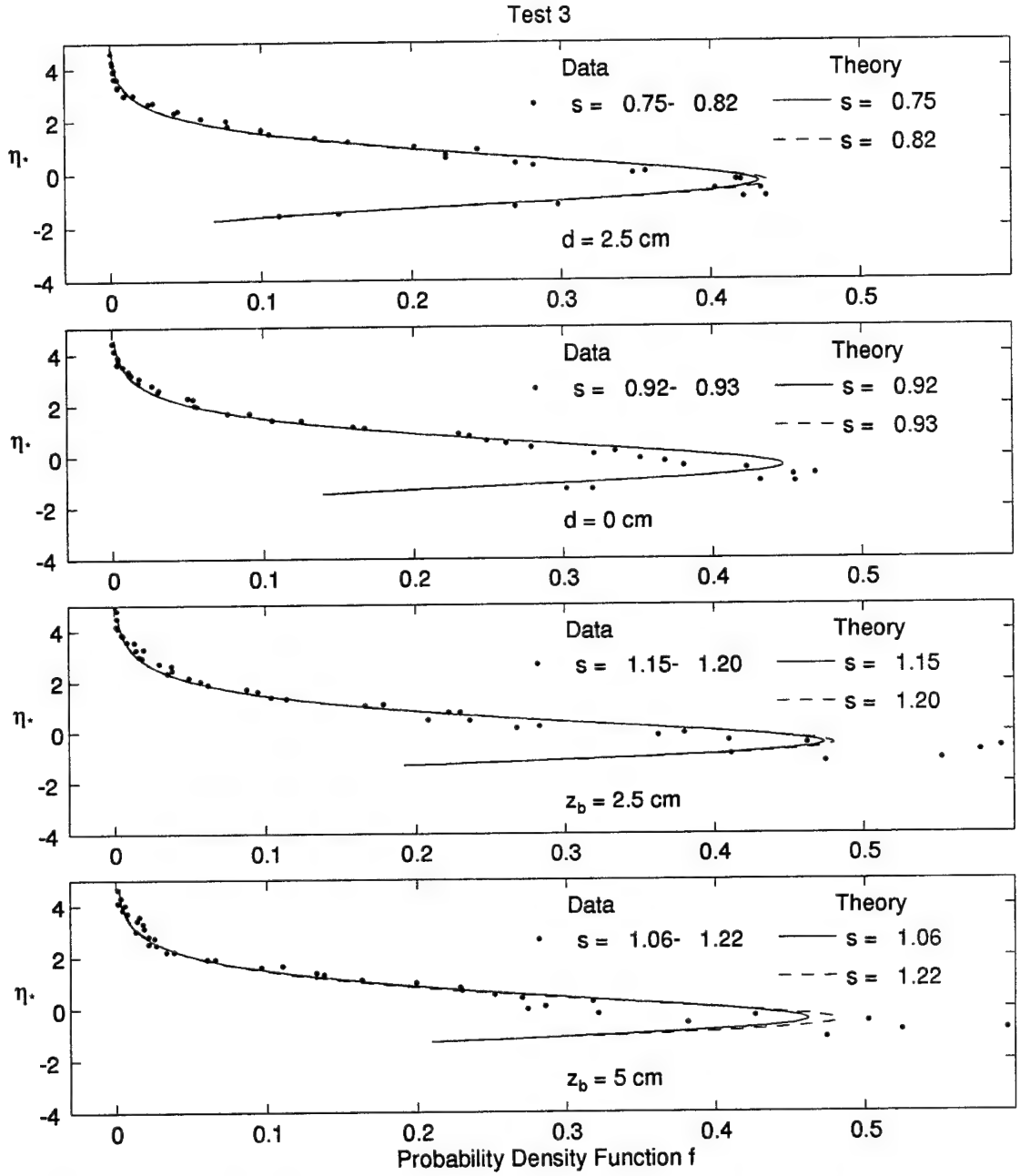

Figure 4.54: Measured and Computed Probability Distributions at Water Depth $d = 2.5$ and 0cm and Bottom Elevation $z_b = 2.5$ and 5cm for Test 3

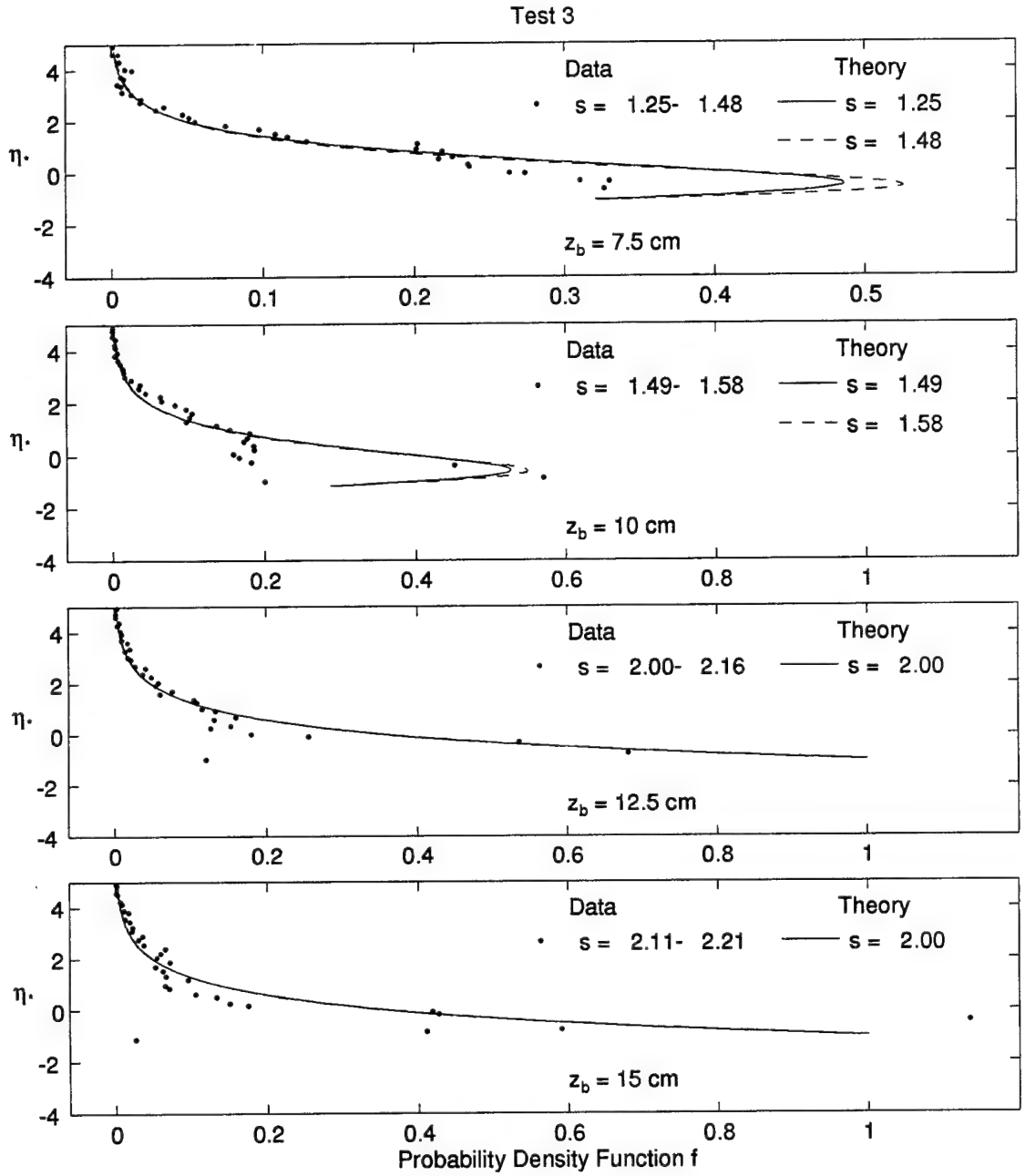

Figure 4.55: Measured and Computed Probability Distributions at Bottom Elevation z_b = 7.5, 10, 12.5, and 15cm for Test 3

Chapter 5

CROSS SHORE HORIZONTAL VELOCITIES

The mean velocity $\overline{u}$, the standard deviation σ_u, the skewness s_u, and the kurtosis K_u for each of the time series of the cross-shore horizontal velocity u measured at the mid-depth below SWL are computed under the assumption of equivalency of the probabilistic and time averaging. The horizontal velocity u is taken to be positive landward and the undertow velocity $\overline{u}$ is negative herein. The normalized horizontal velocity, $u_* = (u - \overline{u})/\sigma_u$, is then calculated using the measured values of $\overline{u}$ and σ_u. The probability density function, $f(u_*)$, for each of the time series of u_* is obtained and compared with the exponential gamma distribution given by equation (2.1) with (2.2) and (2.3) where η_* and s are replaced by u_* and s_u, respectively. The skewness and kurtosis are the same for u and u_*.

5.1 Horizontal Velocity and Linear Theory

To obtain approximate relationships between the free surface and horizontal velocity statistics, local nonlinearity may be neglected and linear progressive long-wave theory may be assumed to be approximately valid locally even inside surf zones (Guza and Thornton 1980). The oscillatory components of the horizontal velocity and free surface elevation may then be related in the following form:

$$(u - \overline{u}) \simeq \sqrt{\frac{g}{\overline{h}}}\,(\eta - \overline{\eta}) \tag{5.1}$$

in which g = gravitational acceleration and $\overline{h}$ = mean water depth given by $\overline{h} = (d + \overline{\eta})$ with d = still water depth. If equation (5.1) holds, the following relationships can be derived

$$\sigma_u \simeq \sqrt{\frac{g}{\overline{h}}}\sigma \quad ; \quad s_u \simeq s \quad ; \quad K_u \simeq K \tag{5.2}$$

in which σ, s and K are the standard deviation, skewness, and kurtosis of the free surface elevation η. Furthermore, the probability density functions of $u_* = (u - \overline{u})/\sigma_u$ and $\eta_* = (\eta - \overline{\eta})/\sigma$ become approximately the same because $u_* \simeq \eta_*$ under the assumption of (5.1) with $\sigma_u \simeq \sqrt{g/\overline{h}}\sigma$.

In order to estimate the undertow velocity $\overline{u}$, the horizontal velocity u at the mid-depth is assumed to be approximately equal to the depth-averaged velocity U. The time-averaged continuity equation, $\overline{hU} = 0$, for the impermeable beach yields (Kobayashi *et al.* 1989)

$$\overline{U} = -\left(\overline{h}\right)^{-1} \overline{(\eta - \overline{\eta})\left(U - \overline{U}\right)} \tag{5.3}$$

in which use is made of $h = (d + \eta)$. Substitution of $u \simeq U$ and equation (5.1) into (5.3) yields

$$\overline{u} \simeq -\sqrt{g\overline{h}}\left(\frac{\sigma}{\overline{h}}\right)^2 = -\frac{\sqrt{g\overline{h}}}{8}\left(\frac{H_{\rm rms}}{\overline{h}}\right)^2 \tag{5.4}$$

5.2 Spacial Variations of Statistical Values in Horizontal Velocity

Figures 5.1 – 5.3 show the cross-shore variations of the measured values of $\overline{u}$, σ_u, s_u and K_u in the still water depth d = 10–66 cm for tests 1–3, with the values also listed in Tables 5.1 – 5.3. The two data points at each cross-shore location, except for the landward two locations in Figure 5.1, correspond to the repeated velocity measurements for test 1. The repeatability of the velocity measurements is good except for the undertow velocity $\overline{u}$ in the shallow water. The computed values of $\overline{u}$, σ_u, s_u, and K_u at each cross-shore location shown in Figures 5.1 – 5.3 are based on equations (5.2) and (5.4) together with the measured values of $\overline{h} = (d + \overline{\eta})$, σ, s, and K at the same location.

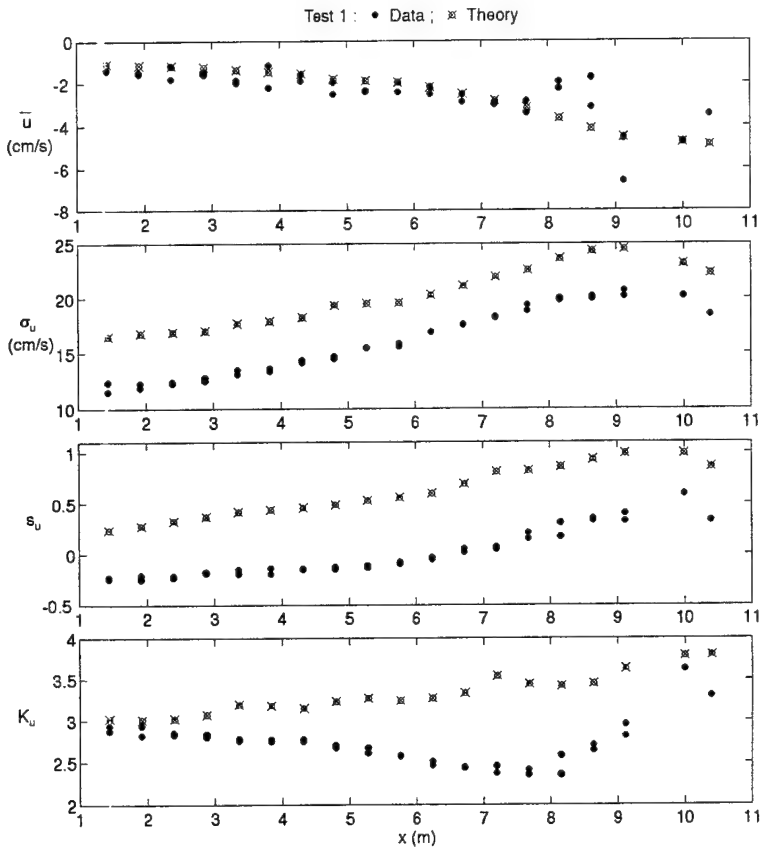

Figure 5.1: Measured and Computed Cross-Shore Variations of $\overline{u}$, σ_u, s_u, and K_u for Test 1

The fair (within about 20% errors) agreement between the measured and computed standard deviation σ_u in Figures 5.1 – 5.3 is expected from the field data intercomparisons made by Guza and Thornton (1980). For d = 10–66 cm with L_p = linear wavelength based on T_p, L_p/d = 5–14, 10–27, and 18–46 for tests 1, 2, and 3, respectively. The long-wave assumption may not be appropriate for test 1. It is noted that Guza and Thornton (1980) limited their analysis to the wind wave frequencies, whereas the measured time series without any filtering are used herein because it is difficult to separate wind wave and low-frequency components for practical applications. The fair agreement between the measured and computed

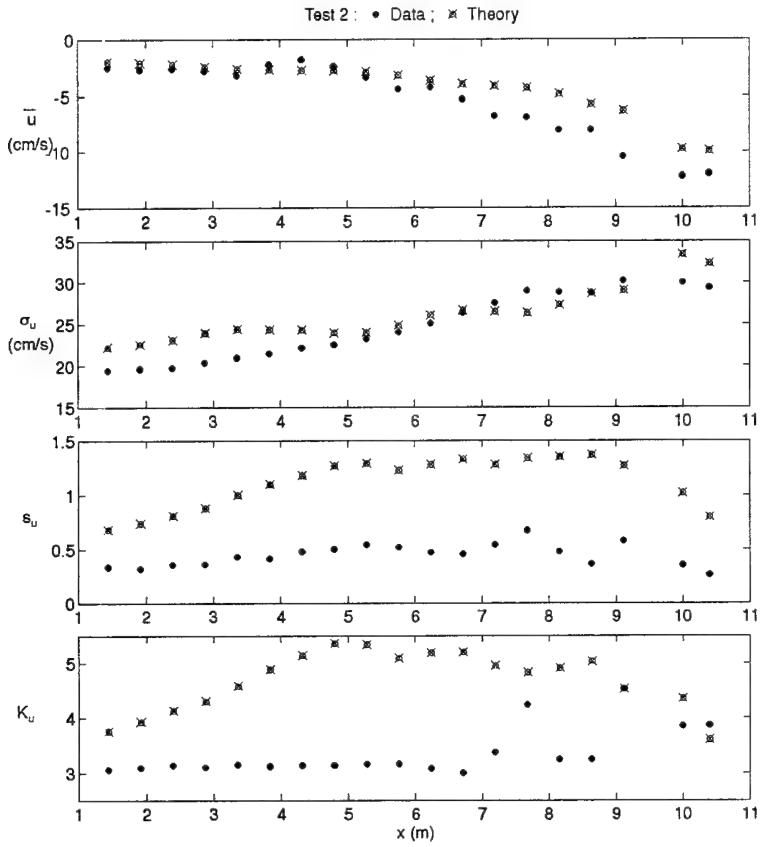

Figure 5.2: Measured and Computed Cross-Shore Variations of $\overline{u}$, σ_u, s_u, and K_u for Test 2

undertow $\overline{u}$ is unexpected because equation (5.4) based on (5.1) does not account for the additional water volume flux due to a roller which increases the magnitude of $\overline{u}$ as shown by Svendsen (1984) for regular waves. The underprediction of the magnitude of $\overline{u}$ in shallow water for tests 2 and 3 may be explained by this roller effect. The landward increases of $|\overline{u}|$ and σ_u in Figures 5.1 – 5.3 are qualitatively consistent with those based on the depth-averaged velocity U computed by Kobayashi and Karjadi (1996) using the finite-amplitude shallow-water equations. In view of equations (5.2) and (5.4), the landward increases of $|\overline{u}|$ and σ_u may simply be explained by the landward increase of $H_{\rm rms}/\overline{h}$ shown in Figures 4.2 – 4.4. In conclusion, the

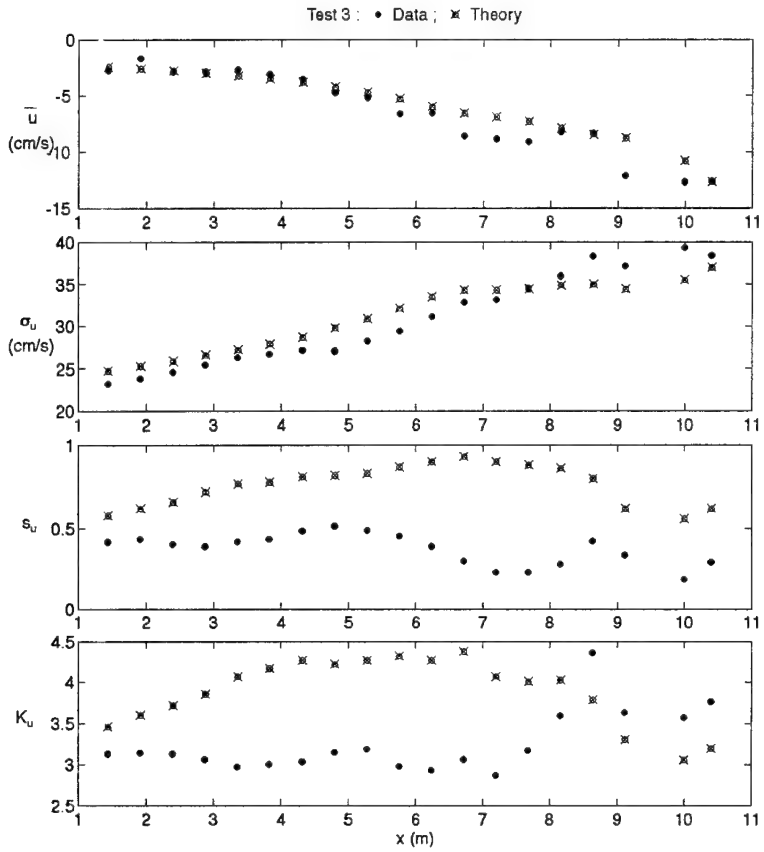

Figure 5.3: Measured and Computed Cross-Shore Variations of $\overline{u}$, σ_u, s_u, and K_u for Test 3

intercomparisons by Guza and Thornton (1980) and Figures 5.1 – 5.3 indicate that the local application of linear long-wave theory is approximately valid for the wave quantities up to the second order or moment in the shoaling and surf zones.

On the other hand, Figures 5.1 – 5.3 show that the skewness and kurtosis representing the third and fourth moments are not predicted well by linear long-wave theory. The skewness s_u of the horizontal velocity u at the mid-depth is always less than the skewness s of the free surface elevation η. This implies that nonlinearity decreases downward from the free surface. The difference $(s - s_u)$ tends to increase landward but fluctuates, partly because of the difficulty in measuring velocities in

very shallow water. On the average, the values of $(s - s_u)$ are on the order of 0.5. The measured values of s_u for the three tests exhibit noticeable differences. The skewness s_u in the shoaling regions in Figures 5.1 – 5.3 increases with the increase of the surf similarity parameter ξ where $\xi = 0.29$, 0.47 and 0.72 for tests 1, 2 and 3, respectively, as listed in Table 3.5. The skewness s_u in this shoaling region for test 1 is small and negative, which implies that the cross-shore velocities are skewed slightly seaward. The kurtosis, K_u, of the mid-depth horizontal velocity, u, and the kurtosis, K, of the free surface elevation, η, exhibit trends similar to s_u and s except that the measured kurtosis, K_u, in shallow water fluctuates widely and may not be very reliable. It is noted that the measured values of s_u and K_u for these three tests are qualitatively similar to the field data of Guza and Thornton (1985).

5.3 Measured and Theoretical Probability Density Functions

The measured probability density function, $f(u_*)$, is compared individually with the exponential gamma distribution based on the measured skewness, s_u. The agreement is good except for slight deviations at the peaks of $f(u_*)$. To show the degree of the overall agreement for tests 1–3, the measured distributions are separated into two groups on the basis of the measured skewness s_u. Figure 5.4 shows the measured distributions with s_u = (-0.25) – 0.36 in comparison with the exponential gamma distributions with $s_u = 0$ and 0.36 where $s_u \geq 0$ is assumed to be consistent with the assumption of $s \geq 0$ made in (2.1). The measured distributions with $s_u = 0.39$ – 0.67 are compared with the exponential gamma distributions with $s_u = 0.39$ and 0.67. The exponential gamma distributions do not deviate much within the specified range of s_u. Figure 5.4 indicates that most of the data points fall between the two theoretical curves, apart from the scatter near the peak of $f(u_*)$. The agreement is similar to those shown in Figures 4.5 – 4.7 for the free surface elevations. It is not certain whether the exponential gamma distribution is

applicable to horizontal velocities near the still water shoreline for lack of data. The individual comparisons are shown in Figures 5.5 – 5.19 for completeness.

Table 5.1: Velocity Data Table Test 1

Run	z_b (m)	$\overline{h}$ (cm)	σ_η (cm)	$\overline{u}$ (cm/s)			σ_u (cm/s)			Skewness			Kurtosis		
				Data		Theory	Data		Theory	S_u		S_η	K_u		K_η
1-18	-0.66	65.81	4.28	-1.37	-1.40	-1.07	11.47	12.33	16.52	-0.25	-0.23	0.24	2.93	2.87	3.02
1-19	-0.63	62.93	4.25	-1.55	-1.48	-1.13	11.84	12.23	16.78	-0.25	-0.21	0.28	2.93	2.82	3.01
1-20	-0.60	59.86	4.18	-1.81	-1.20	-1.18	12.38	12.26	16.92	-0.23	-0.21	0.33	2.85	2.83	3.02
1-21	-0.57	56.72	4.10	-1.46	-1.60	-1.23	12.75	12.45	17.05	-0.19	-0.18	0.37	2.83	2.80	3.07
1-22	-0.54	53.95	4.15	-1.86	-1.99	-1.36	13.03	13.45	17.70	-0.16	-0.19	0.42	2.78	2.76	3.19
1-23	-0.51	50.87	4.08	-2.20	-1.15	-1.44	13.59	13.36	17.92	-0.14	-0.19	0.44	2.75	2.77	3.18
1-24	-0.48	47.99	4.04	-1.58	-1.89	-1.54	14.10	14.34	18.27	-0.15	-0.14	0.46	2.75	2.77	3.15
1-25	-0.45	45.00	4.15	-2.52	-1.96	-1.79	14.67	14.45	19.38	-0.14	-0.13	0.49	2.67	2.70	3.23
1-26	-0.42	41.93	4.04	-2.38	-2.38	-1.88	15.45	15.42	19.54	-0.13	-0.12	0.53	2.61	2.67	3.27
1-27	-0.39	39.03	3.91	-2.42	-1.97	-1.96	15.85	15.54	19.60	-0.08	-0.10	0.56	2.57	2.58	3.24
1-28	-0.36	35.80	3.88	-2.17	-2.52	-2.20	16.87	16.88	20.31	-0.04	-0.05	0.60	2.46	2.51	3.27
1-29	-0.33	32.90	3.87	-2.54	-2.89	-2.49	17.56	17.55	21.13	0.05	0.01	0.69	2.43	2.44	3.33
1-30	-0.30	29.91	3.84	-3.00	-2.91	-2.82	18.28	18.18	21.99	0.04	0.07	0.81	2.37	2.45	3.54
1-31	-0.27	26.95	3.75	-3.41	-2.85	-3.15	19.34	18.81	22.62	0.21	0.15	0.82	2.41	2.35	3.44
1-32	-0.24	23.93	3.69	-1.96	-2.27	-3.64	19.82	19.98	23.63	0.31	0.17	0.86	2.58	2.35	3.42
1-33	-0.21	20.95	3.56	-3.12	-1.76	-4.14	20.15	19.90	24.36	0.35	0.33	0.93	2.64	2.70	3.45
1-34	-0.18	18.06	3.33	-6.64	-4.62	-4.53	20.67	20.15	24.54	0.40	0.32	0.99	2.95	2.81	3.63
1-35	-0.125	12.83	2.65	-4.78	–	-4.79	20.17	–	23.18	0.59	–	0.99	3.62	–	3.79
1-36	-0.10	10.52	2.31	-3.46	–	-4.90	18.46	–	22.31	0.33	–	0.86	3.30	–	3.80

Table 5.2: Velocity Data Table Test 2

				$\overline{u}$ (cm/s)		σ_u (cm/s)		Skewness		Kurtosis	
Run	$z_b(m)$	$\overline{h}$ (cm)	σ_η (cm)	Data	Theory	Data	Theory	S_u	S_η	K_u	K_η
2-18	-0.66	65.80	5.75	-2.50	-1.94	19.43	22.20	0.33	0.68	3.06	3.76
2-19	-0.63	62.89	5.72	-2.64	-2.05	19.60	22.59	0.32	0.74	3.09	3.93
2-20	-0.60	59.93	5.71	-2.61	-2.20	19.71	23.10	0.35	0.81	3.14	4.13
2-21	-0.57	56.97	5.77	-2.78	-2.43	20.36	23.94	0.36	0.88	3.10	4.30
2-22	-0.54	53.96	5.72	-3.22	-2.59	20.92	24.39	0.43	1.00	3.15	4.58
2-23	-0.51	50.94	5.55	-2.24	-2.65	21.42	24.36	0.41	1.10	3.12	4.89
2-24	-0.48	47.91	5.37	-1.82	-2.72	22.10	24.30	0.48	1.18	3.14	5.14
2-25	-0.45	44.92	5.13	-2.41	-2.74	22.49	23.97	0.50	1.27	3.14	5.36
2-26	-0.42	41.91	4.96	-3.34	-2.84	23.19	24.00	0.54	1.29	3.16	5.34
2-27	-0.39	38.94	4.95	-4.44	-3.16	23.97	24.85	0.52	1.23	3.16	5.09
2-28	-0.36	36.08	5.00	-4.23	-3.61	25.04	26.07	0.47	1.28	3.08	5.19
2-29	-0.33	33.03	4.89	-5.31	-3.95	26.33	26.65	0.45	1.33	3.00	5.20
2-30	-0.30	30.07	4.64	-6.82	-4.09	27.46	26.50	0.54	1.28	3.37	4.95
2-31	-0.27	27.10	4.38	-6.93	-4.26	28.92	26.35	0.67	1.34	4.23	4.83
2-32	-0.24	24.42	4.31	-8.10	-4.82	28.76	27.32	0.48	1.35	3.24	4.91
2-33	-0.21	21.20	4.22	-8.07	-5.71	28.73	28.71	0.36	1.37	3.24	5.03
2-34	-0.18	18.30	3.97	-10.47	-6.31	30.20	29.07	0.58	1.27	4.52	4.53
2-35	-0.125	13.31	3.89	-12.23	-9.76	29.95	33.40	0.35	1.02	3.85	4.35
2-36	-0.10	11.31	3.47	-12.00	-9.92	29.37	32.32	0.26	0.80	3.86	3.61

Table 5.3: Velocity Data Table Test 3

				$\overline{u}$ (cm/s)		σ_u (cm/s)		Skewness		Kurtosis	
Run	$z_b(m)$	$\overline{h}$ (cm)	σ_η (cm)	Data	Theory	Data	Theory	S_u	S_η	K_u	K_η
3-18	-0.66	65.79	6.41	-2.75	-2.41	23.19	24.75	0.42	0.58	3.13	3.46
3-19	-0.63	62.85	6.41	-1.70	-2.58	23.76	25.32	0.43	0.62	3.14	3.60
3-20	-0.60	59.81	6.39	-2.93	-2.76	24.55	25.88	0.40	0.66	3.13	3.72
3-21	-0.57	56.84	6.40	-2.86	-2.99	25.44	26.59	0.39	0.72	3.06	3.86
3-22	-0.54	53.82	6.37	-2.68	-3.22	26.26	27.20	0.42	0.77	2.97	4.07
3-23	-0.51	50.81	6.35	-3.08	-3.49	26.69	27.90	0.43	0.78	3.00	4.17
3-24	-0.48	47.78	6.33	-3.56	-3.80	27.15	28.68	0.48	0.81	3.03	4.27
3-25	-0.45	44.77	6.36	-4.76	-4.23	27.01	29.77	0.51	0.82	3.15	4.22
3-26	-0.42	41.78	6.37	-5.20	-4.71	28.20	30.87	0.49	0.83	3.19	4.27
3-27	-0.39	38.77	6.38	-6.62	-5.28	29.36	32.09	0.45	0.87	2.98	4.32
3-28	-0.36	35.85	6.40	-6.56	-5.98	31.08	33.48	0.39	0.90	2.93	4.27
3-29	-0.33	32.80	6.27	-8.62	-6.55	32.77	34.29	0.30	0.93	3.06	4.38
3-30	-0.30	29.90	5.99	-8.86	-6.87	33.09	34.31	0.23	0.90	2.87	4.07
3-31	-0.27	26.99	5.71	-9.10	-7.28	34.45	34.42	0.23	0.88	3.17	4.01
3-32	-0.24	24.23	5.48	-8.26	-7.89	35.92	34.87	0.28	0.86	3.59	4.03
3-33	-0.21	21.45	5.17	-8.37	-8.43	38.27	34.96	0.42	0.80	4.36	3.79
3-34	-0.18	18.75	4.76	-12.14	-8.74	37.14	34.43	0.33	0.62	3.63	3.31
3-35	-0.125	13.93	4.23	-12.69	-10.78	39.27	35.50	0.18	0.56	3.57	3.06
3-36	-0.10	11.93	4.08	-12.59	-12.65	38.37	37.00	0.29	0.62	3.76	3.20

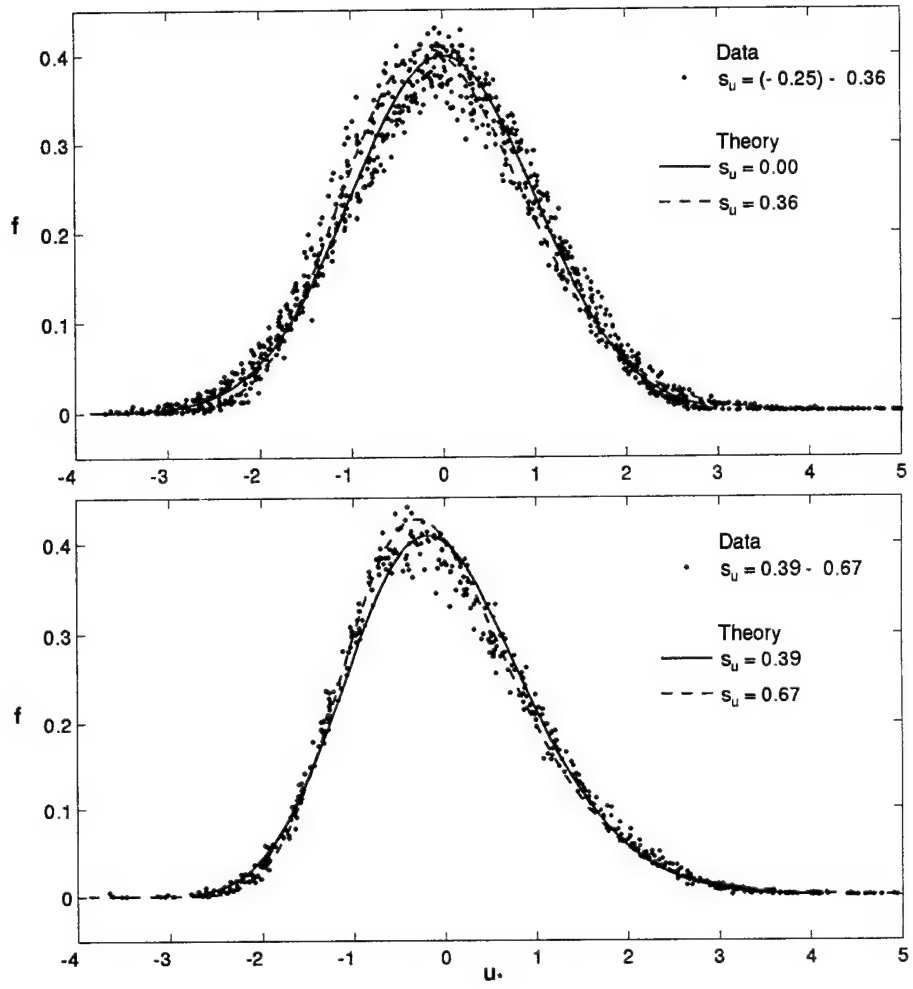

Figure 5.4: Measured and Computed Probability Distributions of Horizontal Velocities for Tests 1–3

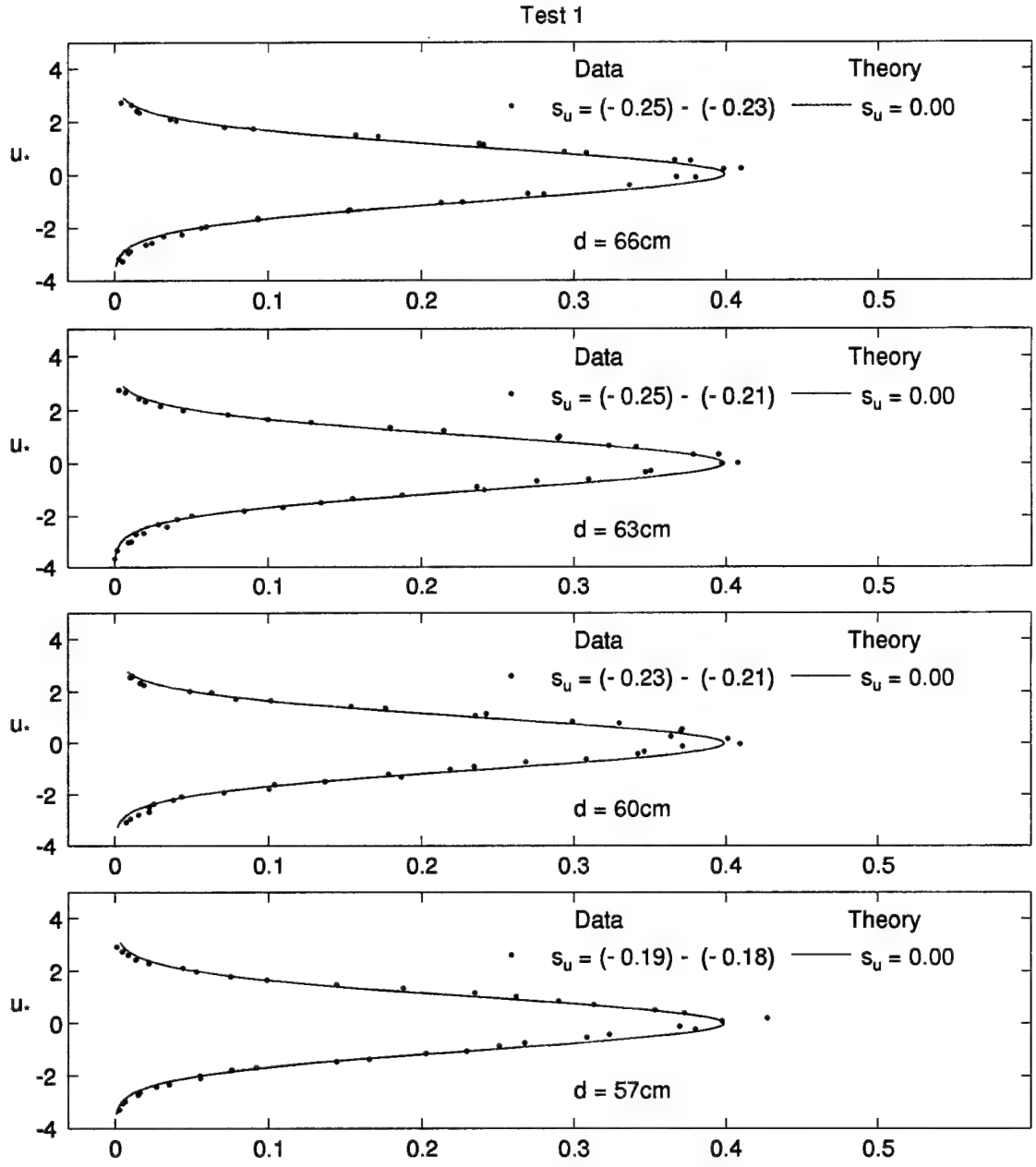

Figure 5.5: Measured and Computed Probability Distributions for Horizontal Velocity at Water Depth d = 66, 63, 60, and 57cm for Test 1

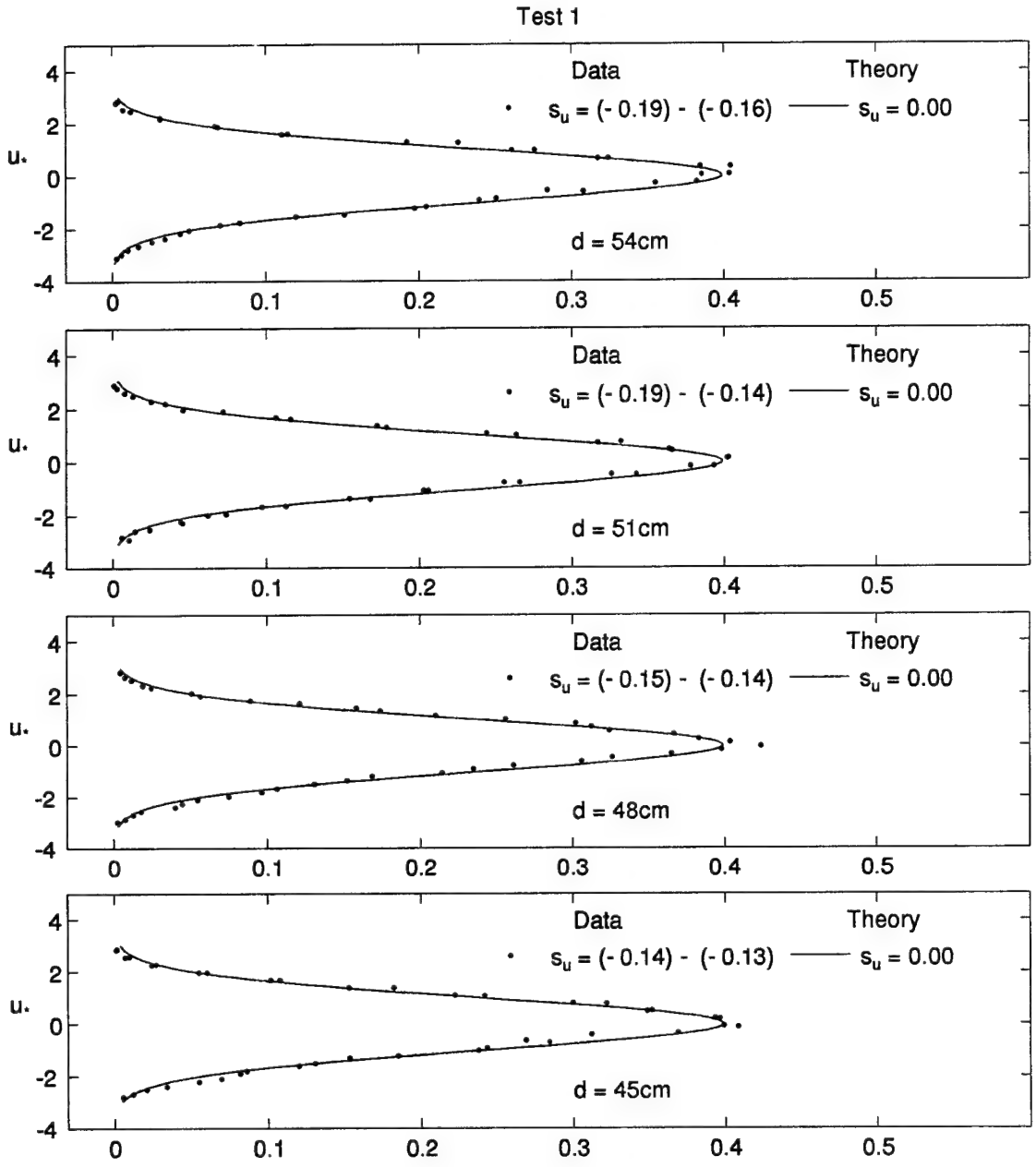

Figure 5.6: Measured and Computed Probability Distributions for Horizontal Velocity at Water Depth d = 54, 51, 48, and 45cm for Test 1

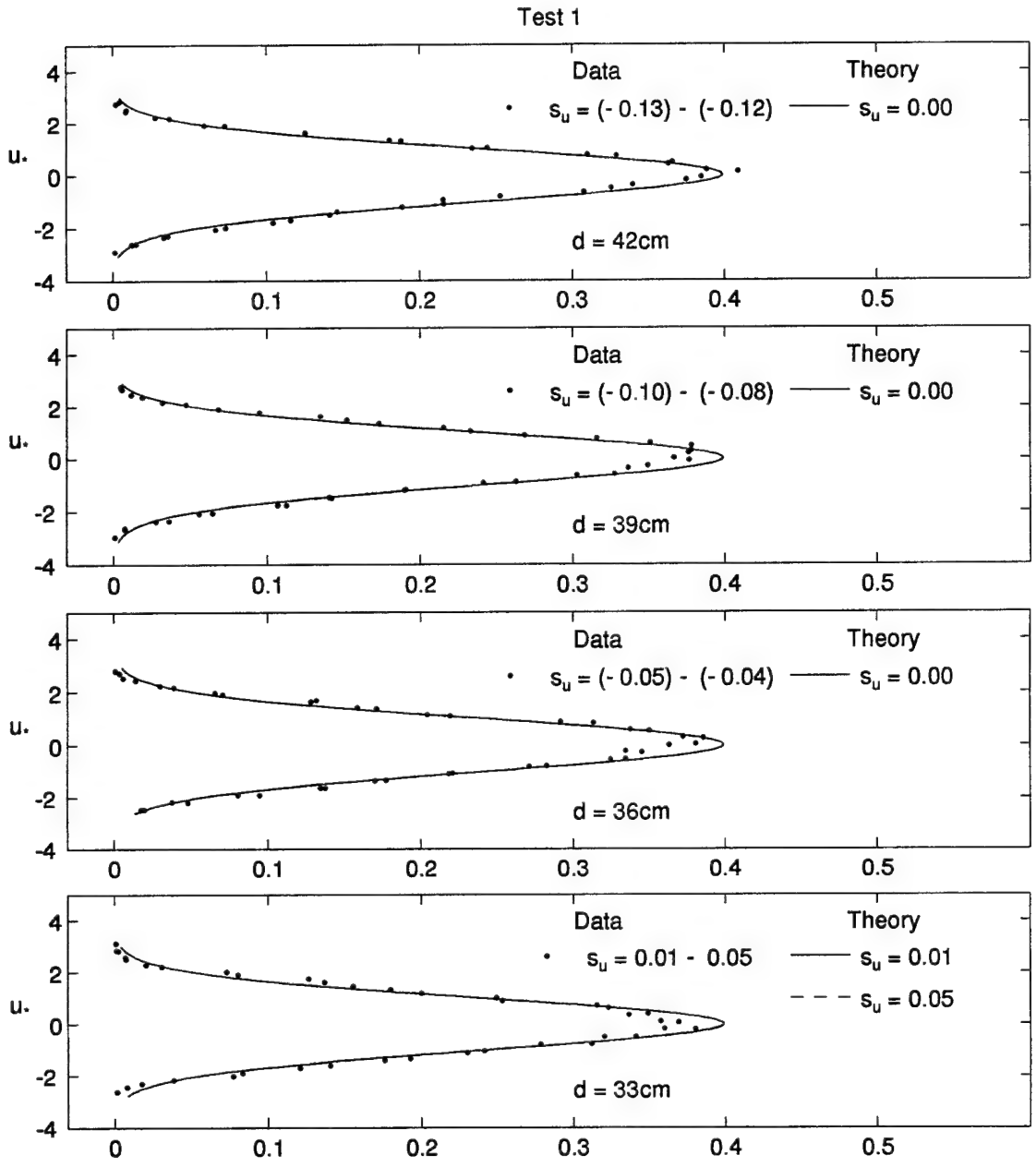

Figure 5.7: Measured and Computed Probability Distributions for Horizontal Velocity at Water Depth $d = 42$, 39, 36, and 33cm for Test 1

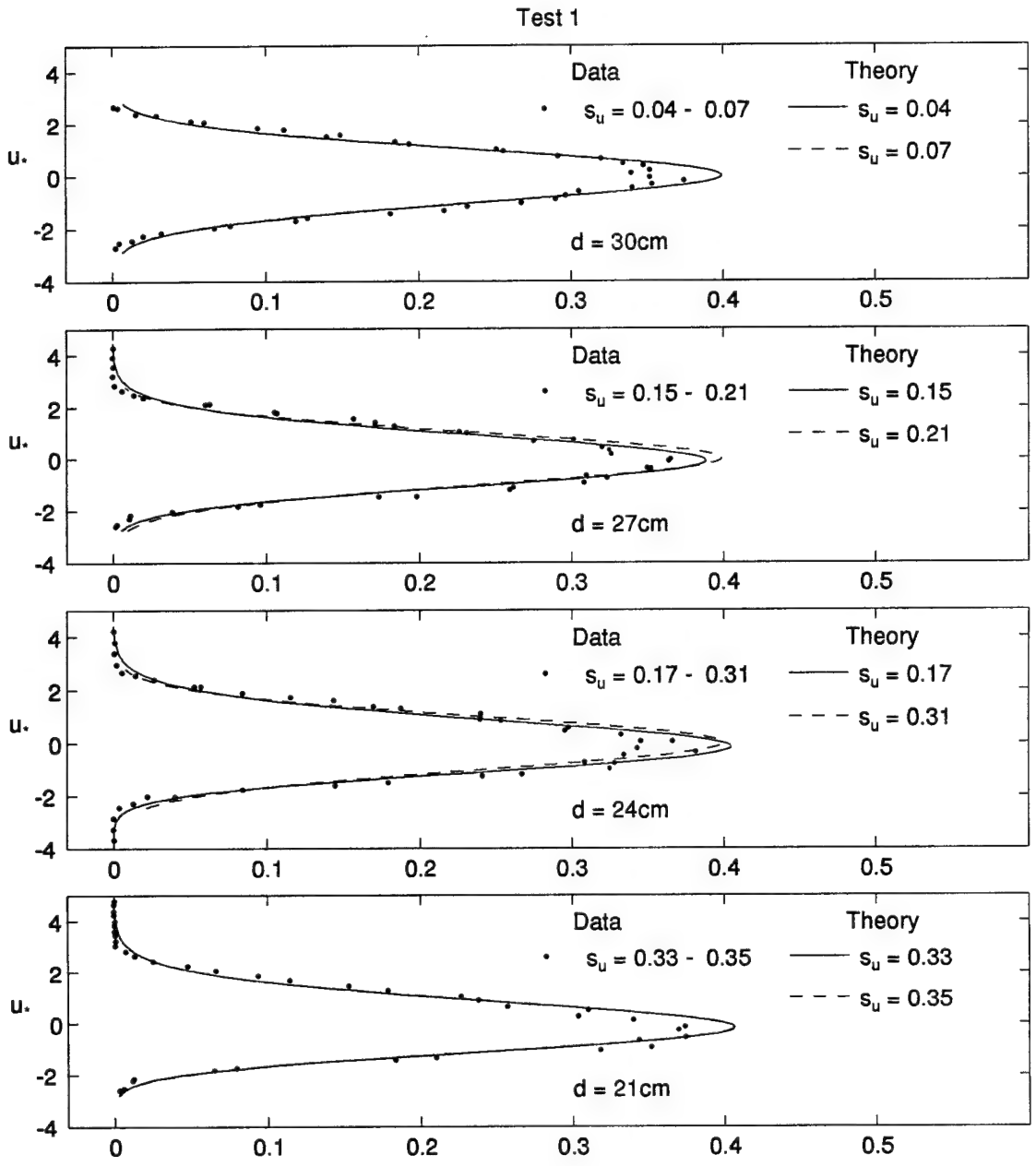

Figure 5.8: Measured and Computed Probability Distributions for Horizontal Velocity at Water Depth $d = 30$, 27, 24, and 21cm for Test 1

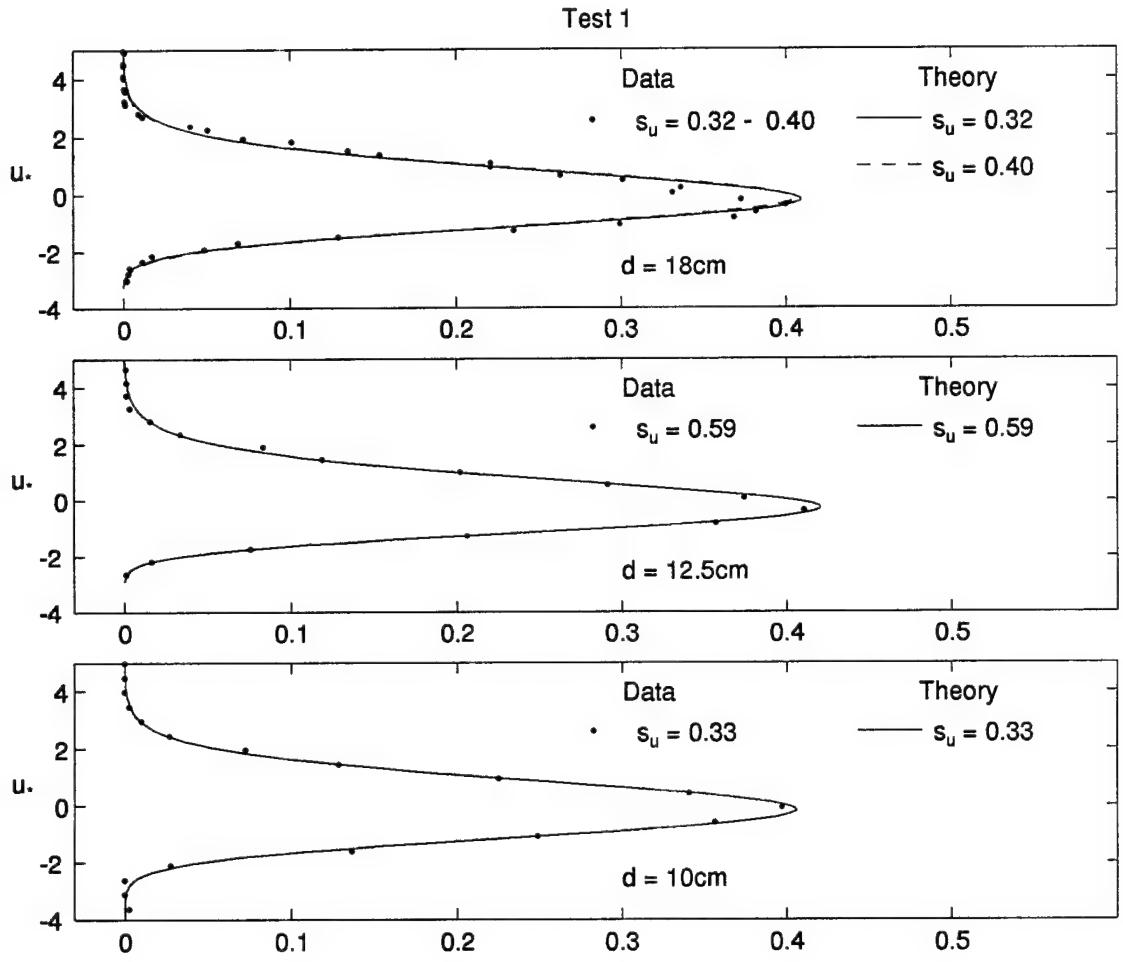

Figure 5.9: Measured and Computed Probability Distributions for Horizontal Velocity at Water Depth $d = 18$, 12.5, and 10cm for Test 1

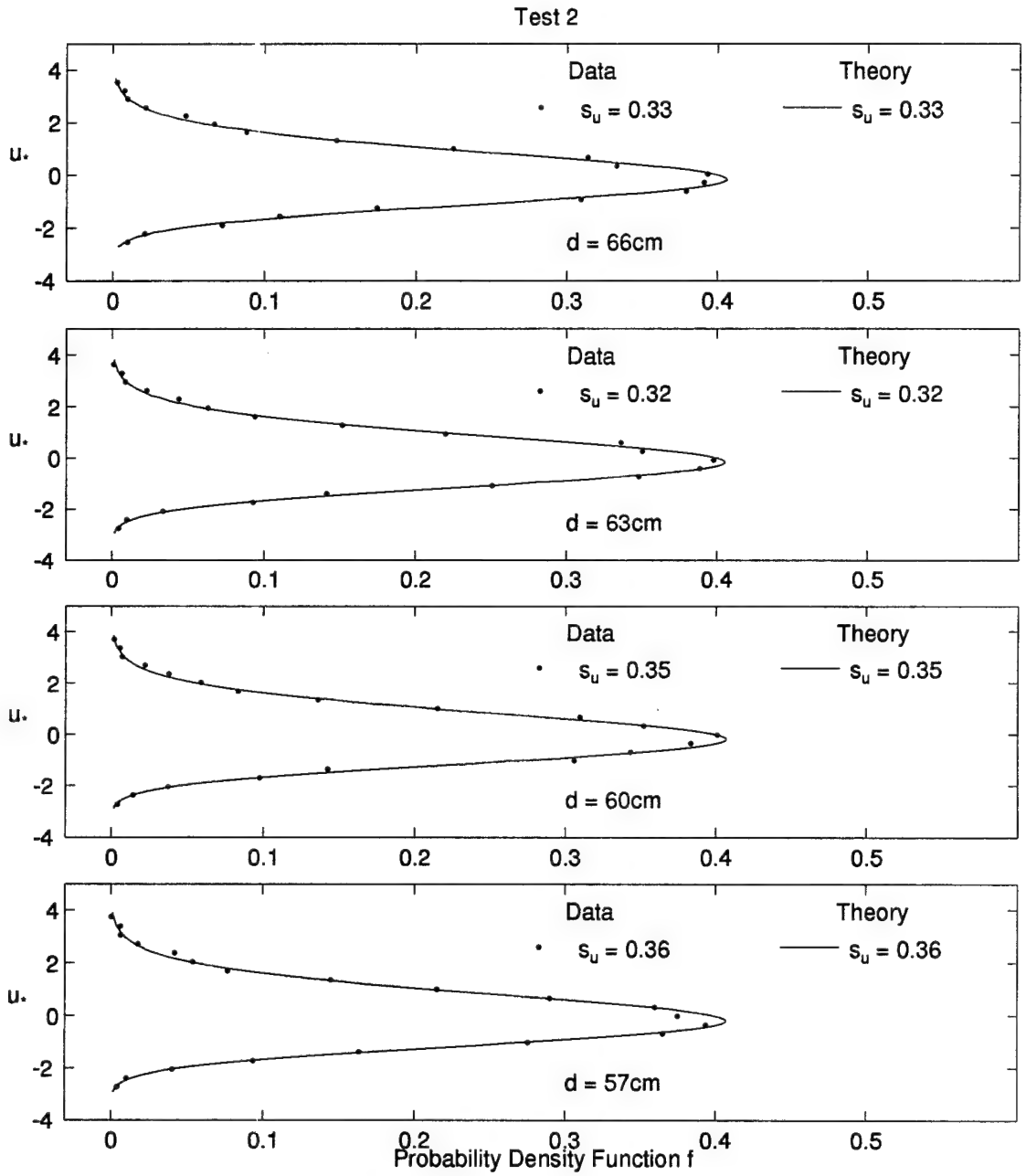

Figure 5.10: Measured and Computed Probability Distributions for Horizontal Velocity at Water Depth d = 66, 63, 60, and 57cm for Test 2

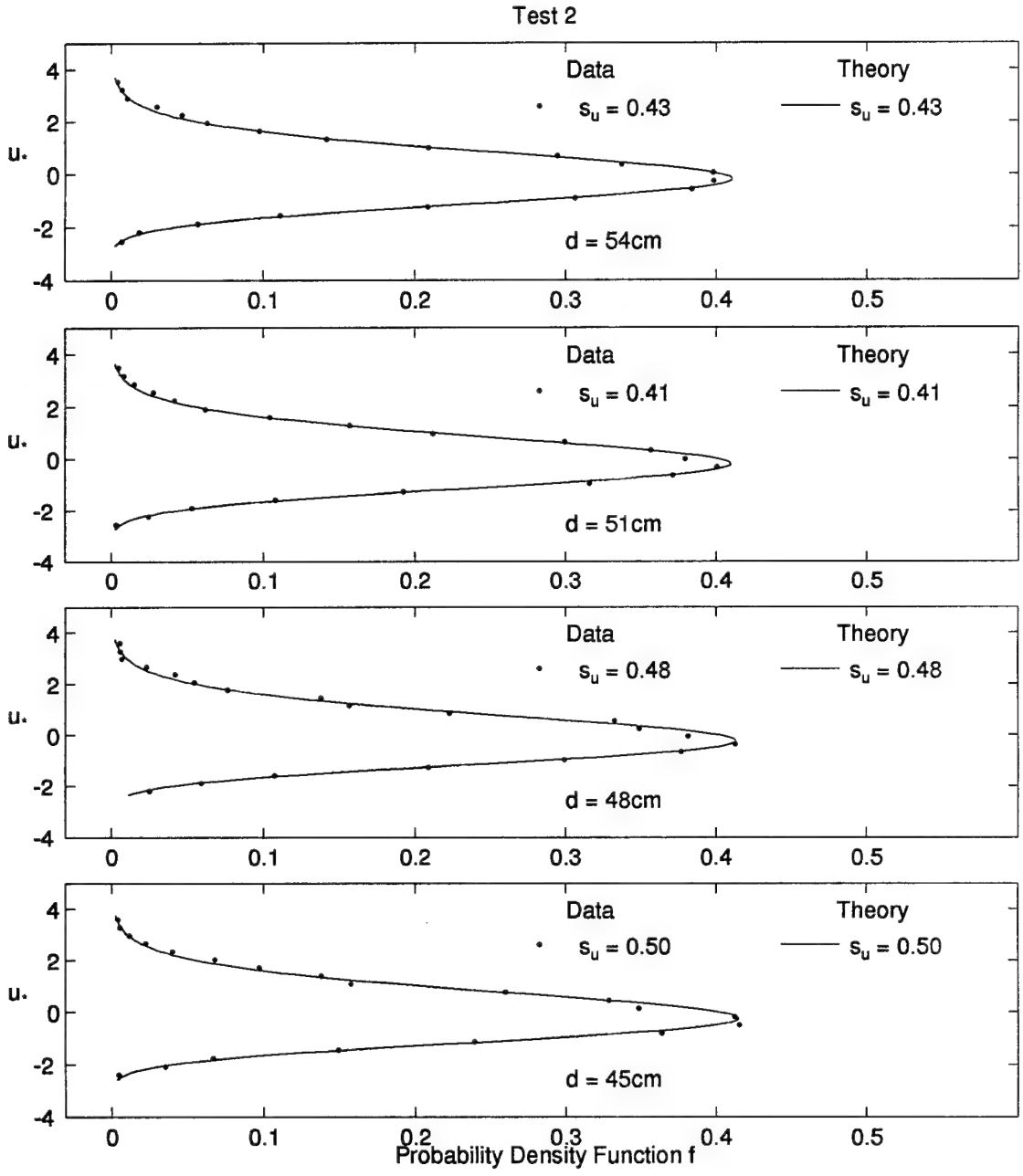

Figure 5.11: Measured and Computed Probability Distributions for Horizontal Velocity at Water Depth d = 54, 51, 48, and 45cm for Test 2

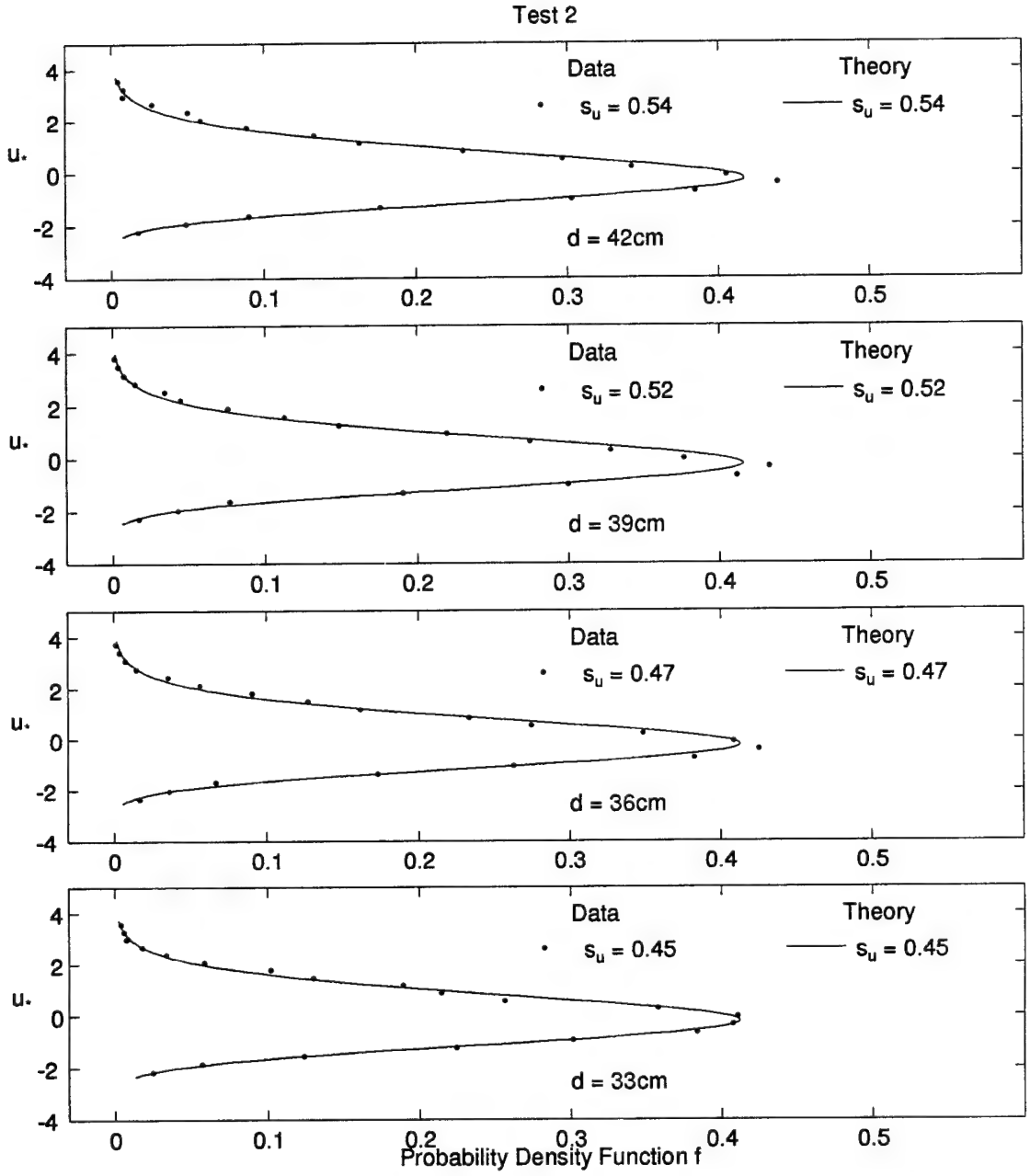

Figure 5.12: Measured and Computed Probability Distributions for Horizontal Velocity at Water Depth d = 42, 39, 36, and 33cm for Test 2

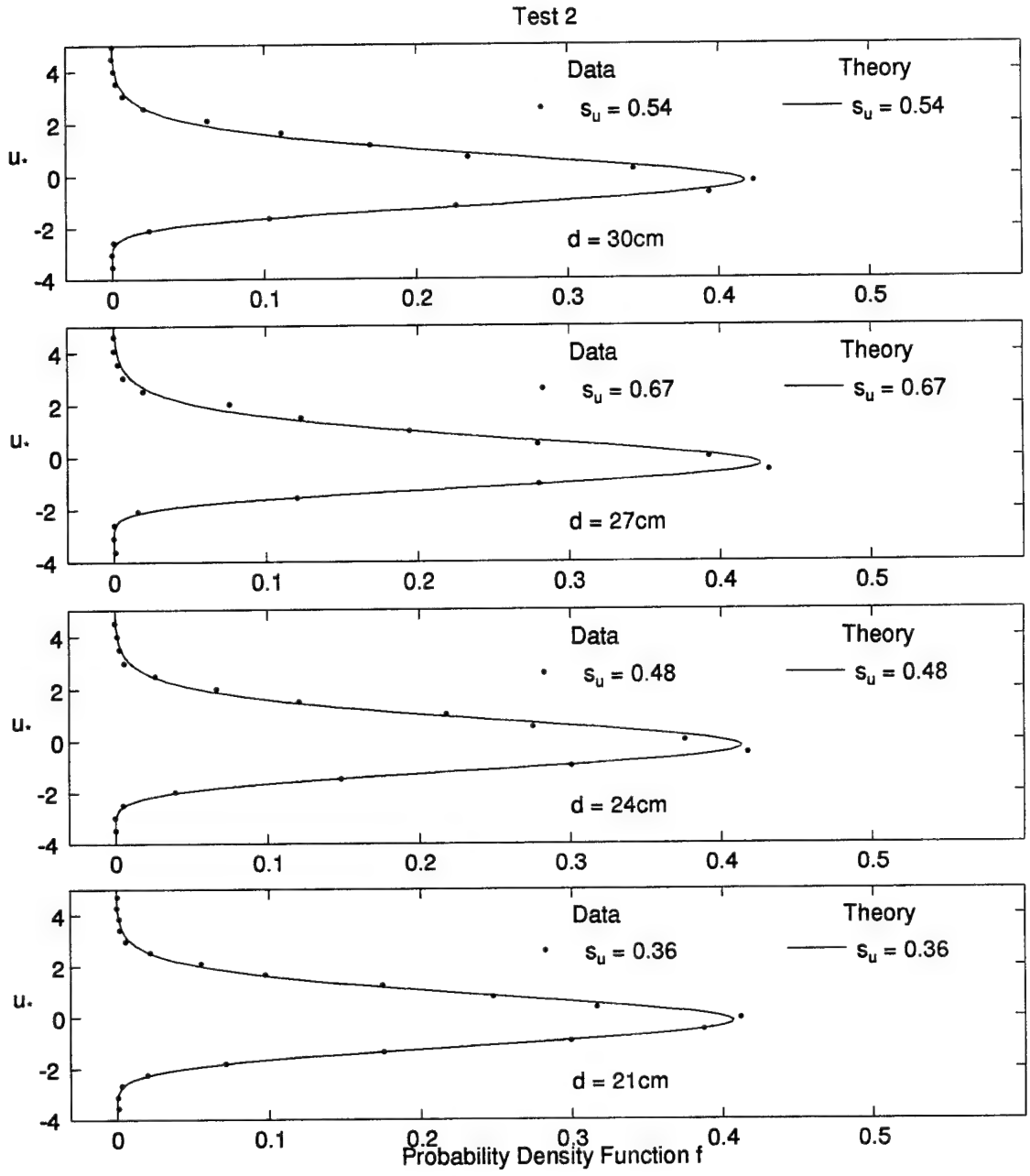

Figure 5.13: Measured and Computed Probability Distributions for Horizontal Velocity at Water Depth d = 30, 27, 24, and 21cm for Test 2

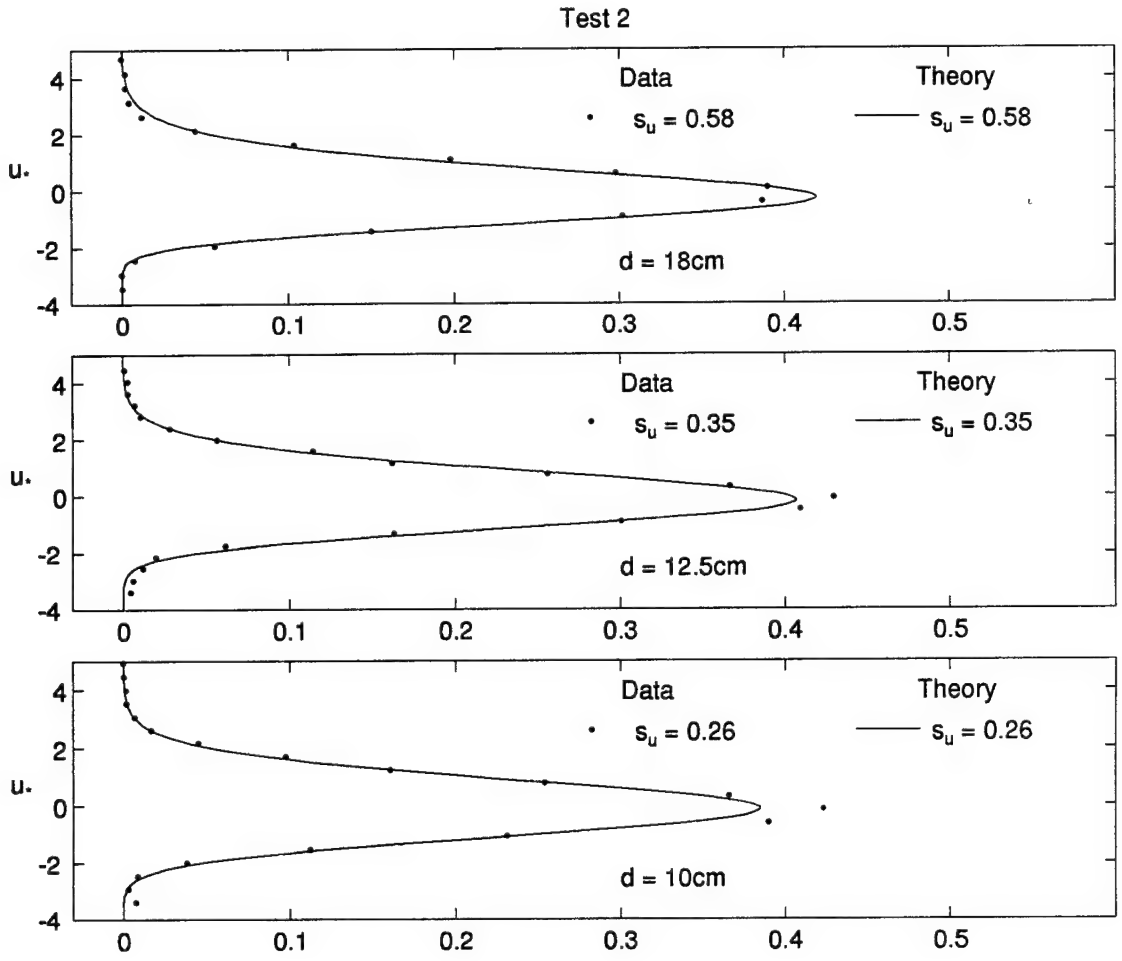

Figure 5.14: Measured and Computed Probability Distributions for Horizontal Velocity at Water Depth $d = 18$, 12.5, and 10cm for Test 2

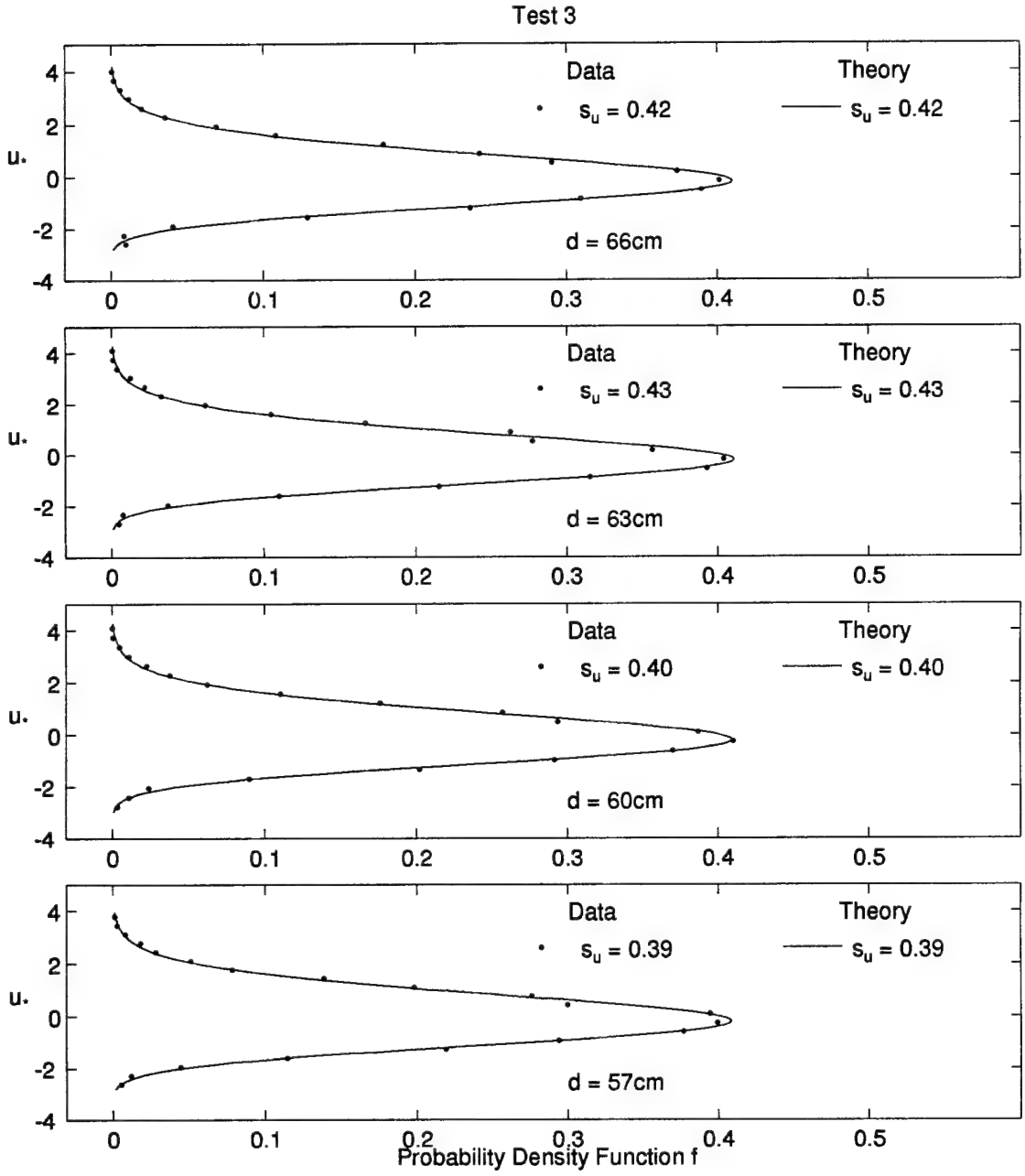

Figure 5.15: Measured and Computed Probability Distributions for Horizontal Velocity at Water Depth d = 66, 63, 60, and 57cm for Test 3

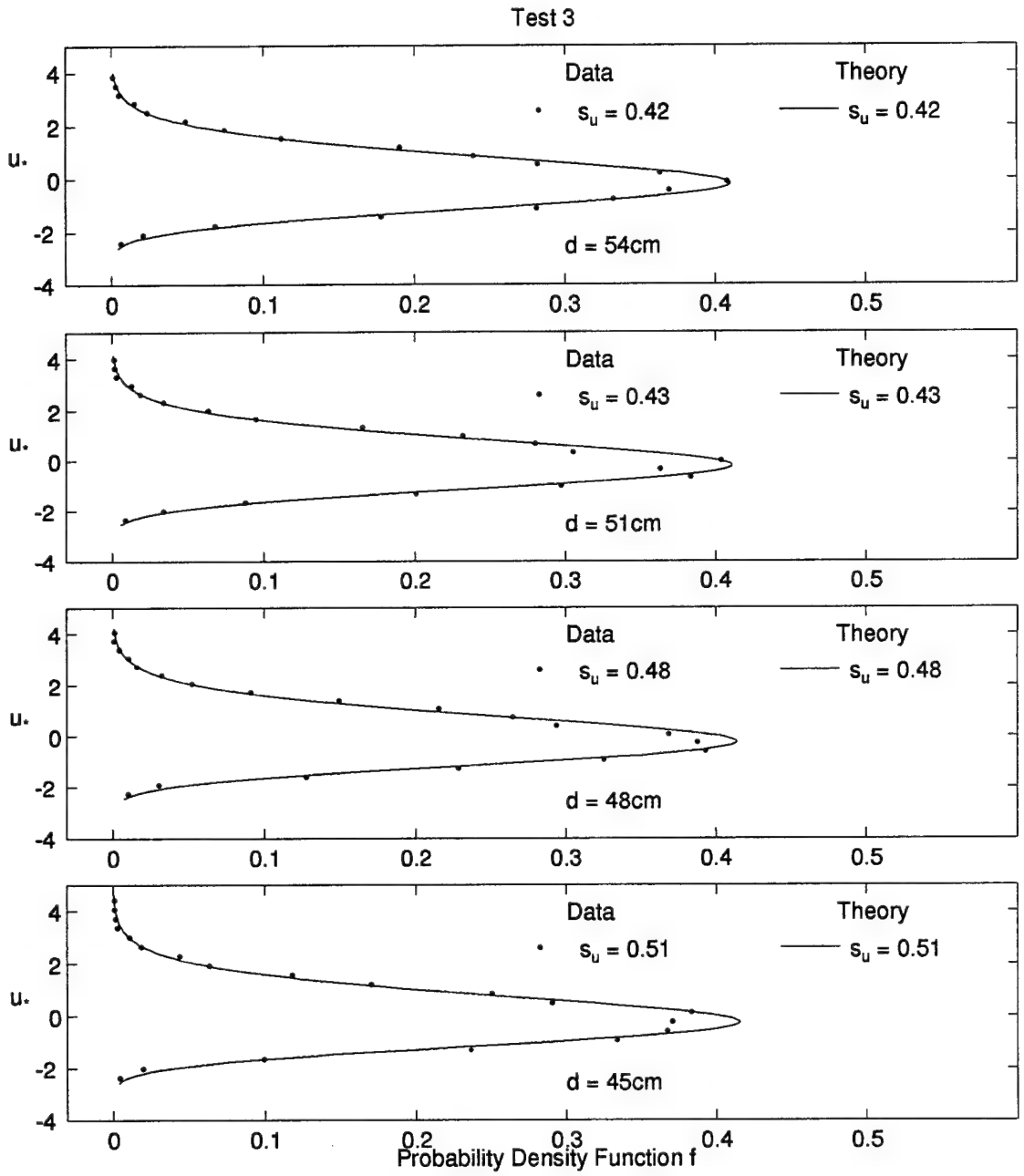

Figure 5.16: Measured and Computed Probability Distributions for Horizontal Velocity at Water Depth d = 54, 51, 48, and 45cm for Test 3

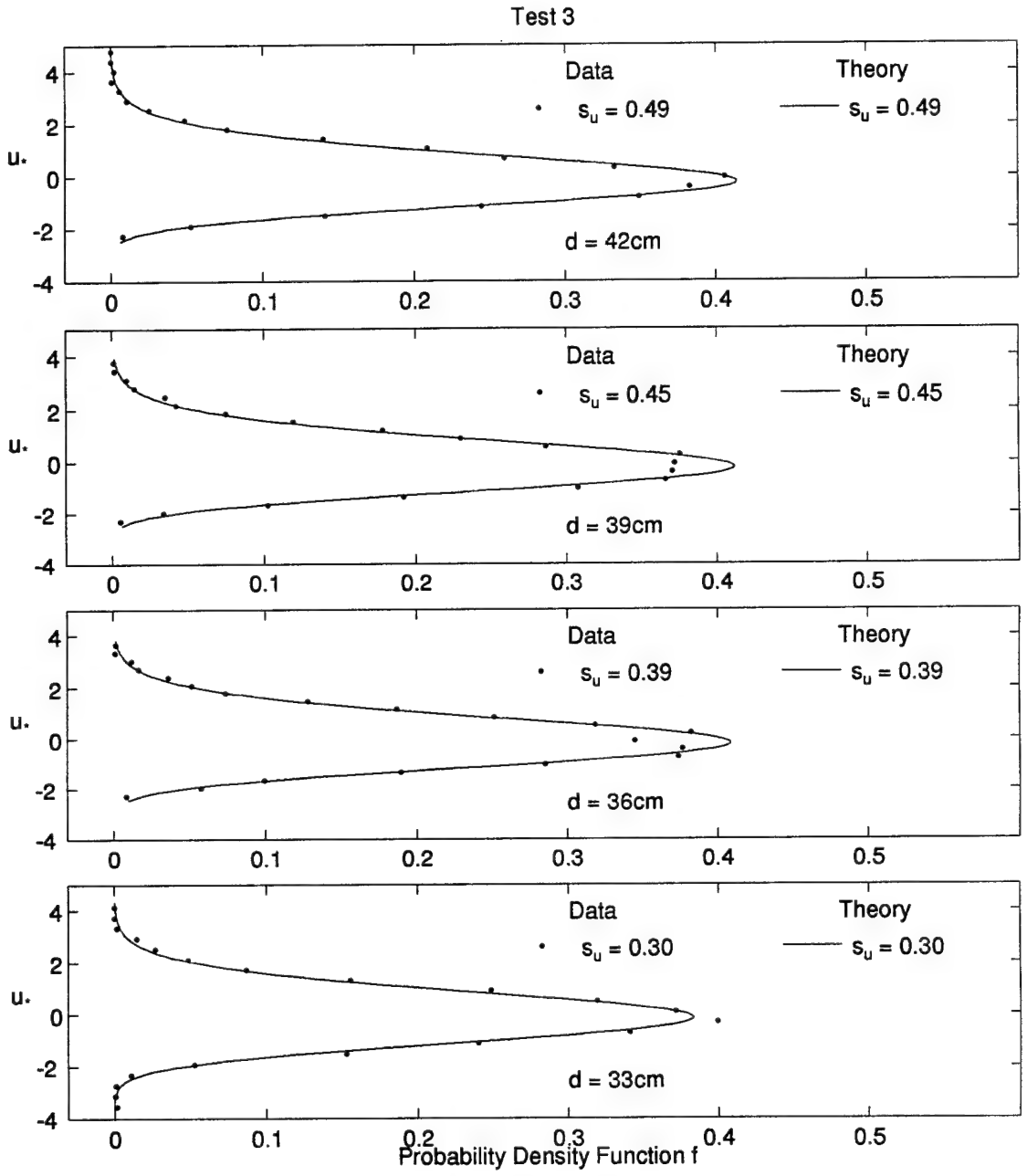

Figure 5.17: Measured and Computed Probability Distributions for Horizontal Velocity at Water Depth d = 42, 39, 36, and 33cm for Test 3

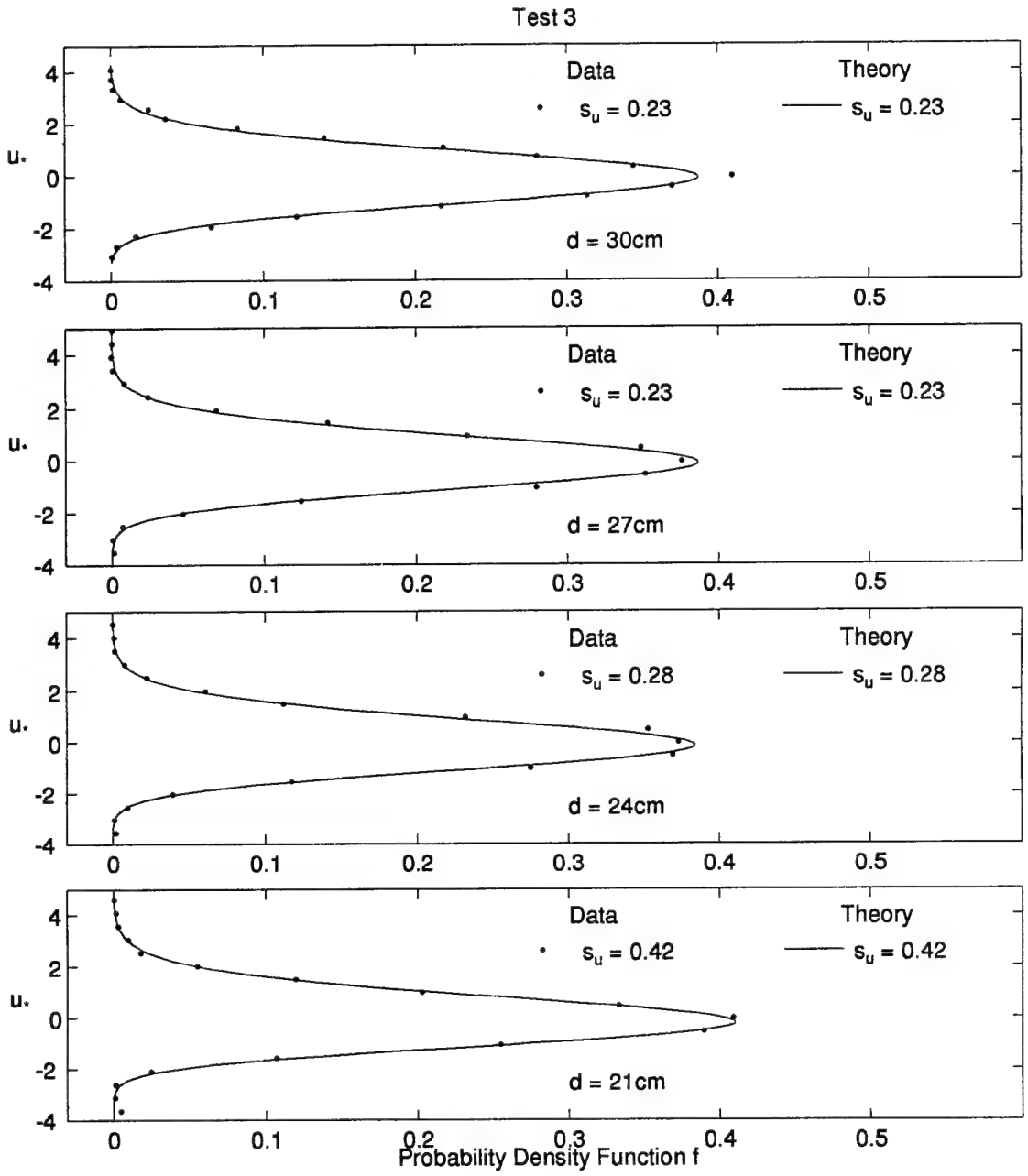

Figure 5.18: Measured and Computed Probability Distributions for Horizontal Velocity at Water Depth d = 30, 27, 24, and 21cm for Test 3

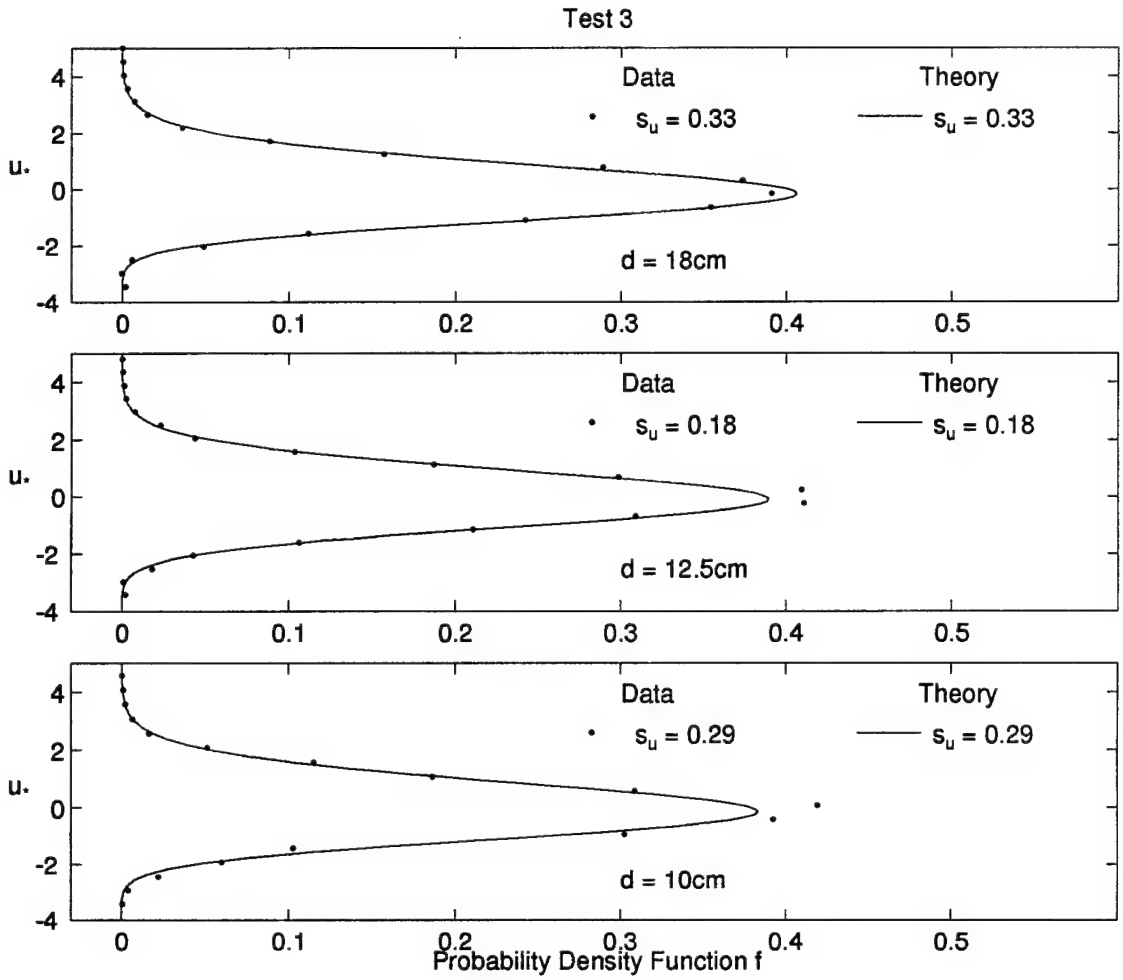

Figure 5.19: Measured and Computed Probability Distributions for Horizontal Velocity at Water Depth $d = 18$, 12.5, and 10cm for Test 3

Chapter 6

CONCLUSION

Three irregular wave tests were conducted on a 1:16 smooth slope to investigate the detailed cross-shore variations of the probability distributions and statistics of the free surface elevations and mid-depth horizontal velocities in the shoaling, surf and swash zones. The exponential gamma distribution is adopted in this study because it becomes Gaussian for zero skewness and exponential for the skewness of two. The exponential gamma distribution with the measured mean, standard deviation, and skewness is shown to be capable of describing all the measured probability distributions in a unified manner.

The lower limit of the exponential distribution of the free surface elevation, η, is assumed to be imposed by the bottom elevation in the swash zone. This assumption yields $H_{\rm rms}/\overline{h} = \sqrt{8}$, where $\overline{h}$ = mean water depth, and $H_{\rm rms}$ = root-mean-square wave height defined as $H_{\rm rms} = \sqrt{8}\sigma$ with σ = standard deviation of η. The measured values of $H_{\rm rms}/\overline{h}$ gradually increase in the surf zone and rapidly approach this upper limit of approximately three in the swash zone. The measured skewness, s, of η increases landward and then decreases toward the still water shoreline but increases again in the swash zone to rapidly approach the upper limit of $s = 2$. The measured kurtosis, K, of η can also be explained by the relation between K and s derived from the exponential gamma distribution. The major conclusion is that the probability distribution and statistics of η in the swash zone are very different from those in the surf zone. The simple relationships of $H_{\rm rms} = \sqrt{8}\ \overline{h}$ and $s = 2$ are useful in predicting the wave motion in the swash zone.

The mean (undertow) $\overline{u}$, and the standard deviation, σ_u, of the horizontal velocity, u, measured at the mid-depth below SWL in the shoaling and surf zones are expressed in terms of $\overline{h}$ and H_{rms} using linear progressive long-wave theory. These simple relationships together with the measured values of $\overline{h}$ and H_{rms} can explain the measured cross-shore variations of $\overline{u}$ and σ_u fairly accurately. The skewness, s_u, of u is found to be always smaller than the corresponding skewness, s, of η, indicating the vertical decrease of nonlinearity. This can not be explained by linear long-wave theory. The kurtosis, K_u, of u exhibits a similar trend but the measured values are less reliable in shallow water.

To utilize the exponential gamma distribution and the simple relationships presented herein for practical applications, a time-averaged model will need to be developed to predict the cross-shore variations of $\overline{h}$, σ, s, and s_u. The equivalency of probabilistic and time averaging will allow one to estimate various even and odd moments associated with time-averaged cross-shore sediment transport rates as was done by Guza and Thornton (1985) using the Gaussian distribution which predicts zero odd moments.

REFERENCES

Abramowitz, M., and Stegun, I.A. (1972). *Handbook of mathematical functions.* Dover, New York, N.Y.

Battjes, J.A. (1974). "Surf similarity." *Proc. 14th Coast. Engrg. Conf.*, ASCE, 1, 466–480.

Battjes, J.A., and Janssen, J.P.F.M. (1978). "Energy loss and set-up due to breaking of random waves." *Proc. 16th Coast. Engrg. Conf.*, ASCE, 1, 569–587.

Battjes, J.A., and Stive, M.J.F. (1985). "Calibration and verification of a dissipation model for random breaking waves." *J. Geophy. Res.*, 90(C5), 9159–9167.

Bitner, E.M. (1980). "Non-linear effects of the statistical model of shallow-water wind waves." *J. Applied Ocean Res.*, 2(2),63–73.

Bouws, E., Gunther, H., Rosenthal, W., and Vincent, C.L. (1985). "Similarity of the wind wave spectrum in finite depth water. 1: Spectral form." *J. Geophys. Res.*, 90(C1),975–986.

Cox, D.T., Kobayashi, N., and Kriebel, D.L. (1994). "Numerical model verification using SUPERTANK data in surf and swash zones." *Proc. Coast. Dynamics '94*, ASCE, 248–262.

Dally, W.R., and Dean, R.G. (1986). "Transformation of random breaking waves on surf beat." *Proc. 20th Coast. Engrg. Conf.*, ASCE, 1,109–123.

Douglass, S.L. (1992). "Estimating extreme values of run-up on beaches." *J. Wtrwy. Port, Coast., and Oc. Engrg.*, ASCE, 118(2),220–224.

Goda, Y. 1985. *Random seas and design of maritime structures.* Univ. of Tokyo Press. Tokyo, Japan.

Gran, S. (1992). *A Course in ocean engineering.* Elsevier, New York, N.Y.

Guza, R.T., and Thornton, E.B. (1980). "Local and shoaled comparisons of sea surface elevations, pressures, and velocities." *J. Geophys. Res.*, 85(C3),1524–1530.

Guza, R.T., and Thornton, E.B. (1982). "Swash oscillations on a natural beach." *J. Geophys. Res.*, 87(C1),483–491.

Guza, R.T., and Thornton, E.B. (1985). "Velocity moments in nearshore." *J. Wtrwy. Port, Coast., and Oc. Engrg.*, ASCE, 111(2),235–256.

Holman, R.A., and Sallenger, A.H. (1985). "Setup and swash on a natural beach." *J. Geophys. Res.*, 90(C1),945–953.

Huang, N.E., and Long, S.R. (1980). "An experimental study of the surface elevation probability distribution and statistics of wind-generated waves." *J. Fluid Mech.*, 101(1),179–200.

Kobayashi, N., DeSilva, G.S., and Watson, K.D. (1989). "Wave transformation and swash oscillation on gentle and steep slopes." *J. Geophys. Res.*, 94(C1), 951–966.

Kobayashi, N., Herrman, M.N., Johnson, B.D, and Orzech, M.D. "Probability distribution of surface elevation in surf and swash zones." *J. Wtrwy. Port, Coast., and Oc. Engrg.*, ASCE. (submitted).

Kobayashi, N., and Karjadi, E.A. (1996). "Obliquely incident irregular waves in surf and swash zones." *J. Geophys. Res.*, 101(C3), 6527–6542.

Kobayashi, N., and Raichle, A.W. (1994). "Irregular wave overtopping of revetments in surf zones." *J. Wtrwy. Port, Coast. and Oc. Engrg.*, ASCE, 120(1), 56–73.

Kobayashi, N., and Wurjanto, A. (1992). "Irregular wave setup and run-up on beaches." *J. Wtrwy. Port, Coast., and Oc. Engrg.*, ASCE, 118(4),368–386.

Kraus, N.C., Lohrmann, A., and Cabrera, R. (1994). "New acoustic meter for measuring 3D laboratory flows." *J. Hydraulic Engrg.*, ASCE, 120(3),406–412.

Kriebel, D.L. (1994). "Swash zone wave characteristics from SUPERTANK." *Proc. 24th Coast. Engrg. Conf.*, ASCE, 2,2207–2221.

Longuet-Higgins, M.S. (1963). "The effect of non-linearities on statistical distributions in the theory of sea waves." *J. Fluid Mech.*, 17,459–480.

Mase, H., and Kobayashi, N. (1991). "Transformation of random breaking waves and its empirical numerical model considering surf beat." *Proc. Coast. Sediments '91*, ASCE, 1.688–702.

Raubenheimer, B., Guza, R.T., Elgar, S., and Kobayashi, N. (1995). "Swash on a gently sloping beach." *J. Geophys. Res.*, 100(C5),8751–8760.

Svendsen, I.A. (1984). "Mass flux and undertow in a surf zone." *Coast. Engrg.*, 8, 347–365.

Tayfun, M.A. (1980). "Narrow-band nonlinear sea waves." *J. Geophys. Res.*, 85(C3), 1548–1552.

Thompson, E.F. (1980). "Shallow water surface wave elevation distributions." *J. Wtrwy. Port, Coast., and Oc. Engrg.*, ASCE, 106(2),285–289.

Thornton, E.B., and Guza, R.T. (1982). "Energy saturation and phase speeds measured on a natural beach." *J. Geophys. Res.*, 87(C12),9499–9508.

Thornton, E.B., and Guza. R.T. (1983). "Transformation of wave height distribution." *J. Geophys. Res.*, 88(C10),5925–5938.

Wolfram, S. (1991). *Mathematica.* 2nd ed., Addison-Wesley, Redwood City, Cal.

Appendix A

COMPLETE FREE SURFACE STATISTICAL DATA FOR TEST SETS 1–3

Complete free surface statistical data is given below for each gage location for test 1. Each gage is indexed by its x position and the corresponding water depth where $z_b = -d$.

Table A.1: Test 1 Gage Data

x	z_b	$\overline{\eta}$	$\overline{h}$	H_{rms}	s	*Kurtosis K*	
(m)	*(cm)*	*(cm)*	*(cm)*	*(cm)*		*data*	*theory*
0.00	-75.0	0.03	75.03	12.44	0.36	3.23	3.26
0.38	-72.6	-0.13	72.47	12.49	0.38	3.20	3.29
0.50	-71.9	-0.19	71.71	12.38	0.36	3.17	3.25
1.44	-66.0	-0.19	65.81	12.11	0.24	3.02	3.11
1.60	-65.0	-0.17	64.83	12.12	0.24	2.99	3.11
1.76	-64.0	-0.02	63.98	11.95	0.22	2.99	3.10
1.92	-63.0	-0.07	62.93	12.01	0.28	3.01	3.16
2.08	-62.0	-0.08	61.92	11.94	0.31	3.07	3.19
2.24	-61.0	-0.11	60.89	11.78	0.31	3.01	3.19
2.40	-60.0	-0.14	59.86	11.82	0.33	3.02	3.22
2.56	-59.0	-0.16	58.84	11.76	0.35	3.04	3.25
2.72	-58.0	-0.09	57.91	11.67	0.36	3.05	3.25

Table A.1: (Test 1 Gage Data, continued)

x	z_b	$\overline{\eta}$	$\overline{h}$	H_{rms}	s	*Kurtosis K*	
(m)	*(cm)*	*(cm)*	*(cm)*	*(cm)*		*data*	*theory*
2.88	-57.0	-0.28	56.72	11.61	0.37	3.07	3.27
3.04	-56.0	-0.07	55.93	11.62	0.37	3.08	3.27
3.20	-55.0	-0.09	54.91	11.63	0.37	3.10	3.27
3.36	-54.0	-0.05	53.95	11.74	0.42	3.19	3.35
3.52	-53.0	-0.08	52.92	11.67	0.40	3.15	3.33
3.68	-52.0	-0.10	51.90	11.56	0.39	3.14	3.30
3.84	-51.0	-0.13	50.87	11.55	0.44	3.18	3.39
4.00	-50.0	-0.06	49.94	11.43	0.43	3.15	3.36
4.16	-49.0	-0.15	48.85	11.32	0.43	3.16	3.37
4.32	-48.0	-0.01	47.99	11.43	0.46	3.15	3.42
4.48	-47.0	-0.11	46.89	11.49	0.46	3.14	3.42
4.64	-46.0	-0.09	45.91	11.55	0.44	3.13	3.38
4.80	-45.0	-0.00	45.00	11.75	0.49	3.23	3.48
4.96	-44.0	-0.10	43.90	11.68	0.49	3.21	3.48
5.12	-43.0	-0.10	42.90	11.53	0.49	3.23	3.48
5.28	-42.0	-0.07	41.93	11.42	0.53	3.27	3.55
5.44	-41.0	-0.14	40.86	11.23	0.54	3.26	3.58
5.60	-40.0	-0.15	39.85	11.02	0.52	3.18	3.53
5.76	-39.0	0.03	39.03	11.07	0.56	3.24	3.61
5.92	-38.0	-0.12	37.88	11.02	0.57	3.22	3.64
6.08	-37.0	-0.18	36.82	10.98	0.56	3.20	3.61
6.24	-36.0	-0.20	35.80	10.98	0.60	3.27	3.72
6.40	-35.0	-0.24	34.76	10.79	0.60	3.23	3.72

Table A.1: (Test 1 Gage Data, continued)

x	z_b	$\overline{\eta}$	$\overline{h}$	H_{rms}	s	*Kurtosis K*	
(m)	*(cm)*	*(cm)*	*(cm)*	*(cm)*		*data*	*theory*
6.56	-34.0	-0.26	33.74	10.86	0.62	3.22	3.77
6.72	-33.0	-0.10	32.90	10.94	0.69	3.33	3.95
6.88	-32.0	-0.15	31.85	10.77	0.72	3.34	4.01
7.04	-31.0	-0.15	30.85	10.79	0.74	3.42	4.07
7.20	-30.0	-0.09	29.91	10.85	0.81	3.54	4.28
7.36	-29.0	-0.14	28.86	10.61	0.80	3.42	4.24
7.52	-28.0	-0.13	27.87	10.63	0.78	3.31	4.18
7.68	-27.0	-0.05	26.95	10.60	0.82	3.44	4.32
7.84	-26.0	-0.16	25.84	10.44	0.80	3.32	4.25
8.00	-25.0	-0.13	24.87	10.34	0.77	3.22	4.17
8.16	-24.0	-0.07	23.93	10.44	0.86	3.42	4.44
8.32	-23.0	-0.06	22.94	10.29	0.87	3.37	4.46
8.48	-22.0	-0.09	21.91	10.06	0.85	3.29	4.40
8.64	-21.0	-0.05	20.95	10.06	0.93	3.45	4.67
8.80	-20.0	0.01	20.01	9.86	0.95	3.49	4.71
8.96	-19.0	0.05	19.05	9.69	0.97	3.59	4.80
9.12	-18.0	0.06	18.06	9.41	0.99	3.63	4.87
9.28	-17.0	0.08	17.08	9.07	1.04	3.71	5.03
9.44	-16.0	0.12	16.12	8.67	1.03	3.68	4.99
10.00	-12.5	0.30	12.80	7.53	1.00	3.78	4.90
10.00	-12.5	0.35	12.85	7.47	0.98	3.79	4.83
10.40	-10.0	0.57	10.57	6.55	0.88	3.72	4.48
10.40	-10.0	0.52	10.52	6.48	0.90	3.97	4.55

Table A.1: (Test 1 Gage Data, continued)

x	z_b	$\overline{\eta}$	$\overline{h}$	H_{rms}	s	*Kurtosis K*	
(m)	*(cm)*	*(cm)*	*(cm)*	*(cm)*		*data*	*theory*
10.40	-10.0	0.45	10.45	6.54	0.85	3.80	4.38
10.40	-10.0	0.55	10.55	6.53	0.83	3.71	4.35
10.80	-7.5	0.65	8.15	5.61	0.67	3.39	3.90
10.80	-7.5	0.79	8.29	5.61	0.68	3.37	3.92
10.80	-7.5	0.85	8.35	5.76	0.71	3.44	4.00
10.80	-7.5	0.83	8.33	5.74	0.69	3.30	3.93
11.20	-5.0	1.14	6.14	4.74	0.57	3.09	3.64
11.20	-5.0	1.14	6.14	4.74	0.54	2.98	3.58
11.20	-5.0	1.22	6.22	4.87	0.60	3.05	3.71
11.20	-5.0	1.21	6.21	4.90	0.56	2.91	3.62
11.60	-2.5	1.48	3.98	4.19	0.36	2.96	3.26
11.60	-2.5	1.48	3.98	4.21	0.41	2.96	3.33
11.60	-2.5	1.54	4.04	4.27	0.41	3.12	3.34
11.60	-2.5	1.60	4.10	4.31	0.42	3.08	3.35
12.00	0.0	1.75	1.75	3.17	0.64	3.10	3.81
12.00	0.0	1.69	1.69	3.19	0.67	3.13	3.90
12.00	0.0	1.83	1.83	3.36	0.57	2.90	3.65
12.00	0.0	1.83	1.83	3.38	0.58	2.97	3.66
12.40	2.5	3.09	0.59	1.88	1.60	5.72	7.29
12.40	2.5	3.20	0.70	1.90	1.59	5.66	7.24
12.40	2.5	3.16	0.66	2.03	1.63	5.73	7.41
12.40	2.5	3.16	0.66	2.03	1.69	6.26	7.68
12.80	5.0	5.26	0.26	0.98	2.24	9.76	9.00

Table A.1: (Test 1 Gage Data, continued)

x	z_b	$\overline{\eta}$	$\overline{h}$	H_{rms}	s	*Kurtosis K*	
(m)	*(cm)*	*(cm)*	*(cm)*	*(cm)*		*data*	*theory*
12.80	5.0	5.31	0.31	0.96	2.24	9.88	9.00
12.80	5.0	5.56	0.56	1.26	1.97	8.16	8.89
12.80	5.0	5.49	0.49	1.32	1.98	8.13	8.91
12.80	5.0	5.48	0.48	1.30	1.95	7.91	8.78

Complete free surface statistical data is given below for each gage location for test 2. Each gage is indexed by its x position and the corresponding water depth where $z_b = -d$.

Table A.2: Test 2 Gage Data

x	z_b	$\overline{\eta}$	$\overline{h}$	H_{rms}	s	*Kurtosis K*	
(m)	*(cm)*	*(cm)*	*(cm)*	*(cm)*		*data*	*theory*
0.00	-75.0	-0.32	74.68	16.85	0.52	3.51	3.55
0.38	-72.6	-0.24	72.36	16.71	0.60	3.58	3.72
0.50	-71.9	-0.11	71.79	16.53	0.62	3.60	3.76
1.44	-66.0	-0.20	65.80	16.28	0.68	3.76	3.92
1.60	-65.0	-0.28	64.72	16.16	0.67	3.74	3.90
1.76	-64.0	-0.23	63.77	15.94	0.69	3.84	3.95
1.92	-63.0	-0.11	62.89	16.17	0.74	3.93	4.09
2.08	-62.0	-0.16	61.84	16.06	0.73	3.89	4.04
2.24	-61.0	-0.21	60.79	15.81	0.74	3.97	4.08
2.40	-60.0	-0.07	59.93	16.14	0.81	4.13	4.26
2.56	-59.0	-0.12	58.88	16.00	0.78	4.06	4.20

Table A.2: (Test 2 Gage Data, continued)

x	z_b	$\overline{\eta}$	$\overline{h}$	H_{rms}	s	*Kurtosis K*	
(m)	*(cm)*	*(cm)*	*(cm)*	*(cm)*		*data*	*theory*
2.72	-58.0	-0.12	57.88	15.78	0.81	4.16	4.28
2.88	-57.0	-0.03	56.97	16.32	0.88	4.30	4.49
3.04	-56.0	-0.08	55.92	16.13	0.87	4.27	4.47
3.20	-55.0	-0.08	54.92	15.80	0.89	4.30	4.51
3.36	-54.0	-0.04	53.96	16.19	1.00	4.58	4.88
3.52	-53.0	-0.14	52.86	15.85	0.98	4.45	4.82
3.68	-52.0	-0.14	51.86	15.41	1.01	4.55	4.92
3.84	-51.0	-0.06	50.94	15.71	1.10	4.89	5.24
4.00	-50.0	-0.17	49.83	15.38	1.10	4.88	5.26
4.16	-49.0	-0.22	48.78	14.92	1.14	5.06	5.40
4.32	-48.0	-0.09	47.91	15.19	1.18	5.14	5.55
4.48	-47.0	-0.19	46.81	14.84	1.17	5.11	5.51
4.64	-46.0	-0.20	45.80	14.42	1.19	5.17	5.59
4.80	-45.0	-0.08	44.92	14.52	1.27	5.36	5.90
4.96	-44.0	-0.13	43.87	14.21	1.23	5.22	5.76
5.12	-43.0	-0.15	42.85	13.84	1.22	5.16	5.71
5.28	-42.0	-0.09	41.91	14.04	1.29	5.34	5.98
5.44	-41.0	-0.14	40.86	13.87	1.25	5.18	5.84
5.60	-40.0	-0.12	39.88	13.64	1.23	5.12	5.75
5.76	-39.0	-0.06	38.94	13.99	1.23	5.09	5.75
5.92	-38.0	-0.11	37.89	13.70	1.22	5.05	5.70
6.08	-37.0	-0.13	36.87	13.80	1.23	5.09	5.74
6.24	-36.0	0.08	36.08	14.13	1.28	5.19	5.95

Table A.2: (Test 2 Gage Data, continued)

x	z_b	$\overline{\eta}$	$\overline{h}$	H_{rms}	s	*Kurtosis K*	
(m)	*(cm)*	*(cm)*	*(cm)*	*(cm)*		*data*	*theory*
6.40	-35.0	-0.05	34.95	13.74	1.25	5.03	5.84
6.56	-34.0	-0.06	33.94	13.69	1.24	5.01	5.80
6.72	-33.0	0.03	33.03	13.84	1.33	5.20	6.13
6.88	-32.0	-0.03	31.97	13.42	1.30	5.04	6.02
7.04	-31.0	-0.04	30.96	13.30	1.26	4.93	5.88
7.20	-30.0	0.07	30.07	13.13	1.28	4.95	5.96
7.36	-29.0	-0.02	28.98	12.78	1.27	4.82	5.90
7.52	-28.0	-0.01	27.99	12.71	1.26	4.84	5.87
7.68	-27.0	0.10	27.10	12.38	1.34	4.83	6.19
7.84	-26.0	0.05	26.05	11.99	1.32	4.76	6.09
8.00	-25.0	0.04	25.04	11.92	1.30	4.77	6.04
8.16	-24.0	0.42	24.42	12.20	1.35	4.91	6.23
8.32	-23.0	0.28	23.28	11.77	1.32	4.80	6.13
8.48	-22.0	0.34	22.34	11.60	1.33	4.88	6.15
8.64	-21.0	0.20	21.20	11.93	1.37	5.03	6.30
8.80	-20.0	0.16	20.16	11.34	1.30	4.79	6.04
8.96	-19.0	0.17	19.17	11.03	1.26	4.61	5.85
9.12	-18.0	0.30	18.30	11.22	1.27	4.53	5.89
9.28	-17.0	0.25	17.25	10.58	1.19	4.33	5.61
9.44	-16.0	0.26	16.26	10.17	1.15	4.27	5.42
10.00	-12.5	0.81	13.31	11.01	1.02	4.35	4.97
10.40	-10.0	1.22	11.22	9.74	0.78	3.40	4.18
10.40	-10.0	1.40	11.40	9.88	0.82	3.82	4.32

Table A.2: (Test 2 Gage Data, continued)

x	z_b	$\overline{\eta}$	$\overline{h}$	H_{rms}	s	*Kurtosis K*	
(m)	*(cm)*	*(cm)*	*(cm)*	*(cm)*		*data*	*theory*
10.80	-7.5	1.82	9.32	9.25	0.85	3.83	4.39
10.80	-7.5	1.78	9.28	9.19	0.86	4.01	4.42
11.20	-5.0	2.27	7.27	8.34	0.73	3.48	4.05
11.20	-5.0	2.21	7.21	8.28	0.87	4.28	4.45
11.60	-2.5	2.82	5.32	7.64	0.84	3.60	4.38
11.60	-2.5	2.78	5.28	7.52	0.91	3.97	4.59
12.00	0.0	3.32	3.32	6.69	1.15	4.13	5.43
12.00	0.0	3.39	3.39	6.58	1.15	4.37	5.42
12.40	2.5	5.12	2.62	5.21	1.45	4.94	6.64
12.40	2.5	4.57	2.07	5.25	1.40	4.74	6.43
12.80	5.0	6.67	1.67	3.66	1.54	5.54	7.03
12.80	5.0	6.36	1.36	3.56	1.54	5.25	7.03
13.20	7.5	8.31	0.81	2.33	2.32	9.79	9.00
13.20	7.5	8.15	0.65	2.23	2.30	9.82	9.00
13.60	10.0	11.07	1.07	1.78	3.02	14.77	9.00
13.60	10.0	10.48	0.48	1.96	2.75	12.72	9.00
13.60	10.0	10.45	0.45	1.95	2.76	13.17	9.00
14.00	12.5	13.40	0.90	1.44	1.75	8.55	7.93
14.00	12.5	13.37	0.87	1.43	1.34	7.26	6.20
14.00	12.5	13.22	0.72	1.23	2.67	13.57	9.00
14.00	12.5	12.94	0.44	1.06	2.02	9.04	9.00

Complete free surface statistical data is given below for each gage location

for test 3. Each gage is indexed by its x position and the corresponding water depth where $z_b = -d$.

Table A.3: Test 3 Gage Data

x	z_b	$\overline{\eta}$	$\overline{h}$	H_{rms}	s	*Kurtosis K*	
(m)	*(cm)*	*(cm)*	*(cm)*	*(cm)*		*data*	*theory*
-1.00	-76.2	-0.24	75.96	18.40	0.42	2.98	3.36
0.38	-72.6	-0.30	72.30	18.16	0.50	3.22	3.50
0.50	-71.9	-0.27	71.63	18.30	0.53	3.29	3.57
1.44	-66.0	-0.21	65.79	18.12	0.58	3.46	3.66
1.60	-65.0	-0.36	64.65	18.18	0.57	3.49	3.64
1.76	-64.0	-0.39	63.61	18.11	0.59	3.56	3.68
1.92	-63.0	-0.15	62.85	18.13	0.62	3.60	3.76
2.08	-62.0	-0.26	61.74	18.21	0.62	3.64	3.77
2.24	-61.0	-0.27	60.73	18.10	0.64	3.70	3.80
2.40	-60.0	-0.19	59.81	18.09	0.66	3.72	3.86
2.56	-59.0	-0.27	58.73	18.14	0.65	3.70	3.83
2.72	-58.0	-0.27	57.73	18.13	0.69	3.86	3.95
2.88	-57.0	-0.16	56.84	18.10	0.72	3.86	4.01
3.04	-56.0	-0.31	55.69	18.13	0.70	3.84	3.98
3.20	-55.0	-0.27	54.73	18.00	0.72	3.93	4.03
3.36	-54.0	-0.18	53.82	18.02	0.77	4.07	4.14
3.52	-53.0	0.20	53.20	18.01	0.75	4.02	4.09
3.68	-52.0	-0.28	51.72	17.86	0.75	4.06	4.10
3.84	-51.0	-0.19	50.81	17.97	0.78	4.17	4.17
4.00	-50.0	-0.35	49.65	17.96	0.76	4.13	4.13
4.16	-49.0	-0.32	48.68	17.83	0.76	4.12	4.13

Table A.3: (Test 3 Gage Data, continued)

x	z_b	$\overline{\eta}$	$\overline{h}$	H_{rms}	s	*Kurtosis K*	
(m)	*(cm)*	*(cm)*	*(cm)*	*(cm)*		*data*	*theory*
4.32	-48.0	-0.22	47.78	17.90	0.81	4.27	4.27
4.48	-47.0	-0.29	46.71	17.86	0.77	4.10	4.16
4.64	-46.0	-0.31	45.69	17.75	0.76	4.11	4.14
4.80	-45.0	-0.23	44.77	18.00	0.82	4.22	4.29
4.96	-44.0	-0.26	43.74	17.98	0.78	4.13	4.20
5.12	-43.0	-0.32	42.68	17.94	0.79	4.15	4.22
5.28	-42.0	-0.22	41.78	18.01	0.83	4.27	4.33
5.44	-41.0	-0.33	40.67	18.07	0.81	4.20	4.27
5.60	-40.0	-0.33	39.67	17.98	0.79	4.24	4.21
5.76	-39.0	-0.23	38.77	18.05	0.87	4.32	4.45
5.92	-38.0	-0.28	37.72	18.09	0.84	4.21	4.37
6.08	-37.0	-0.38	36.62	17.96	0.82	4.19	4.30
6.24	-36.0	-0.15	35.85	18.11	0.90	4.27	4.54
6.40	-35.0	-0.32	34.68	18.14	0.87	4.30	4.47
6.56	-34.0	-0.38	33.62	17.91	0.85	4.38	4.40
6.72	-33.0	-0.20	32.80	17.73	0.93	4.38	4.66
6.88	-32.0	-0.29	31.71	17.57	0.90	4.28	4.56
7.04	-31.0	-0.35	30.65	17.28	0.80	4.41	4.24
7.20	-30.0	-0.10	29.90	16.95	0.90	4.07	4.54
7.36	-29.0	-0.21	28.79	16.68	0.85	4.12	4.40
7.52	-28.0	-0.29	27.71	16.52	0.68	4.69	3.91
7.68	-27.0	-0.01	26.99	16.16	0.88	4.01	4.50
7.84	-26.0	-0.12	25.88	15.82	0.75	3.91	4.09

Table A.3: (Test 3 Gage Data, continued)

x	z_b	$\overline{\eta}$	$\overline{h}$	H_{rms}	s	*Kurtosis K*	
(m)	*(cm)*	*(cm)*	*(cm)*	*(cm)*		*data*	*theory*
8.00	-25.0	-0.16	25.18	15.81	0.88	4.18	4.50
8.16	-24.0	0.23	24.23	15.51	0.86	4.03	4.42
8.32	-23.0	0.13	23.13	15.18	0.74	4.15	4.07
8.48	-22.0	0.21	22.21	14.59	0.67	4.16	3.88
8.64	-21.0	0.45	21.45	14.62	0.80	3.79	4.26
8.80	-20.0	0.49	20.49	14.53	0.70	3.51	3.97
8.96	-19.0	0.53	19.53	13.79	0.64	3.32	3.82
9.12	-18.0	0.75	18.75	13.48	0.62	3.31	3.77
9.28	-17.0	0.81	17.81	13.31	0.60	3.08	3.71
9.44	-16.0	0.96	16.96	12.84	0.62	3.14	3.75
10.00	-12.5	1.43	13.93	11.96	0.56	3.06	3.61
10.40	-10.0	1.85	11.85	11.56	0.62	3.20	3.77
10.40	-10.0	2.01	12.01	11.53	0.62	3.20	3.76
10.80	-7.5	2.25	9.75	10.96	0.57	3.10	3.64
10.80	-7.5	2.39	9.89	11.07	0.57	3.08	3.64
11.20	-5.0	2.82	7.82	10.52	0.60	3.24	3.71
11.20	-5.0	2.97	7.97	10.50	0.60	3.27	3.71
11.60	-2.5	3.58	6.08	9.37	0.82	3.37	4.31
11.60	-2.5	3.77	6.27	9.41	0.75	3.27	4.10
12.00	0.0	4.16	4.16	8.24	0.93	3.53	4.64
12.00	0.0	4.38	4.38	8.37	0.92	3.64	4.62
12.40	2.5	5.35	2.85	6.83	1.20	4.35	5.64
12.40	2.5	5.48	2.98	6.83	1.15	4.16	5.45

Table A.3: (Test 3 Gage Data, continued)

x	z_b	$\overline{\eta}$	$\overline{h}$	H_{rms}	s	*Kurtosis K*	
(m)	*(cm)*	*(cm)*	*(cm)*	*(cm)*		*data*	*theory*
12.80	5.0	7.24	2.24	5.23	1.22	4.52	5.71
12.80	5.0	7.28	2.28	5.45	1.06	3.92	5.10
13.20	7.5	8.80	1.30	3.59	1.48	5.34	6.77
13.20	7.5	8.87	1.37	4.26	1.25	4.33	5.81
13.60	10.0	11.00	1.00	3.03	1.49	4.72	6.79
13.60	10.0	10.89	0.89	3.19	1.58	5.13	7.21
14.00	12.5	13.17	0.67	2.32	2.00	7.23	9.00
14.00	12.5	13.15	0.65	2.60	2.16	7.90	9.00
14.40	15.0	15.36	0.36	1.97	2.21	7.85	9.00
14.40	15.0	15.59	0.59	2.32	2.11	7.44	9.00